TAMPEREEN TEKNILLINEN YLIOPISTO
TAMPERE UNIVERSITY OF TECHNOLOGY

PEKKA LAURIKAINEN

CHARACTERIZATION OF THE AGEING OF GLASS FIBRE-REINFORCED POLYMERS

Master of Science Thesis

Examiners: Assistant Professor Essi Sarlin and University Lecturer, Docent Terttu Hukka
The topic and examiners approved on 9. August 2017

ABSTRACT

PEKKA LAURIKAINEN: Characterization of the ageing of glass fibre-reinforced polymers
Tampere University of Technology
Master of Science Thesis, 85 pages, 28 Appendix pages
August 2017
Master's Degree Programme in Materials Science
Major: Polymers and Biomaterials
Examiner: Assistant Professor Essi Sarlin, University Lecturer, Docent Terttu Hukka

Keywords: Ageing, Fiber-reinforced plastics, Glass Fibres, Glass structure, Glass corrosion, Polymer Chemistry, Thermosetting polymers.

This work was carried out as a part of the research in ageing and corrosion of composite materials at Tampere University of Technology. The subject is of great interest for both academia and industry and collaboration with industrial partners is included in the form of materials and even some testing. The aim of this work is to compile and provide information on the chemistry related to the ageing of glass fibre-reinforced unsaturated polyester, vinyl ester and epoxy matrix composites in aqueous environments and to examine suitable methods of observing these processes.

The ageing in the polymer matrix is a combination of physical and chemical phenomena, which are determined by the used resin. Hydrolysis, for example, is a major chemical degradation process for all polyester structures; present both in unsaturated polyester and vinyl ester resins. Physical ageing includes plasticizing of the resin, swelling and removal of unreacted resin, all caused by diffusion of water into the structure. Post-curing is likely if the ageing environment has high temperatures. For glass fibres, these environments cause chemical reactions that lead to corrosion of the glass. The severity depends on the composition and structure of the glass, the latter of which is not fully understood. Based on literature review, possible structures of the glass materials are presented and their expected correlation the corrosion is explained. The ageing at the interphase between fibre reinforcements and the resin matrix, in turn, is a complex phenomenon that has been studied with varying success for several decades. It has been shown that the sizing applied on the glass fibre surface has a significant role in the properties of the interphase, but the scope of this work is not sufficient to analyse the role of sizing in detail.

The extent of the ageing phenomena, for various materials representing parts of the composite, were examined with several methods. Weighing of the samples during the ageing procedure and optical microscopy and thermal analysis methods after the ageing were used to examine a vinyl ester resin. Scanning electron microscopy and energy-dispersive X-ray spectroscopy, inductively coupled mass spectrometry and mechanical testing were in turn used to examine the changes in glass fibres. Infrared spectroscopy was also utilized to find changes of in the chemical structure of both the resin matrix and the fibre reinforcements. The loss of properties at the interphase was tested with a recently developed microbond tester, developed at Tampere University of Technology. The results of these tests agree with the phenomena found in literature well, but further need for research is identified in many areas of the ageing behaviour.

TIIVISTELMÄ

PEKKA LAURIKAINEN: Lasikuitulujitteisten polymeerimateriaalien vanhenemisen karakterisointi
Tampereen teknillinen yliopisto
Diplomityö, 85 sivua, 28 liitesivua
Elokuu 2017
Materiaalitekniikan diplomi-insinöörin tutkinto-ohjelma
Pääaine: Polymers and Biomaterials
Tarkastajat: Apulaisprofessori Essi Sarlin, Yliopistonlehtori, dosentti Terttu Hukka

Avainsanat: Vanheneminen, Kuitulujitteiset muovit, Lasikuidut, Lasin kemiallinen rakenne, Lasin korroosio, Polymeerikemia, Kertamuovit.

Tämä työ suoritettiin osana Tampereen teknillisessä yliopistossa tehtävää materiaalien vanhenemiseen ja korroosioon liittyvää tutkimusta. Aihe on sekä tutkimuksen, että teollisuuden kannalta merkittävä ja tässäkin työssä on mukana materiaaleja ja testausapua yhteistyökumppaneilta teollisuudessa. Työn päämääränä on koota olemassa olevaa tietoa tyydyttymätön polyesteri, vinyyliesteri ja epoksi pohjaisten lasikuitukomposiittien vanhenemisesta vesipohjaisissa ympäristöissä, sekä tarkastella niiden vanhenemisprosessien havainnointiin ja testaukseen sopivia menetelmiä.

Polymeerimatriisin vanheneminen on yhdistelmä fysikaalisia ja kemiallisia ilmiöitä, jotka riippuvat suuresti hartsin kemiallisesta rakenteesta. Hydrolyysi – esimerkiksi, on merkittävä kemiallinen hajoamisprosessi kaikissa polyesterirakenteissa, kuten esimerkiksi tyydyttymättömissä polyesterihartseissa ja vinyyliesteri hartseissa. Fysikaalisiin vanhenemisilmiöihin lukeutuvat hartsin plastisointi ja turpoaminen, sekä reagoimattomien hartsin lähtöaineiden poistuminen veden vaikutuksesta. Korkean lämpötilan ympäristöissä vanhenemiseksi lasketaan myös jälkikovettumisreaktiot. Lasikuiduissa vesipohjaiset ympäristöt aiheuttavat kemiallisia reaktioita, jotka pahimmillaan johtavat lasin korroosioon. Reaktioiden eteneminen riippuu merkittävästi lasin koostumuksesta ja rakenteesta, joista jälkimmäistä ei vielä täysin ymmärretä. Tehdyn kirjallisuusselvityksen perusteella, lasien mahdollisia rakenteita ja niiden vaikutusta lasin korroosioon tarkastellaan. Kuitujen ja matriisin välisen rajapinnan vanheneminen on monimutkainen ilmiö, jota on tutkittu vaihtelevalla menestyksellä muutaman vuosikymmenen ajan. Lasikuidun pinnalle lisätyn viimeistelyaineen rooli rajapinnan muodostumisessa on tunnetusti merkittävä, mutta tämän työn laajuus ei riitä viimeistelyaineen kattavaan analyysiin.

Löydettyjen ilmiöiden vaikutuksia eri komposiitin osia edustavissa näytteissä tutkittiin useilla menetelmillä. Vinyyliesterinäytteitä punnittiin, sekä tarkasteltiin optisella mikroskoopilla, sekä termisillä analyysimenetelmillä. Pyyhkäisyelektronimikroskopiaa, röntgenspektroskopiaa massaspektrometriaa, sekä mekaanista testausta hyödynnettiin puolestaan lasikuitujen muutoksien tarkastelussa. Infrapuna spektroskopialla tutkittiin kemiallisen rakenteen muutoksia, sekä hartsissa että lasikuiduissa. Rajapinnan ominaisuuksien heikentymistä tarkasteltiin Tampereen Teknillisessä Yliopistossa kehitetyllä ”microbond”-testilaitteella. Näiden testien tulokset vastaavat hyvin kirjallisuutta, mutta useilla vanhenemisen osa-alueilla todettiin tarve jatkotutkimuksille.

PREFACE

This Master's thesis work is intended as a learning experience and groundwork for further research on the ageing of glass fibre reinforced polymer composites. The subject presents an intriguing problem as a combination of chemistry and materials science. Two similar, yet ultimately very different fields of study.

Firstly, I would like to thank my Thesis instructors; Assistant Professor Essi Sarlin for providing guidance, materials and even the idea and funding for this work and University Lecturer Terttu Hukka for guidance, support and an important different perspective of the subject. I offer thanks also to our industrial collaborators Mari Lindgren at Outotec and Maija Hoikkanen and Rami Haakana at Ahlstrom-Munksjö, for all their interest and support, material or otherwise, they have offered for this work. The Fibrobotics group at Tampere University of Technology led by Mathias von Essen was also instrumental in the work, by providing the equipment and expertise for the fibre tensile and microbond testing. I also value greatly the support of my co-workers at the Plastics and Elastomer Technology research group at Tampere University of Technology. A truly motivated group of people always willing to brainstorm and offer advice on virtually any subject. Finally, significant thanks belongs to my long time life-partner Tuire Marin for both the emotional and academic support she has provided during my time with this work.

In Tampere, Finland, on 23. August 2017

Pekka Laurikainen

CONTENTS

ABBREVIATIONS

ATR	Attenuated Total Reflectance. Used in infrared spectroscopy as a possible interaction method for the IR-beam with a sample.
C-glass	A glass grade, which offers great chemical durability. Rarely used as a reinforcement due to limited mechanical properties
DSC	Differential Scanning Calorimetry
DMTA	Dynamic Mechanical Thermal Analysis, DMA (Dynamic mechanical analysis also widely in use.
E-glass	Borosilicate glass commonly used in reinforcement fibres
ECR-glass	E-glass modification which does not include boron, marketed as having increased durability in acidic environments
EDS	Energy Dispersive X-ray Spectrometry. A chemical analysis method commonly incorporated to SEM.
EP	Epoxy resins
FTIR	Fourier Transform Infrared Spectroscopy
ICP-MS	Inductively Coupled Plasma Mass Spectrometry
IFSS	Interfacial shear strength. Similar to the above but used for the results of tests that more or less directly measure the interface, such as single fibre pull-out or microbond tests.
ILSS	Interlaminar shear strength. A name for a commonly used method and its result. Used to determine the strength of the interface in a PMC.
NBO/BO	Non–bridging/Bridging oxygen. An abbreviation used often in relation to the chemical structure of glasses. Denotes whether an oxygen in the structure of a glass has two covalent bonds or has a covalent bond and an ionic association. In the glass industry, these are often called Q_4 and Q_3 species, respectively.
NMR	Nuclear Magnetic Resonance spectroscopy. Method that can detect the presence of certain nuclei in a material and quantify their amount. Magic angle spinning (MAS) and quantum magic angle spinning (QMAS) variants also offer information of the bonding of the compounds to surrounding substances.
PMC	Polymer Matrix Composite
S-glass	One of the available high mechanical performance glass fibre reinforcement grades.
SEM	Scanning Electron Microscopy/Microscope. Used for both the method and the device itself.
UP	Unsaturated polyester resin
VE	Vinyl ester resin

1. INTRODUCTION

Heated aqueous environments for composite materials are of significant commercial interest and used for example in reactor and chemical transportation tanks. The environments inside such applications are often challenging and failure cases have been reported. The ageing of the materials is often one of the major reasons for the failure. (Dai et al. 2006; Myers et al. 2007; Li et al. 2013; Lindgren et al. 2015) Other acidic ageing environments are of similar interest for example in high-voltage insulators, commonly utilizing E-glass composites. Failure caused by stress corrosion cracking initiated by nitric acid has been reported as a major problem in these applications. (Megel et al. 2001) Glass fibre reinforced composites are also important in marine applications and for example in wind turbines, where water or atmospheric moisture can act as ageing environments (Visco et al. 2008; Guzman & Brøndsted 2015). These research fields have been of great interest for several decades and have led to the development of both reinforcement and resin options with greater resistance to such environments.

However, despite these advances and constant ongoing research, some aspects of the ageing in multi-component materials cause surprising problems. The effects the environments in question have on individual components of the material have earlier been the focus of the research and are therefore well known. (Qiu & Kumosa 1997; Boinard et al. 2000; Ledieu et al. 2004; Jones 2006; Toscano et al. 2016; Sugiman et al. 2016) A problem however arises from the significantly different nature of the components, which causes a division of the field. This division is enhanced by the multitude of options for example for the reinforcement, but also for the matrix. The actual scale of the field of composites is immense and even if one focuses on for example polymer matrix composites, the scope of one's knowledge is almost surely limited to certain material groups to the exclusion of others. More often than not, this leads to oversights in certain areas of the composite behaviour, such as the behaviour of the sizing or assumptions that fibre reinforcements remain unaffected. It has also been shown, for example, that the bonding and the by extension the effects ageing has on the bonding of different types of fibre–resin combinations can be significantly different (Gaur et al. 1994).

This work is intended as preliminary research and information gathering for larger study on the subject. Because of the division of the field, a large-scale effort to compile and evaluate available information is an important first step. The results from the testing, conducted as a part of this work, should also serve in highlighting both problematic areas in the testing and interesting phenomena, which will require significant attention in further research.

The first part of the work consists of an effort to compile the ageing phenomenon identified by many research groups. In this literature review part of the work, significant attention is given to the chemistry of the thermosetting resins and the glass fibres, as the differences between the different material options is expected to be explained by differences in their respective chemical structures. The structure of the interphase between the fibre reinforcements and the polymeric matrix is also discussed to evaluate the importance of this part of the composite, also in terms of ageing of the composite as a whole.

The experimental portion of the work focuses on finding methods for small-scale characterization of different components contributing in a composite. Commonly used methods for composites testing are often in a scale where the properties of individual components are hidden and only the resulting combination of properties is observed. Such methods are, for example, tensile testing of composite laminates and ILSS. These methods are well suited for examination of the significant improvement in properties exhibited by composites compared to the individual materials. However, examination of specific ageing phenomena from such results is virtually impossible. To alleviate the problem a significantly different approach is used. With the information provided in the literature review part of this work, a hypothesis of the advancement of the ageing in composites was formed. This behaviour is the separated into parts, for which experimental methods are selected with the goal of determining the validity and importance of the identified ageing phenomena. When analysing the results, the significance of individual phenomena will be discussed for the material itself, but also for the composite as a whole.

2. AGEING IN POLYMER MATRIX COMPOSITES

The ageing in polymer matrix composites (PMCs) is a subject of great interest in several fields of industry from automotive and electrical to aerospace. However, despite extensive research globally, some aspects of the ageing and degradation of these materials are still poorly understood. These difficulties are primarily caused by problems of reliably examining the interface between the matrix and the reinforcement, which is widely considered as one of the most crucial aspects in the properties of a composite.

2.1 Ageing of the matrix materials

The most common degradation, ageing or corrosion method, for many polymeric materials in aqueous environments is hydrolysis. The terms ageing, degradation and corrosion are used rather arbitrarily to discuss similar phenomenon and the term in use is often determined by the background of the person and the perceived severity of the ageing. In this work, the term ageing will be used when discussing materials subjected to specific environments regardless of the effects, those environments actually have on the properties of the material. Degradation and corrosion can be used to describe specific phenomena, if the term clearly suits better to the situation in question. By this definition, degradation and corrosion can be thought of as effects of the ageing of the material.

2.1.1 Chemical and physical ageing

When discussing the effects of ageing on the properties of the material, the phenomena behind the changes are often divided into chemical and physical ageing. The term physical ageing is used on the effects of the environment, which do not result in chemical changes in the material and can even be reversible. By this definition, chemical ageing is then used to describe the permanent changes in the chemical structures of the material. Hydrolysis is the most important of the chemical ageing phenomena. In hydrolysis, a water molecule breaks a compound via nucleophilic attack and separation to a hydrogen and a hydroxyl group. In polymers this kind of reaction is common for ester groups, which when broken by hydrolysis result in carboxylic acid and alcohol groups in the ends of two now separate compounds. In thermosetting resins, the plasticizing effect of water is widely recognized as one of the most significant form of physical ageing. This plasticizing effect is caused by diffusion of water into the polymer network. (Ehrenstein & Pongratz 2013 pp. 709-713)

In polymeric materials, the most significant hydrolysis reactions are those of esters and amides but some level of vulnerability exists in almost all polymer chain structures that

contain oxygen bridges. The mechanism for acid catalysed hydrolysis of an ester is presented in figure 1.

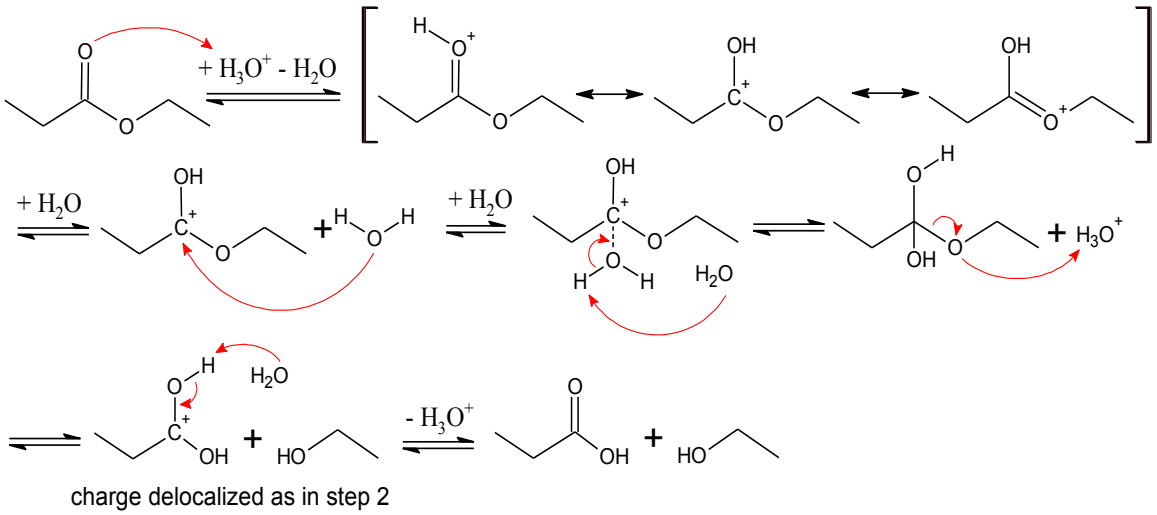

Figure 1. *Acid catalysed hydrolysis of an ester.*

The amount and frequency of these vulnerable points in the polymer structure have a significant contribution to the vulnerability of the material. Other important factors include also the structure dependant catalysis of the reaction by different environments, such as an acidic or basic solution. The spatial configuration of the material can also greatly hinder the access of water to the vulnerable chemical site. (Fried 2003 pp. 271–273, Ehrenstein & Pongratz 2013 pp. 815–816) Of thermosetting polymers, especially unsaturated polyesters (UP) and vinyl esters (VE) are vulnerable to hydrolysis (Gautier et al. 2000).

Most of the effects an aqueous environment has on a solid polymer material are dependent on the diffusion of the solution into the material. The diffusion of water inside a polymer is a complex phenomenon. Defects, such as voids, that can be left over from processing or be created during the ageing enable further and more rapid access of water into the matrix. (Thomason 1995a; 1995b) For pure resin, the diffusion behaviour of water in the polymer network resembles Fick's laws of diffusion. However, despite similarities the diffusion behaviour is rarely true Fickian diffusion. Significant deviations from even this behaviour are also common. These are often referred to as anomalous moisture uptake or anomalous diffusion. Many research groups have studied cases where these types of diffusion are present, so significant amount of literature is available on the subject. (Carter & Kibler 1978; Schutte 1994; Ehrenstein & Pongratz 2013; Pitaressi et al. 2015) As the solvent, for example water, has entered the resin it can cause significant changes in properties. As previously stated water acts as a plasticizer, swelling the polymer network and making relative movement of the polymer chains easier. This causes a lower glass transition temperature and stiffness. The swelling can also cause internal stresses to form in the material as the structure is locally swelled. (Guzman & Brøndsted 2015) Fraga et al. (2003) have however also observed that the swelling, or possible the combination of

swelling and post-curing, can cause defects in the material to become smaller. If present, this phenomenon in turn increases both the glass transition temperature and the stiffness of the material.

What is common for all thermosetting matrices is that the curing reaction never reaches the actual stoichiometric ratio, meaning for example with epoxy (EP) resins that not every possible epoxy and hardener chain end react to form the networked structure. This is caused by the loss of chain mobility at gel point and vitrification. The loss of chain mobility increasingly hinder the ability of the prepolymers and small molecular weight fractions to diffuse and find reactive sites. This effect can be minimized with proper post-curing treatment, in which heat is used to enhance the chain mobility and reactivity, but even then, there are always unreacted sites and whole molecules in the final product. These unreacted resin and curing agent molecules, often called volatiles, plasticize the resin and are usually somewhat soluble to water. Therefore, they are extracted during the swelling caused by an aqueous environment. (Ashbee & Wyatt 1969; Fraga et al. 2003; Visco et al. 2011; Toscano et al. 2016; Wang et al. 2016)

In literature, there is much discussion of the stresses caused by the combination of water and the volatiles, both inside the matrix and at the reinforcement–matrix interface. The potential of swelling or osmotic pressure caused crazing or cracking has been identified for thermosetting polyester and EP resins. For these polyester resins, the most important factor is the osmotic pressure. Osmotic pressure is caused by concentration differences of volatiles, which is balanced by water diffusing to the site of higher concentration (Zumdahl 2009 pp. 867–868). These are largely caused by hydrolysis of the polymer network, with the unreacted prepolymers having only a minor contribution. Because of its better resistance to hydrolysis, vinyl ester resins also show a greater resistance to this kind of cracking behaviour, compared to UP resins. (Gautier et al. 2000; Boinard et al. 2000) In EP resins, hydrolysis on the polymer network is a far lesser factor. Crazing occurs mainly at high water uptake due to uneven crosslink density present in the material. Areas with low crosslinking density can generally swell more as there are less fixed points in the structure. (Apicella & Nicolais 1984; Toscano et al. 2016) This same phenomenon was previously mentioned as causing the formation of internal stresses inside the resin, which is a less severe alternative of the same phenomena. Apicella and Nicolais (1984) also speculated similar crazing at reinforcement interfaces, where curing shrinkage of the resin causes stresses. The effect, this kind of formation of structural defects in the matrix or matrix–reinforcement interface has on the properties of a composite is likely severe. However, especially for EP resins there is much discrepancy in the results of property changes in hygro- and hydrothermally aged EP resins, at least in part caused by the large variation in the chemistry of different resin–curing agent systems (Sugiman et al. 2016).

2.1.2 Thermosetting polyester resins

In order to understand the ageing in thermosetting polyester resins, it is important to understand the chemical structures of the different resin varieties. This enables one to predict the severity of specific ageing phenomena for different resins just from the chemical structure. UP and VE resins are discussed together, as they are processed similarly, used in similar applications and age because of same phenomena. This is because of the similarities in the functional groups responsible for forming crosslinks and the groups most vulnerable to ageing. There are however, significant differences in the respective chemical structures, which is the reason for the differences in their behaviour and why VE resins are not included in UP resins. In terms of ageing, the difference between the two resin groups can be generalized as vinyl ester resins having greater durability in aqueous environments.

UP resins are formed usually by step polymerization reactions of dicarboxylic acids, such as phthalic acids and maleic acid, and glycols to form polyester chains with varying densities of unsaturated sites. Curing is achieved by activation of an unsaturation site, usually with a radical initiator such as a peroxide, which leads to radical polymerization with styrene acting both as a solvent for the resin and as the crosslink former. (Ehrenstein & Pongratz 2013 p. 8) Seawater ageing and analysis of both polyester resin types conducted by Visco and collaborators show a relation between UP resin structure and cured resin free volume. This in turn had a significant effect on water diffusion in the material. As the ageing is largely dependent on the diffusion, the resins with less free volume had better durability despite otherwise similar chemical structure. They also noted that UP curing reactions tend to form quite long polystyrene chains, whereas shorter polystyrene sections are formed with VE resins. (Visco et al. 2008; Visco et al. 2011) In terms of resistance to hydrolysis, one of the key factors is the amount of ester linkages in the structure. In addition, water access to the vulnerable site is important and thus compact structures have greater resistance, both because of slower diffusion and possibly because of the steric hindrance offered by the benzene rings in styrene, if the crosslinking site is close to the ester group in the structure. (Boinard et al. 2000; Visco 2008)

Vinyl ester resins are formed by nucleophilic substitution of unsaturated carboxylic acids to the epoxide groups of an EP resin, resulting in an ester linkage. This is an S_N2 reaction where the “leaving group” is the epoxide oxygen bonded to the carbon at the end of the polymer chain. (Clayden et al. 2001 pp. 411–415) After the substitution, the hydrogen of the hydroxyl group – now bonded to the carbon at the end of the EP structure – is taken by the former epoxide oxygen to balance the charges. Vinyl groups from the unsaturated carboxylic acid are thus at the ends of the VE structure and act as crosslinking sites like the unsaturations in UP resins. Relatively low molecular weight acids are used, so that the crosslinking site is near the ester bond, which also means the benzene ring of the styrene is near the ester bond and thus hinders the access of water to the vulnerable site. Such acid are for example acrylic, methacrylic and cinnamic acid. Methacrylic acid is

often favoured due to the additional steric protection provided by the methyl group. In addition to the steric hindrance, the structure of vinyl ester resins is more resistant to hydrolysis because of the long polymer chain separating each ester linkage. (Boinard et al. 2000; Li 1998)

There is a variety of different resins available for both polyester resin categories. The differences in ageing can however be evaluated by the previously explained factors and knowledge of the chemical structure of the resin. To summarize the advantages offered by vinyl ester resins in aqueous environments are a result of shorter polystyrene chains, which create a structure with limited free volume and provide a steric hindrance for water access to the ester linkage. The polymer chain separating each ester linkage is generally significantly longer in vinyl ester resins. Compared to UP resins, VE resins are however expensive as they are based on epoxy compounds.

2.1.3 Epoxy resins

The structure of EP resins vary greatly between different resins. In general, EP resins are polyfunctional linear or branched organic molecules with the epoxide groups situated at chain ends. Molecular weights are in the range of hundreds of grams per mole. Most EP resins are either bisphenol-A based or novolac resins. The latter results in a more highly crosslinked material due to significant branching, giving the material great thermal and mechanical properties. The material is however also quite brittle. (Ehrenstein & Pongratz 2013; Wang et al. 2016) In addition to the resin, the curing agent also has a significant effect on the final properties of the material. Unlike with polyester resins, the curing reaction on EP resins is a S_N2 nucleophilic substitution reaction, similar to the reaction described earlier to make VE resin from an epoxy. In this case, a suitable polyfunctional curing agent, or "hardener" as they are often called, reacts with the epoxide groups at the resin chain ends, creating an alternating structure of resin and curing agent. Common curing agents include di- and other polyamines and organic acid anhydrides. (Fried 2003 pp. 379–380; Ehrenstein & Pongratz 2013 pp. 8–9) The different chemistry of epoxies make them far less vulnerable to hydrolysis because there are no ester groups in the polymer chains if amine hardeners are used. In bisphenol-A based epoxies there are oxygen linkages in the chain structure but these kind of ether structures are stable against nucleophilic attack. (Clayden et al. 2001 p. 434) However, in epoxies cured with an anhydride curing agent, the addition reaction between the anhydride and the epoxide result in ester groups. (Fried, 2003 pp. 380).

2.1.4 Overview of the ageing of the matrix

To elucidate the differences in the chemical structure of the different resins commonly used, simple prepolymers for an UP, a VE and an EP resin are presented in figure 2. These structures represent some of the simplest structures for each thermosetting resin group.

However, UP resins and EP curing agents are often used as complex mixtures to tailor the processibility and the final properties of the resin.

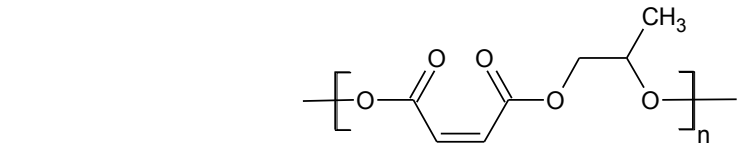

Unsaturated polyester prepolymer from maleic acid and 1,2-propylene glycol

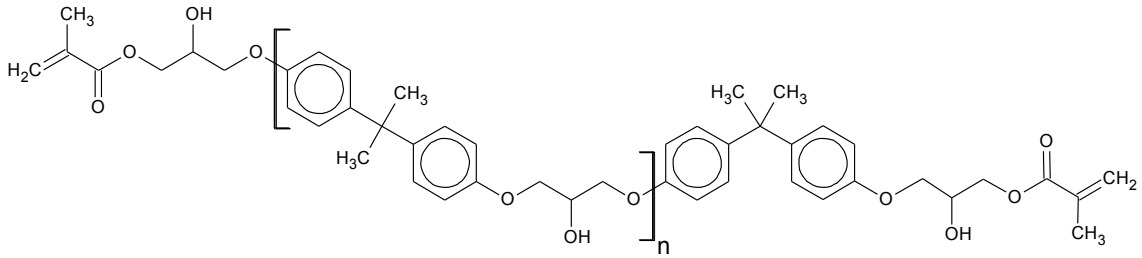

Vinyl ester prepolymer from bisphenol-A epoxy (DGEBA) and methacrylic acid

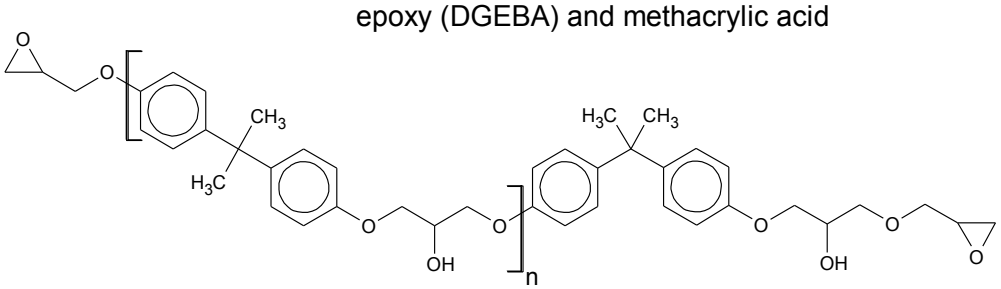

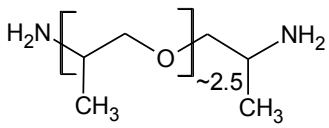

Epoxy resin prepolymers: bisphenol-A epoxy (DGEBA) and poly(oxypropylene) diamine

Figure 2. *Significant, simple prepolymers for UP, VE and EP resins. DGEBA is an abbreviation for diglycidyl ether of bisphenol-A. Based on epoxide equivalent weight data available, the* n *in DGEBA repeating unit is very low. (Li 1998; Epikote 2007; Jeffamine 2007)*

As previously stated UP and VE resins contain a significant volume of styrene, which acts as a comonomer to the compounds depicted in figure 2. To start the crosslinking reaction these resins also require an initiator, which is usually a peroxide, and a catalyst such as cobalt naphthenate solution. These reagents have no significant contribution to the chemical properties of the cured resin. However, they do contribute significantly to the processing of the material.

The importance of each aspect of ageing for a specific resin is determined by the chemical structure of the resin. The amount of free volume and chemically vulnerable sites being among the most important, as they determine the diffusion rate and vulnerability to hydrolysis, respectively. Through the effect it has on the diffusion rate, the free volume in the chemical structure determines the amount of time it takes for notable ageing of the resin to begin, once the resin is subjected to the solution environment. (Boinard et al.

2000; Fraga et al. 2003) Only after the diffusion into the material has advanced sufficiently, do the other factors presented here – possibly excluding hydrolysis on the material surface – become relevant. Once water penetrates the resin, the affected portion exhibits lower stiffness and glass transition due to the plasticizing effect of the water. Vulnerable sites in polyester resins start to break down via hydrolysis. However, without the catalysing effect of the hydronium ions from the acidic environment, the hydrolysis is very slow or even non–existent. Early on, even in acidic environments, it is probable that the hydrolysis is not significant due to the larger size of the acid constituents of the solution. The larger size makes their diffusion into the material slower, so a certain time lag can be expected in the start of any significant hydrolysis inside the material. (Ehrenstein & Pongratz 2013 p. 710)

As the diffusion advances, the structure of the polymer starts to swell. Smaller molecular weight fractions not bonded to the major polymer network, whether they are unreacted resin feedstock or fractions separated by hydrolysis, are mixed with the penetrating solution. The swollen polymer network can allow them to better travel inside the structure, which then enables the volatiles to either leave the structure, or if other factors are favourable as well, find a reacting site. This combination makes the effects of the advance of the ageing hard to predict as the structure can be simultaneously affected by post-curing, hydrolysis, plasticizing effect of the solution and removal of volatiles. From these the first and last two have opposing effects on the properties of the material. (Fraga et al. 2003; Guzman & Brøndsted 2015)

Any defects in the resin, such as bubbles trapped in the material during processing, present a significantly easier path for the solution to access further into the resin. These kind of defects can however be formed in the structure because of the ageing as well. EP resins in particular can cure with very significant differences in the crosslink density in different parts of the material. The swelling of these different regions is then also significantly different, which can result in high internal stresses and in severe cases cracking. Similar effects are also possible for UP and VE resins but their significance is small. In UP and VE resins, defects formed during ageing are more likely the result of pockets high concentration of monomers and oligomers from uncured resin or hydrolysis products. These concentration differences result in increased water diffusion and osmotic pressure between different parts of the resin, which can become high enough to break the structure. The stresses and osmotic pressure required for this type of cracking is however very high and therefore not likely to cause any catastrophic damage to the material. Combined with external stresses however, the situation can be much more severe. (Apicella & Nicolais 1984; Gautier et al. 2000; Boinard et al. 2000; Toscano et al. 2016)

2.2 Glass structure and ageing

In all composite materials, one of the important roles of the matrix is to protect the reinforcement material from the environment. However, with commonly used thermosetting matrix materials the access of water and other media to the reinforcement is always an issue. As previously discussed, slow but inevitable diffusion of water through the matrix – depending on the properties of the resin – will eventually happen with all thermosetting resins. This process will also reach the matrix–reinforcement interface, enabling interaction of the environment with the reinforcement fibres. (Ehrenstein & Pongratz 2013 pp.709-713)

Most significant of the effects water has on glass fibres is the depletion of metal ions, namely calcium and aluminium but also others, from the glass structure. This type of corrosion is generally caused by acidic, and to a lesser extent basic media, but also even by water due to the presence H_3O^+ ions. The process starts with diffusion of the media inside the glass. The penetration depth of the media into the glass fibre is one of the factors of interest when examining the resistance of the material to the corroding media. (Qiu & Kumosa 1996) When the media is not acidic, for example water, the process is controlled more by interfacial properties than diffusion. This is based on the observed kinetics being linear for such cases (Ehrenstein & Pongratz 2013, p. 703). This also means that the penetration depth is not very deep. In a study by Qiu and Kumosa (1996), it was observed that the acidic nature of the corroding media is however not the only crucial factor when determining its effectiveness in corroding the glass fibres. In the study four different acid solutions, namely hydrochloric, nitric, sulphuric and oxalic acids were used. Some trend in relation to pH of the aqueous acid solution was noted but a more significant difference was observed between sulphuric and oxalic acids and hydrochloric and nitric acids. The latter two caused relatively low weight loss even at low pH, whereas sulphuric and oxalic acids caused significant weight loss. This phenomenon has been attributed to the formation precipitates and complexes by the conjugates of the acids and the metal ions removed from the glass structure and replaced by hydrogen. The process could be something along the mechanism presented in figure 3. (Qiu & Kumosa 1996)

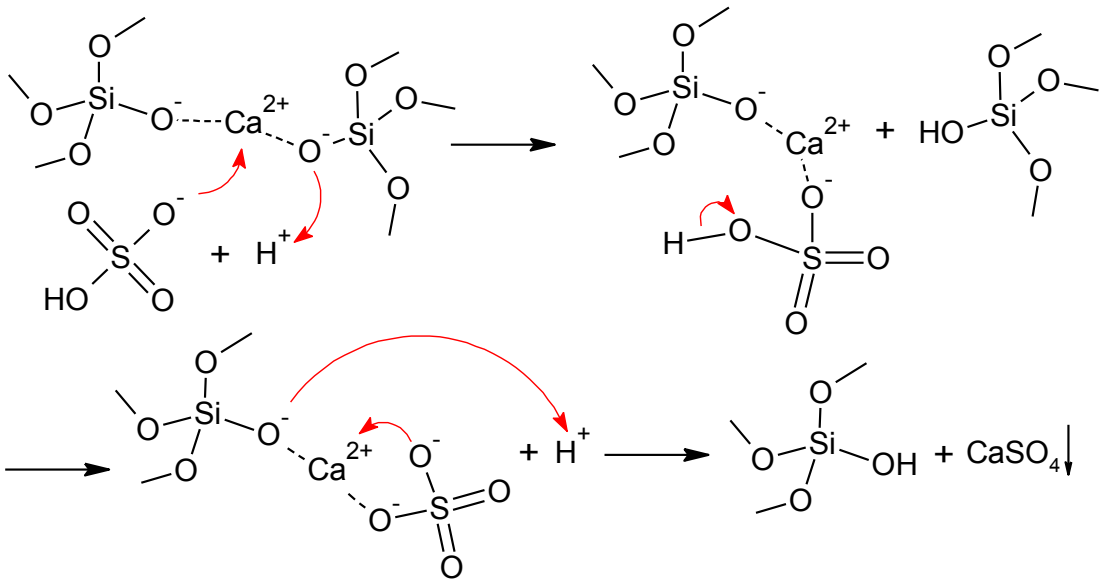

Figure 3. *A possible mechanism of leaching enhanced by the anions of sulphuric acid. Unmarked bonds indicate continuation of the glass network.*

It can be expected that, as presented in figure 3, the effectiveness of leaching is also related to the dissociation of the second hydrogen from sulphuric acid. This is true whether it actually is the HSO_4^- or the SO_4^{2-} that is most responsible for this leaching behaviour. Figure 3 was created with the assumption, that in a process leading to a change in pH, the feedstock that causes less change would have preference. Regardless of which sulphuric acid conjugate has preference, it is of interest to examine the changes in sulphuric acid behaviour with concentration and temperature. Sulphuric acid solution as an environment has some unique properties, as it is the only common acid with a strong initial dissociation and a weak secondary dissociation step. This causes complex behaviour in the composition and pH of the solution with different concentrations and temperatures. In broad terms, increase in both temperature and concentration leads to higher relative HSO_4^{2-} fraction. However, increasing the concentration still leads to an increase in the concentration of all sulphuric acid constituents.

As the process of glass "leaching" is somewhat limited in the metals and structures it targets, or at least clear preferences can be observed, the chemical composition of the glass determines the vulnerability of the material. Generalized composition ranges for some glass fibre grades, as presented in Wallenberger et al. (2001) are collected in table 1. It should however be noted that these values vary significantly according to the manufacturer and literary reference in question and therefore are presented purely for demonstrative purposes.

Table 1. *Glass fibre compositions. Glass types are: E – aluminoborosilicate glass, ECR – boron free E–glass modification, S/R – High tensile strength and modulus glass (Wallenberger et al. 2001)*

	E [%]	**Boron–free E [%]**	**ECR [%]**	**S or R [%]**
SiO_2	52–56	59 / 60.1	58.2	60–65.5
CaO	21–23	22.6 / 22.1	21.7	0–9
Al_2O_3	12–15	12.1 / 13.2	11.6	23–25
MgO	0.4–4	3.4 / 3.1	2	6–11
B_2O_3	4–6	-	-	-
TiO_2	0.2–0.5	1.5 / 0.5	2.5	-
Na_2O	0–1	0.9 / 0.6	1.0	0–0.1
K_2O	-	- / 0.2	0.2	-
Fe_2O	0.2–0.4	0.2 / 0.2	0.1	0–0.1
Others	0.2–0.7	- / 0.1	2.9	0–1

In the proposed reaction of metal ion leaching, components presented most vulnerable to it in acidic environments are calcium and aluminium, yet when compared to E-glass the grade considered more resistant, ECR-glass has comparable and possibly even higher portions of aluminium and calcium oxide (Qiu & Kumosa 1996). The difference in degradation behaviour is attributed to the structure not including boron. While boron is also a constituent vulnerable to leaching, in many cases it is reported as being extracted slowly, and so the difference in chemical durability between the two glass grades is not so straightforward. (Ehrenstein & Pongratz 2013 pp. 703)

A more detailed examination of the problem is presented for example in the works of Jones (2006a; 2006b; Jones & Stewart 2010), who has examined the kinetics of the corrosion of E-glass fibres in different acidic environments. His research indicates that the corrosion of glass fibres in acidic environments is complex and depends greatly on the constituents of both the glass and the acid. In fact, the results presented by Jones indicate that the use of boron free ECR-glass as a universal solution for greater resistance against acidic environments is could be somewhat misguided. The leaching of boron is a major factor in the corrosion of E-glass in organic acids, especially in oxalic acid. However, its contribution to the corrosion by many other acids, for example sulphuric acid is presented as insignificant. The leaching of aluminium and calcium by sulphuric acid is however significant, causing the glass to corrode quickly. The weakness of E glass compared to ECR is not well explained, as the major difference is the lack of boron in ECR. Jones also noted that the ion interactions make the effect of pH more complicated. For example in the case of E-glass fibre corrosion by oxalic acid, he noted a maximum point when comparing the corrosion of the fibre to the pH of the acid solution. As an explanation he offered that at low hydrogen ion concentrations, meaning relatively high

pH, the ion exchange is not as favoured and proceed slowly, as can be easily expected. At very low pH the effectiveness of the corrosion can however be hindered by anions binding to metal cations on the glass surface, but the actual process is not entirely understood. (Jones 2006b) For example, no explanation was offered on what differentiates the complexes that facilitate the leaching from complexes that stay bound to the glass phase and hinder the corrosion.

The leaching of the metal ions, which as discussed above is determined by the acid and glass compositions, determines how the corrosion of the glass fibre propagates. A significant part of this is also the actual chemical structure of the glass. Accurate analysis of the glass structure is a complex field, with many problems relating to the interpretation of results from analysis and the verification of the proposed structural models. (Shelby 2005 p. 80) In the book by Shelby (2005 pp. 81–92), structural models for silicate glasses and their modifications including aluminosilicate glasses are discussed. Based on the presented guidelines a schemactic presentation of the structure of ECR-glass was constructed with the purpose of providing visual aid in understanding the "weak points" caused by the leached metals in the glass structure. This is presented in figure 4.

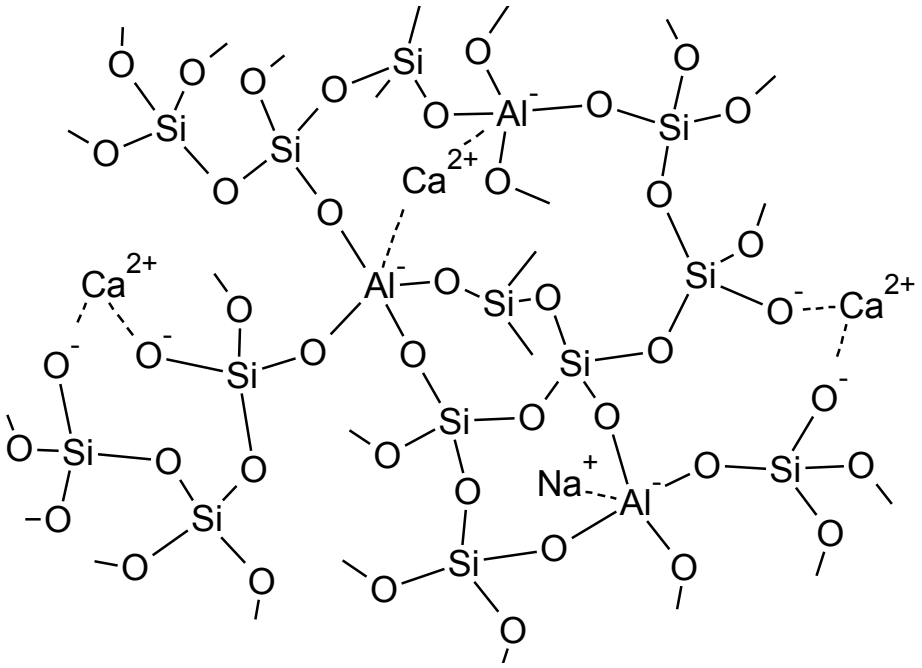

Figure 4. *Schematic presentation of the structure of ECR-glass, based on Zachariasen's rules (Shelby 2005) and NMR studies on the bonding of aluminium in glass. (Du & Stebbins 2005; Neuville et al. 2007) Effort has been made to match the ratios of the constituents to those presented in table 1.*

Despite which ions are exchanged to hydrogen, this causes stresses to form in the structure. The stresses are caused by the smaller volume of hydrogen, compared to the replaced ion. In fibres that are in solution environments, hydrogen bonded water alleviates the problem, but drying often removes such water from the structure. Network modifiers like calcium are quite easily extracted by the corroding media. (Qiu & Kumosa 1996;

Jones & Stewart 2010) If network formers – such as boron or aluminium – are also extracted due to the corrosion, the resulting strength loss and penetration depth of the corrosion in the fibres is often more significant. The depth and severity of the corrosion can be visually inspected by extraction of the fibres from the corroding environment followed by washing and drying. The stress caused by the shrinkage, combined with the residual stresses from the fibre manufacture, can lead to the formation of cracks on the glass fibre surface. These cracks have been categorized as either spiral or axial cracks. Spiral cracks are formed in the cases where the penetration depth of the corrosion is rather small, while axial cracks form in the more severe cases. It should be noted, that excluding significant corrosion, these two crack types are not simultaneously observed because the cracks form during the drying of the fibres and therefore correspond to the corrosion as a whole, rather than being a continuous process during the exposure. In cases of severe corrosion, the axial cracking alone is insufficient to relieve the stresses caused by the shrinkage and as a result, the fibre surface cracks in radial directions as well. (Ehrenstein & Pongratz 2013; Qiu & Kumosa 1996; Li et al. 2013)

Even the previously presented results do not appreciate all the relevant factors. In the work of Li et al. (2013), evaluation has been done on the behaviour of the glasses with varying boron contents. Their work also considered the alteration of the glass structure, depending on whether or not there is boron incorporated in the glass structure. Based on the findings, they offered a theory on the difference in corrosion between boron–free and boron containing glass, analogous to ECR and E glass. They suggested that because boron and aluminium function as similar constituents, and because the stabilization of $[AlO_4]^-$ and $[BO_4]^-$ structures via Ca^{2+} ions is likely created by linking two of these structures with Ca^{2+} associated NBOs (non–bridging oxygen), there is actually nanometre scale phase separation present in E-glass. An example of this can also be seen in the ECR structure presentation in figure 4. However, one could easily argue whether or not this can be considered phase separation. Another possible and a more severe case, this could be understood as, is a structure presented in figure 5.

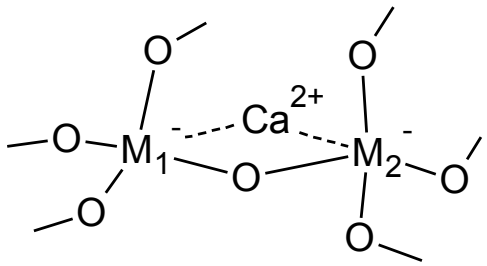

Figure 5. *Two charged network-forming structures bonded together with an oxygen bridge. M_1 and M_2 can be either Al or B in E-glass. The presence of such a structure is hypothetical and unconfirmed.*

These aluminium and boron rich zones act as sites for the acid to leach, resulting in destabilization and eventually severe corrosion of the glass. This however fails to account for the results indicating no significant leaching of boron for E-glass fibres. The materials

reported in the study also had higher Al_2O_3 and CaO and lower SiO_2 fractions, along with increased boron content, which considering the previously presented results could account for at least a part of the higher corrosion rate. Li et al. (2013) also proposed that the corrosion of boron–free glass is determined by the corrosion of the silica network, which is in other studies likely considered an unaffected portion of the glass, based on it being rarely even mentioned. It is however evident that the structures of E and other glass grades are very complex and simultaneously critical in understanding the corrosion of glass fibres.

Further insight to the chemical structure of glass fibres can be found from a multitude of magic angle spinning (MAS NMR) and quantum magic angle spinning NMR (QMAS NMR) studies conducted with the aim of discerning the preferred positioning and bonding of the glass constituents. (Du & Stebbins 2005; Kiczenski et al. 2005; Neuville et al. 2006; Angeli et al. 2007; Wu & Stebbins 2009) According to the study by Du and Stebbins (2005), the relative positioning of boron and aluminium in glasses similar to E glass depend significantly on the network modifying cation. Alkaline cations, namely Na^+ and K^+ cause the structure to follow an avoidance principle with B–O–M and Al–O–M type bonding, where M is 4-coordinated boron or aluminium. This is quite easily explained by the fact that such structures cause a significant localized negative charge build, which is not easily balanced by a +1 cation. Alkaline-earth cations, mainly Ca^{2+}, which is known to be abundant in E-glass, can more easily balance the negative charge of such structures due to its high charge and small size. This causes a more random distribution, as the structures like the one presented in figure 5 become a valid option alongside other possible structures.

In the work by Angeli et al. (2006) – discussed in more detail below – an effort was made on determining whether it is sodium (Na^+) or calcium (Ca^{2+}) that more readily balances the negative overall charge of the $[AlO_4]^-$ tetrahedra. They concluded, that when present, sodium is preferred as the one that balances the $[AlO_4]^-$ in pristine glass but is readily leached and replaced by calcium as a charge compensator. A more accurate presentation of the situation is actually that the higher field strength calcium prefers to coordinate with NBOs instead of stabilizing the four-coordinated aluminium or boron when the composition enables NBOs to be formed (Wu & Stebbins 2008). This is easily explained by the free electron pairs of the NBOs.

Some studies also examine specifically the structures of leached glass with NMR methods. Angeli et al. (2006) conducted leaching with acidic and basic solutions on glass powders from high boron content silicate glasses. Their characterization of the “gel” layer formed on the glass surface, analogous to the previously mentioned shell of the core–shell observed with glass fibres, clearly shows the formation of an almost purely silica based layer on the glass in after immersion in nitric acid. In basic solutions however, all oxides excluding boron are observed in the gel layer with the relative portions varying on the initial glass composition. One of the aspects of this result one must consider is what it

indicates in terms of the results presented by Jones & Stewart (2010), where uncertainty could be expected on whether the boron concentration of the solution properly represents the amount of leached boron. Considering the difference in acid between these two results, some uncertainty remains, but at least in nitric acid almost all of the leached boron ends up in the solution along with the aluminium, sodium and calcium. In other studies results are however presented that, indicate the possibility of boron precipitates, which cause errors in terms of boron observed in the solution (Scheetz et al. 1985). Another aspect of glass leaching in aqueous environments presented in literature was silica network "repolymerization" and how the initial glass structure affects this process during the leaching. Especially with acid leached glasses, the NMR results show a shift in the Si spectra from Q^2 and Q^3 species towards significantly increased Q^4 population. In the structure, this means that the amount of silicon connected to two or one non–bonding oxygen is lesser for the leached glass "gel" structure. The mechanism of this repolymerization is explained as a condensation reaction between silanol groups created as protons from the solution attach to NBOs. This is supported by the result that the repolymerization appears to be more significant for glasses with initially more NBOs. (Angeli et al. 2006) Figure 6 presents a visual presentation of the silica repolymerization process.

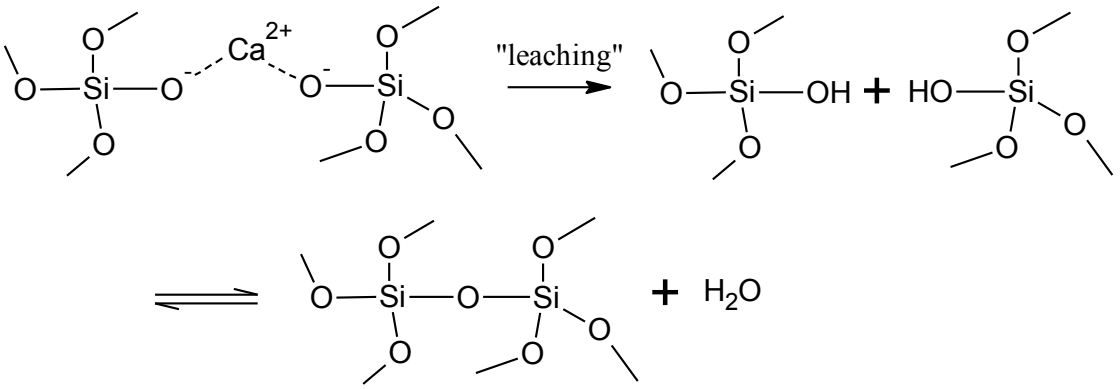

Figure 6. *Silica network repolymerization in an aqueous environment.*

Ignatyev et al. (2003) have also observed such silanol condensation reactions taking place. Their observations include an important intermediate in which a water molecule is hydrogen bonded to both hydroxyl groups, indicating such reaction is unlikely to take place without the presence of water. These results, along with other literature on the leaching behaviour of borosilicate glasses, offer a possible explanation for the end of the corrosion propagation in glasses. When an equilibrium between the hydrolysis and condensation of the oxygen linkages between network formers in the glass structure is reached, if no other propagation pathways – such as leachable cations or changed network formers – are found the corrosion stops. The chemical structure of the pristine glass and the acid in question, considering the significant literature on the subject, appear to determine both the point in which this equilibrium is achieved and the rate at which it is achieved. (Angeli et al. 2006; Jégou et al. 2000; Ledieu et al. 2004). Unfortunately, the

overview of the subject is still not well defined and different studies offer some conflicting results on the subject.

Based on these literature findings a following mechanism is hypothesized to prevail in the ageing of glass fibres in aqueous environments. Initially small molecules and ions present in the solution reach the glass surface. This effect can be expected to be significant when there is a polymer matrix present hindering the diffusion of larger compounds more significantly than smaller ones. These small solution particles are most likely water and hydrogen or more accurately hydronium ions. Initial interactions include reactions of NBOs to create silanol groups, releasing the metal ion and some hydrolysis of the silica network. In very resistant glass grades, one could predict that the "repolymerization" of the silica network can also begin significantly and thus the reaction could largely be limited to this, if no other relevant, solution particles arrive to the glass surface later on.

In an acidic environment it can however be expected that after some diffusion rate dependent time, also the conjugate ions of the acid arrive at the glass surface and begin to interact more strongly with the metal ions in the glass structure. Depending on the composition of the glass there can be significant degradation when calcium or sodium stabilizing four-coordinated complexes are leached, severity depending naturally of the structural part in question. When two oxygen linked four-coordinated groups are destabilized and subsequently leached from the structure the size of the network portion lost is significant, which can be expected to facilitate greater penetration of the solution to the glass in the form of pores of a significant size. Other options for the phase separation-like structures likely also cause similar weakness. Based on this type of mechanism the stability of the glass is determined by the size and number of the acid vulnerable sections in the network and the amount of NBOs facilitating more effective network self-repair. The results where boron was not found in the solution after the leaching could be a result the gel layer restructuring as a borosilicate network and/or precipitation of the boron compounds on the fibre surface.

2.3 Ageing of the interphase

The aging of the fibre–matrix interface is one of the greatest questions still without adequate explanation in the subject of composite ageing. The interface/interphase region is generally considered as the most important factor in the final properties of PMC, as it is responsible for transferring the loads from the matrix to the fibres. (Ashbee & Wyatt 1969) The contribution on the sizing in this regard is significant. (Johansson et al. 1967; Reilly & Thomason 2010) In this chapter, special attention is given to the broader aspects and the chemistry of the silanes acting as coupling agents in the interface. Because the sizing recipes are often proprietary information, not readily available outside the companies that make them, and the broad field of research they present, the specifics of sizing recipes and their effect on the overall ageing of the composites are however excluded from this work.

2.3.1 Sizing

The composition of the sizing in commercial glass fibres is very complex. Major constituents include for example water, UP or EP resin, starch and other ingredients acting as film formers, antistatic and antifoaming agents and processing aids for the fibre manufacture. (Thomason 1995c; Reilly & Thomason 2010; Dey et al. 2014) It has also been shown that also these ingredients, especially the film formers, have a significant effect on the resulting interfacial properties of the glass fibre in a composite (Dey et al. 2014). More research in this field is still required to understand the properties and ageing of the interface/interphase created by the complex sizing formulations commonly used in the industry. Significant knowledge of the matter exists in glass fibre companies, but is often proprietary information and therefore mostly unavailable.

Sizings are also used with most other fibrous reinforcements with differences related to their compatibility with the fibre itself. (Rudzinski et al. 2011) The effectiveness of silanes as coupling agents between glass fibres and the polymer matrix are a result of ability of silicon to form stable dual reactive compounds quite easily. Dual reactivity in this instance means that the compound is capable of reactions with organic and inorganic substances simultaneously. (Pape 2017) To elaborate how this is achieved, the structures of a few commonly used silanes are presented in figure 7.

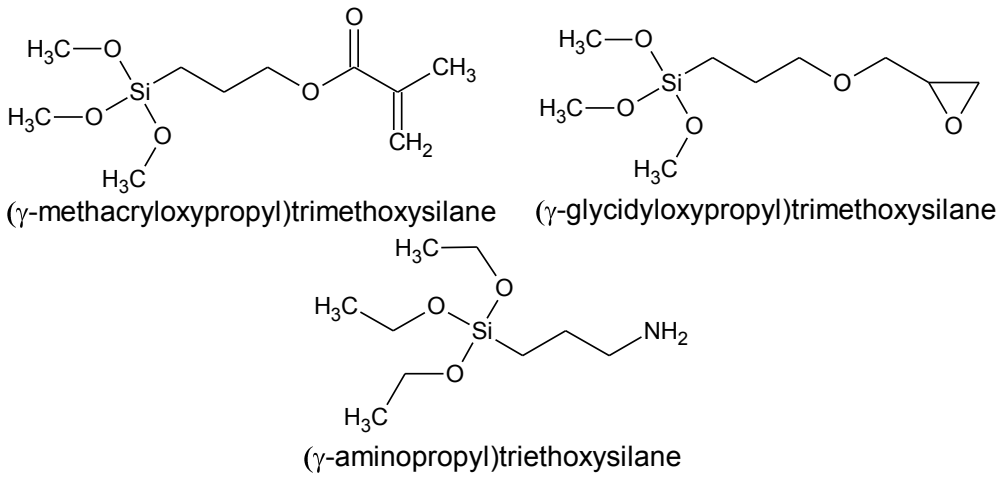

Figure 7. *Structures of commonly used silanes, in glass fibre sizing formulations. Based on (Reilly & Thomason 2010)*

These silanes belong to the category called organosilanes because of the Si–C bond linking the silicon and the organic chain portion of the silane. In these, like in practically every other case as well, the organic chain and its functional groups bind the silane to the organic matrix. The bonding to glass fibres is achieved when the water present in the sizing hydrolyses the alkoxy groups. This leads to the formation of silanol groups that are capable of the same condensation reaction described previously in chapter 2.2 and can therefore bond to the glass surface. The reaction is an equilibrium reaction, meaning not all the silanol groups are reacted to form covalent bonds between the silane and the glass.

(Pape 2017) These unreacted silanols coordinate via hydrogen bonding, holding the sizing in place. This could be one of the factors causing the often-observed aging behaviour of the sizing. It has been reported that the loss of the "physisorbed" portion of the silane is one of the major factors in the aging of the sizing (Plonka et al. 2004). The contribution of the sizing to the overall ageing in fibre–reinforced composites, especially in the interfacial region, cannot be excluded since the chemistry of the interface region is determined by the chemistry of the sizing. The sizing also improves the glass fibre properties by filling small surface flaws created in processing. (Schutte 1994; Reilly & Thomason 2010; Pape 2017)

2.3.2 Interphase structure and ageing

In a review article of glass fibre composite aging, focused on the effects on silane coupling agents to the ageing of composites, Schutte (1994) offered a view of the interphase region as a three-phased structure consisting of a monolayer and layers of chemi- and physisorped silane. This nomenclature will be used in this section for the sake of simplicity, even though there is doubt on the validity of these names. The layers can be characterized by a decreasing level of chemical bonding and structural order. The mono-, or at least a very thin, only a couple of silane molecules thick layer, formed on the glass surface is almost fully chemically bonded with the glass, and probably to a significant degree to neighbouring silanes via Si–O–Si bonds. On top of this layer, there are silane molecules with a high number of chemical linkages and when possible, hydrogen bonding binding them together to form an organized structure that is also bonded to the previous layer to some extent. Schutte called this the chemisorped layer. On top of this chemisorped layer is the physisorped layer consisting mainly of silanes held in place by weaker interactions and some chemical linkages to neighbouring silanes. The two sorped layers are most distinguishable by their ease of removal. For the outer layer even washing in cold water is sufficient to remove the layer, whereas the chemisorped layer requires boiling water or similar more aggressive environment. This structural model has been evidenced with multiple experimental methods, for example radio labelled traces from which the thicknesses of the layers of (γ-aminopropyl)triethoxysilane (γ-APS) on a borosilicate glass were determined as approximately 1, 10 and 270 monolayer equivalents. (Schutte 1994; Schrader 1974)

Using radioactive tracer techniques, Johansson et al. (1967) studied the nature of silane coupling agent bonding on both the glass fibre and the resin. One of the significant findings made was that the sizing treatment affected the nature of the silane–resin interaction significantly. Retention of resin bonded to silane films that were dried after adsorption from an aqueous solution, showed a notable dependence on the silane film thickness in tetrahydrofuran extraction of the resin. However, coupling agent films cured with refluxing tetrahydrofuran extraction at 65 °C showed no similar dependence. The first of these was attributed to the swelling of the silane film by the resin, resulting in both

chemical bonding and mechanical interlocking via chain entanglement. On the latter case, no such swelling happens. It is however unclear, whether the reason is increased crosslinking in the silane film or removal of some of the sorped silane layers. This oversight is likely at least partly because the layered structure had not yet been identified. The resins used in the study were ^{14}C-traced equivalents of the three silanes presented in figure 7; (γ-aminopropyl)triethoxysilane, (γ-glycidyloxypropyl)trimethoxysilane and (γ-methacryloxypropyl)trimethoxysilane. Interestingly, Johansson et al. identified the environmental attack on the E-glass surface as a major reason for silane coating removal in boiling water.

The ageing of the interface or interphase in glass fibre reinforced composites appears, similarly to that of the matrix, to be a combination of physical and chemical processes effecting in the interphase region. The optimal interphase region is sometimes described as one, where on top of the chemically bonded monolayer of silanes there is an interpenetrating network of crosslinked silanes and matrix resin, with some chemical bonding between these two as well (Pape 2017; Schutte 1994; Johansson et al. 1967). Once water and possible other reagents reach the interphase region, hydrolysis on both the glass surface and in the resin can begin. As previously stated the hydrolysis of the glass surface eventually leads to the detachment of the silane coupling agent from the glass surface. Resin hydrolysis especially with UP and VE resins also contribute to the interphase degradation directly via the loss of the interpenetrating network and indirectly if water-soluble low molecular weight products are created that lead to the generation of osmotic pressure at the interphase. (Ashbee & Wyatt 1969; Boinard et al. 2000) Hydrolysis of the silane crosslinks can also be expected, at least in higher solution temperatures, leading to further loss of the interpenetrating network between the coupling agent film and the resin (Schutte 1994). Water can easily interact with the hydrogen bonds, which also makes the silane layers less stable.

2.3.3 Overview of the ageing of the composite

Much like the composite itself, the ageing in a PMC is more than the sum of its parts. The ageing of the resin, the fibre reinforcement and the interphase region, largely determined by the surface treatment of the fibres each have distinctive phenomena related to the chemical and physical interactions with the ageing environment. Research done over several decades has elucidated many of these phenomena and their correlation with the chemistry of the materials is well known. However, there are still many aspects of the ageing of a composite as a whole, which are still not fully understood. These are mostly related to the effects the products of chemical ageing in different components of the resin have on the others. (Sethi & Ray 2015) This is unsurprising, as these phenomena take place inside – and are very hard to duplicate outside – the actual composite. This field of study will likely be one of the major upcoming challenges for the composite industry, but a successful approach would prove valuable to the industry as a whole.

The protective effect the matrix has on the reinforcement fibres, as a hindrance through which the solution environment has to travel to access the fibre was discussed earlier in chapter 2.2. The role of the interphase region in this is not straightforward, but it is safe to assume it cannot be ignored. The swelling of the matrix, the interaction of the solution with the silane and the volatiles and leaching products travelling to and from the interphase region are all relevant factors when determining the loss of properties at the interface and by extension in the composite as a whole. This combined with the plasticizing and possible chemical degradation of the matrix and the corrosion of the fibre reinforcement means that the properties of a composite, unsuited for a specific environment, can degrade significantly. Even in materials, which resist these environments the effects of the ageing should be noted and corresponding protective measures taken in the manufacture of the composite part. (Myers et al. 2007)

3. MATERIALS AND METHODS

This chapter describes the selected materials and experimental methods used in the practical part of the work. The materials were selected with the aim of being relevant yet with as simple chemical structures as possible. This makes determination of chemical changes easier, as the changes are not directly observable. Even with these relatively simple materials, for example the characteristic vibrations of many structural groups in the resin infrared spectra overlap, making accurate evaluation difficult.

3.1 Materials

The materials chosen for this study represent the common chemical structures of thermosetting matrices used in the composite industry, when increased chemical resistance is required. Derakane 441-400 epoxy vinyl ester resin – provided by Ashland Finland – represents the polyester resins. It is often used in the manufacture of large chemical containers and reaction vessels, due to a combination of good chemical stability, mechanical properties and favourable processing conditions. Derakane 441-400 is a polyester created by a step polymerization reaction of bisphenol-A diglycidyl ether and a methacrylic acid. This structure is presented in figure 2 in the previous chapter. The styrene content of 441 is relatively low, 33%, which acts as a comonomer for the crosslinking reaction. The chain growth reaction is initiated with methyl ethyl ketone peroxide (MEKP). A 6% cobalt naphthenate solution is used as an accelerator.

A comparative simple epoxy resin – EPON 828 a bisphenol-A diglycidyl ether – was used. The resin was chosen because it is commonly featured in articles of similar subject making comparison to results found in literature easier. To keep the chemistry of the resin as simple as possible a simple amine curing agent Jeffamine D-230, a polyether diamine kindly supplied by Huntsman, was used creating a simple two component system whereas many commercial epoxy resins use mixtures of several amines to tailor the properties of the resin.

The glass fibre grades used in this work are Ahlstrom R338 and Jushi E6CR17. These glass fibres represent modern compositional ranges for E and ECR glass fibres, which are the most common glass fibre variants because of their relatively cheap price and good mechanical and insulation properties. The most significant difference between the two glass types is that boron free ECR type glasses generally exhibit greater resistance to ageing in aqueous environments. The Ahlstrom R338 and Jushi E6CR17 fibres are referred to as E- and ECR-glass, respectively, in short. The full names of the grades are also used where deemed necessary for clarity.

3.2 Microbond sample preparation

The sample preparation method, for the FIBRObond device, has been filed for an international patent under the patent application: A method and a device for forming a droplet or droplets on a fibre, PCT/FI2017/050431, which was filed on the 9th of June 2017. The method was used to create the microbond samples used in this work and its applicability for several resin options was tested.

When suitable curing procedure and reagent ratios are followed, careful mechanical mixing is should be sufficient for homogeneous resin material formation with these kind of resins. Significant problems were however noted during microdroplet sample manufacture with the picolitre scale volumes, which resulted in poor curing of the resins. Based on the observations made on the behaviour of the 441 resin, and on previous work presented on microdroplet testing of a similar Derakane 441-45 resin, the cause of the problem was identified as vaporization of the styrene from the resin droplets (Dirand et al. 1996). The vapour pressure of styrene in standard conditions is 0.81 kPa and can be expected to be even higher in the very small volume droplets, created on the glass fibre surface (Haynes 2017). This effect was counteracted by placing the droplet sample holders in a high styrene content atmosphere, such as a closed container, which contains the 441 resin left over from the batch. Droplets created without this modification did not cure even with excessive post-cure treatments, apparently because the styrene content was insufficient for proper curing. The result are droplets that exhibit waxy plastic deformation when an effort was made to test the samples.

Similar problems arose with the Epon 828 epoxy resin cured with Jeffamine D-230, but because of altogether different reasons. Since the mixture contained no substances with significant vapour pressures, the similar vaporization can be excluded as an explanation. Instead based on the observations made during droplet sample manufacture – where a resin droplet travelled along the fibre surface with no apparent force moving it, for relatively long distances before finally stopping – the expected reason for incomplete curing of the resin was likely phase separation of the resin and the curing agent during the droplet manufacture. This explanation is supported by two separate observations. A somewhat similar combination of Araldite 5052 resin cured with the standard 5052 hardener, which is a mixture of several terminal polyamines and has a significantly higher viscosity than Jeffamine D-230, did not exhibit this issue. This was speculated to be, because of the significantly lesser difference in the viscosity of the resin and the hardener compared to the Epon 828–Jeffamine D-230 combination. The other supporting observation was made when the curing of the Epon 828–Jeffamine D-230 combination was allowed to slowly advance until significant rise in viscosity is observed. The droplet samples made from these batches cured to a glassy state and exhibited sufficient mechanical properties to enable the microdroplet testing. The suggested explanation is that phase separation in this sample is no longer possible, as significant covalent bonding exists between the resin and the amine oligomers.

Other possible, albeit more unlikely explanation for the insufficient curing of the EP resin is atmospheric moisture interacting with the resin system, which hinders the crosslinking reaction. Allowing the cure reaction to advance in a closed container could prevent some of this interaction, as it is likely limited to the surface of the large resin volume, leaving most of the batch unaffected. The idea of such interaction is a result of previous observations of a “leathery” skin formed in some epoxy samples cured in open moulds. There are however no other significant observations supporting this behaviour. These problems in the curing of small resin volumes warrant further study, both for their significance in terms of the viability of the FIBRObond method and because such behaviour has not been widely reported and could reveal interesting information about the curing reactions themselves.

3.3 Ageing conditions

Sulphuric acid solution is one common environment, when composite reactor vessels are concerned. It is also of interest to understand the contribution of the water in such environments. In many cases, most of the effects of such environments have on the composite properties are attributed to the strongly acidic nature of the solution, but as shown by many of the results presented in chapter 2, water also has contributes in the degradation of composite properties. This makes the prediction of accelerated ageing environments difficult, which is one of the reasons why the conditions used in this work are similar to the environments the materials are subjected to in actual applications.

3.3.1 Vinyl ester samples

For the resin samples, the ageing times used ageing times are long, as the advance of ageing is controlled by diffusion of solution constituents into the material. The ageing is however done by full immersion of the test specimen and without protective layers, often used in composite structures from which environmental resistance is required. This way the diffusion can occur from all surfaces simultaneously and the ageing begins immediately after sample immersion. The protective layers mentioned previously are, however, often from the same resin as the composite itself. The protection of the actual structural composite is thus achieved by providing a layer of the matrix, through which the solution environment must diffuse. The ageing tests conducted therefore also provide information of the diffusion speed through this kind of protective layer.

Due to safety concerns and overall time requirements of the sulphuric acid environments used in this work, most of the ageing involved in this work were done at Outotec Research Center in Pori, Finland. To examine the behaviour of the resin, relatively large sheets with dimensions roughly 10 × 10 cm were made from the Derakane 441-400 resin. The effect of three solutions were tested: deionized water and sulphuric acid solutions with 50 and 500 grams of sulphuric acid per litre of solution (50 and 500 g/dm^3). The solutions were

held at a constant temperature of 95 °C during the testing. Seven sheets, in three different thicknesses were made, with identical curing procedure. Recommendations given by the resin supplier were followed to ensure sufficient curing of the resin. Before exposure, the resin samples were weighed carefully in order to examine the weight change in the samples during exposure. For comparative purposes a single 3 millimetres thick 5 × 10 cm sheet was made accordingly to the "clear casting" procedure given in the Derakane technical datasheet to provide a reference sample for DMTA and FTIR measurements of the aged sheets (Derakane® 2009).

The resin samples were distributed and immersed in the solutions so that there is one "thin" and one "thick" sheet in each solution. Additionally, one sheet of an intermediate thickness was exposed to the more dilute sulphuric acid solution. Thicknesses of the sheets were controlled by using similar resin weights. The resulting sample thicknesses are roughly three, four and five millimetres. An overview chart of the solutions and vinyl ester samples is presented in table 2.

Table 2. *Ageing environments and initial sample weights for the vinyl resin sheets.*

Approximate sample thickness [mm]	Deionized water [g]	50 g/dm^3 sulphuric acid solution [g]	500 g/dm^3 sulphuric acid solution [g]
3	31.6243	33.0034	34.3283
4	–	48.3572	–
5	62.01	74.004	64.849

The ageing was carried out for a period of 1008 hours or 42 days. The weight of the samples was examined at specific intervals to examine the diffusion of the solution into the resin sheets. The weighing intervals are short at first, in order to view the early fast diffusion accurately. Then as the material is expected to reach equilibrium-like behaviour, the time between each weighing was gradually increased. This assumes a diffusion behaviour that at least resembles Fick's law, which is often the case. At each weighing, the samples are rinsed clean of the ageing solution and then dried from the surface so that only the solution inside the material contributes to the weight change.

3.3.2 Glass fibres

Bundles of glass fibres from both Jushi E6CR and Ahlstrom R338 grades were immersed in deionized water, sulphuric acid solution with a pH of 2 and a sulphuric acid solution with 50 grams of acid per litre of solution (50 g/dm^3). The ageing was done both at room temperature and at 95 °C, but the room temperature ageing was mostly done to observe differences in leached species in the ICP-MS examination and therefore only one fibre bundle per environment was used. The pH 2 sulphuric acid solutions used correspond to 0.59–1.46 g/dm^3 solutions. The exact concentration varies due to the pH of the deionized water, which is between 5.5 and 6.26 in the glass fibre ageing tests. For simplicity, the pH 2 sulphuric acid environment will be marked as a 1 g/dm^3 sulphuric acid solution, so

comparison to the other sulphuric acid environments is easier. The difference in environments compared to the resin sheet ageing environments is because of the expected poor resistance of the unprotected glass fibres to the acid solution. Also, in the actual composite applications the diffusion of H_3O^+ and conjugate base species is expected to be slower than that of water molecules, which likely causes lower sulphuric acid concentrations near the embedded glass fibres than are in the actual solution environment outside the composite. For each solution, four bundles of each fibre grade were immersed and subsequently removed after different exposure times. After careful washing to ensure no further ageing takes place, these different bundles represent the state of the glass after one day, two days, one week and two weeks of exposure to each solution.

3.3.3 Microbond samples

Microbond samples were also aged in order to test the method as a direct way to analyse the effects the solution environment has on the interface, as was done for example by Gaur and Miller (1990) and Gaur et al. (1994) for Kevlar, E-glass and carbon fibres. For this purpose, special sample holders were manufactured from AISI 316L corrosion resistant stainless steel. Batches of samples were aged in 1 g/dm^3 sulphuric acid solution and in deionized water. The solutions were kept at a constant temperature of 95 °C during the ageing. The 50 g/dm^3 environment was excluded due to the observed severity of this environment, especially to the E-glass grade. It was therefore expected, that the properties of the fibre would be weakened too much for the samples to be tested. Several of the samples sent to the 1 g/dm^3 solution exposure were lost because the epoxy adhesive, used to attach the glass fibres to the sample holder, lost adhesion with the metal when exposed to the ageing environment. Because of this and some scheduling difficulties with the device, which was still under development during this work, the initial plan of several parallel samples from both environments were postponed and only some results from deionized water ageing are presented in this work.

In all of the aforementioned ageing procedures, an important aspect was to examine the concentration and volume of the solutions so that the conditions of the ageing do not change because. This is especially important in the heated environments where water evaporation is significant. The pH of the solutions was measured to keep track of the sulphuric acid concentration. The pH was however allowed to change because of, for example leaching reactions with the glass.

3.4 Experimental methods

The chapter describes briefly the experimental methods used in characterization of the ageing of the resin matrix, fibre reinforcements and the interface. The VE resin weights were measured during the ageing at Outotec Research Center as were the ICP-MS for the glass fibre ageing solutions. These methods were already discussed in the previous

chapter. The advanced testing methods used in this work include a microbond test device still under development, called FIBRObond. Information about the operating principle and significance of the test is presented in this chapter.

3.4.1 Optical microscopy

The resin sheets were examined with Leica DM2500 M optical microscope. Both the outer surface and the inside of the sample were examined. The latter was achieved by transillumination and was used in an effort to determine the presence of other defects, created during ageing or otherwise, inside the resin sheets. Similar microscopic observations of crack generation with ageing was done by Gautier et al. (2000). In this work the method is, however, included to more show its applicability and evaluate the amount of defects formed and not to evaluate the crack geometry as done by Gautier et al. The amount of defects in different environments is evaluated visually as accurate image analysis would require different sample conditions to minimize the effect of defects at different depths and thus shown slightly out of focus.

3.4.2 Thermal analysis

Thermal properties of the matrix, before and after ageing, are examined with dynamic mechanical analysis (DMA) and differential scanning calorimetry (DSC). The approximately 3 millimetres thick, aged Derakane 441-400 resin sheets were tested with Mettler Toledo DMA/STDA861 to determine possible changes in mechanical properties and for example the glass transition temperature. If such changes, for example in the flexural modulus are, observed it can indicate either degradation of the polymer structure or post curing, depending on the properties are worse or better for the aged sample (Fraga et al. 2003) For comparison, the DSC was also used to determine thermal properties such as the glass transition temperature, T_g. The DSC analysis was done with Netzsch DSC 204 F1. The method can also offer valuable information on the degree of curing in the resin samples, when two heating cycles are used for the same sample. Post-curing can be observed from both an exothermic reaction peak and a shift to higher temperatures in the glass transition (Ehrenstein et al. 2004 p. 31).

The DMTA testing was done in three-point bending mode because of the reliability of the modulus given by a properly conducted experiment. The sample dimensions are also relatively large, which in this case is an advantage as the small localized changes or defects created during ageing affect the results less, making the preparation of representative samples straightforward. An offset force of 150% of the force amplitude was used to ensure proper sample contact with the device and an amplitude sweep was conducted to identify the linear viscoelastic region of the material. Differences in the materials were expected to be small enough that the amplitude sweep of one of the samples was deemed sufficient to determine the measuring parameters for all samples.

The temperature scan used in the actual measurement was a heating from 25 °C to 160 °C at a relatively high heating rate of 5 K/min. The dynamic movement parameters are 1.00 Hz frequency and amplitude of 5.500 N, resulting in 600 µm displacement. The time between the ageing and the DMTA testing was several months, during which time the resin sheets were allowed to dry completely. Due to this, the plasticizing effect of water should be virtually non–existent in the results, so the observed differences should correspond to structural changes in the material.

In the DSC, a sample from each approximately 3 mm thick resin sheet was subjected to two heating cycles from 25 to 200 degrees Celsius, with a liquid nitrogen assisted cooling cycle. The sample mass was approximately 10 milligrams for each material. A heating rate of 10 K/min was used in the DSC measurements. The cooling cycle between the heating cycles was not deemed interesting or relevant for the properties of the resin in the second heating, as might be the case with thermoplastic resins, and thus a higher cooling rate of 20 K/min was used. The samples were cooled to 20 °C so that undershooting of the second heating cycle would not extend to higher temperatures than in the initial heating. Nitrogen was used as purge gas in the DSC measurements.

3.4.3 Fourier transform infrared spectroscopy

FTIR is used with the aim of identifying chemical changes in the matrix and the glass fibres. Especially the changes in absorption bands that indicate the chemical changes presented in chapter 2 for both VE and glass fibre samples are of interest. These changes include, for example, unsaturated carbon bond vibrations, ester group vibrations and oxygen bond vibrations for silicon, aluminium and boron in the glass structure. Changes in these vibration bands indicate post-curing and the hydrolysis of ester groups and glass structure, respectively. The FTIR measurements were conducted with Bruker Tensor 27 spectrometer with a PIKE Technologies GladiATR Attenuated Total Reflectance (ATR) sample holder using a diamond crystal. Glass fibres were measured by crushing then into a fine powder with the sample holder screw normally used to hold the sample in place during ATR measurements.

FTIR measurements were conducted on vinyl ester sheets and both glass fibre grades. Both aged and unaged samples were measured. The vinyl ester samples were measured with a wavenumber range of 400–4000 cm^{-1} and a resolution of 4 cm^{-1}. As the silica Q_4 (no NBOs) bending vibration takes place between wavenumbers 400 and 500 cm^{-1} the full measuring range of the device was utilized at lower wavenumbers to achieve a minimum of 340 cm^{-1}, when measuring the glass fibre samples (Lynch et al. 2007; Marzouk 2010). Thus, the measuring range for glass fibre samples was selected as 340–4000 cm^{-1}. Before the testing, the background was measured with 68 scans of the whole wavenumber range, checked after each sample and measured again when necessary. The samples were measured with 128 scans.

3.4.4 Scanning electron microscopy

Scanning electron microscopy (SEM) images from both glass fibre grades were taken for unaged samples and all ageing conditions. For the heated environments, the fibres are examined at four different time points. For the room temperature environment, only samples that have been exposed to the whole two weeks of ageing are examined. Due to operating permissions and scheduling of the work, different microscopes were used. Heated environment aged Jushi E6CR fibres were viewed with Zeiss ULTRAplus FEG-SEM, whereas a Philips XL-30, which uses a LaB_6 thermal electron emission source, was used for the rest of the samples. The aim of the SEM imaging was to observe surface quality changes and cracking behaviour in the glass fibres.

Additionally the heated environment aged glass fibres were analysed with energy-dispersive X-ray spectroscopy (EDS) during the SEM imaging to receive information of the surface composition of the fibres. Changes in the surface composition could offer valuable information on the corrosion mechanism of the glass. The surface sensitivity of EDS is however limited as the interaction volume of an electron beam is quite significant. For the glass fibre analysis, this means that the X-rays used to analyse the composition of the sample are collected from a significant depth. Due to this, changes in the composition are observable only after the corrosion has penetrated the glass fibre sufficiently to yield data mostly from the altered layer on the glass fibre surface.

3.4.5 Tensile testing

A custom-built fibre tensile tester, developed by the same research group responsible for the FIBRObond device was used in determination of tensile properties of the glass fibres. The extent of the loss of tensile properties caused by ageing is an important part of the effects the fibre reinforcement ageing has on the properties of the composite as a whole. As the properties of fibre samples can vary significantly and poorly representative sample behaviour during the test is common, large amounts of parallel samples should be tested to achieve good accuracy of the results (ASTM D 3379-75 1989). However, the application of the method for this work was hindered by scheduling limitations, due to which only specific samples from the aged glass fibres were tested. The samples were selected based on the results from other methods, in order to select samples that show the effects of the ageing and the difference in durability of the fibre grades. The samples also need retain sufficient properties after the ageing, to withstand the handling required to initiate the testing. Based on these requirements, the following samples were selected for testing: 10 reference samples and 10 samples aged for two weeks in deionized water and in 1 g/dm^3 sulphuric acid from both glass fibre grades, 60 samples in total.

The movements and grips of the device have been designed to minimise erroneous behaviour during the testing, for example from excess radial stresses caused by the grips, which could result in premature breaking of the sample from the grips. The device also

has a camera and optics setup for observing fibre behaviour and more importantly for determination of the fibre diameter, which is needed to calculate the material properties from the test data. The scaling of the camera image was calibrated with a suitable micrometre scale ruler and the diameters were measured with image analysis tools. The samples were tested with crosshead movement speed of 10 μm/s or 0.6 mm/min, which is the more common unit. Accurate determination of crosshead placement during the test was not available. Therefore, the modulus of the fibres and the stress-strain behaviour in general could not be evaluated. The measurements available from the device are the force, fibre diameter and test time. Due to the linear, brittle behaviour of the glass, it is expected that the slope of the stress-time curve is proportional to the modulus of the glass, which enables comparative evaluation of changes in the fibre behaviour.

3.4.6 Inductively coupled plasma mass spectrometry

In order to receive relative information of chemical changes due to leaching and hydrolysis of the glass, inductively coupled plasma mass spectrometry (ICP-MS) was used at Outotec Research Center to identify relevant substances from the glass fibre ageing solutions after all samples were removed. The device used was a Thermo Scientific iCAP 6000 Series ICP Spectrometer. The analysis was done at a very broad material spectrum but results are presented only on those constituents, which present a significant fraction of the glass structure and the presence of which can be used to characterize the way the glass is affected by the solution. All ICP-MS results are taken after the full two-week exposure of the glass fibres. This means the results include all leaching constituents from each of the four fibre bundles, aged for different times, for each fibre–temperature combination. The amount of sample in each case is similar, but not identical. This means that accurate quantitative analysis based on the ICP-MS results is not possible. The methods however gives valuable information on the glass constituents removed from the material during ageing which supports the other compositional analysis methods such as EDS and FTIR.

3.4.7 Microbond method

The aim of the microbond method in this work is to observe the degradation of interfacial properties, with ageing of the microcomposite samples. As with the mechanical testing, due to scheduling most of the intended test series was excluded from this work. The microbond method was first introduced in an article by Miller et al. (1987). Since then several research groups have utilized and further developed the method. Compared to interlaminar shear strength (ILSS) measurements the microbond method measures the properties of the interface more directly. This direct measurement of the interfacial strength also enables more in-depth analysis of the behaviour of the materials near the interface and of the interface itself. Compared to the more traditional single fibre pull-out test, where the fibre is embedded in a resin well, the microbond method can reach much

lower embedded fibre lengths because the meniscus formed by the resin well often contributes to a significant portion of the embedded length, whereas the menisci at the ends of a droplet are almost negligible. (Miller et al. 1987; Gaur & Miller 1990; Dey et al. 2014)

The method is very responsive to the factors that contribute to the interfacial strength but also to variations inside a glass fibre batch, because it measures the properties of the fibre–matrix interface for just one fibre at a time. This also makes sample preparation and analysis of the results difficult, as virtually every small change in the properties and dimensions of the fibre, the resin or the interface changes the measured force required to detach the resin droplet from the fibre surface. This has caused many of the published articles on the subject to present results with significant divergence.

One factor, on which the literature on the subject agrees on, is that the force required to detach the droplet corresponds linearly to the embedded length of the fibre. However due to the very high variance caused by other factors, this behaviour is often obscured or hard to evaluate. One solution, also utilized by the FIBRObond concept, is to make several different sized droplets on a single fibre. This eliminates much of the variance caused by the fibre diameter and for example age of the sizing. The variation caused by these can then be included in the examination by observing several similarly prepared fibres. (Scheer & Nairn 1995; Day & Cauich-Rodrigez 1998; Pandey et al. 2011) This also enables an interesting alternative approach to the determination of the IFSS. The common approach is to determine the IFSS for each tested droplet from the force and contact area separately. Once there is practically no variance from the fibre itself, the linear correlation to embedded length becomes apparent and the IFSS for the resin on that individual fibre can be determined from the slope of the force–area curve. For accurate analysis of the fibre–resin combination, several fibres need to be tested.

Instead of depositing resin droplets on the fibre surface, as described by Miller et al., the sample preparation is done with a separate device called FIBROdrop. A single fibre is attached from both ends to a rigid sample holder, which can easily be attached to both the sample preparation and the testing devices. The sample holder and deposited droplets are presented in figure 8.

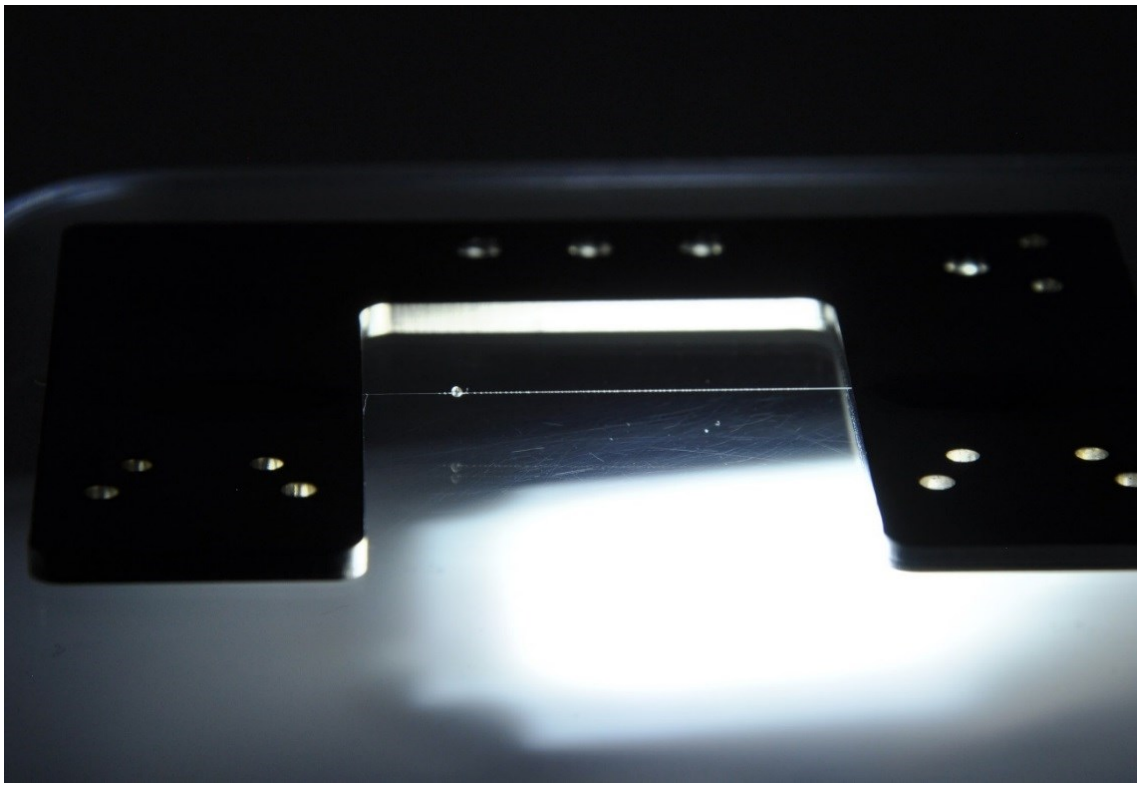

Figure 8. *FIBRObond sample holder. The light refraction reveals the micrometre scale droplets on the glass fibre surface.*

Droplets are created by vertical movement of the fibre through a resin well and the droplet size can be controlled by altering the parameters of the movement, such as velocity and distance. Different resins respond differently to the parameters but the method has so far been applicable to every resin system tested, once the requirements of the material in question are properly taken into account. Some of these factors were discussed earlier for the resins used in this work.

The actual testing device is very similar to the set-up described by Miller et al (1987). The major exception is that the whole device is self-built to ensure compliance to the requirements of testing at such as small scale. A camera set-up is also included to enable observation and recording of the test. The testing device is presented in figure 9.

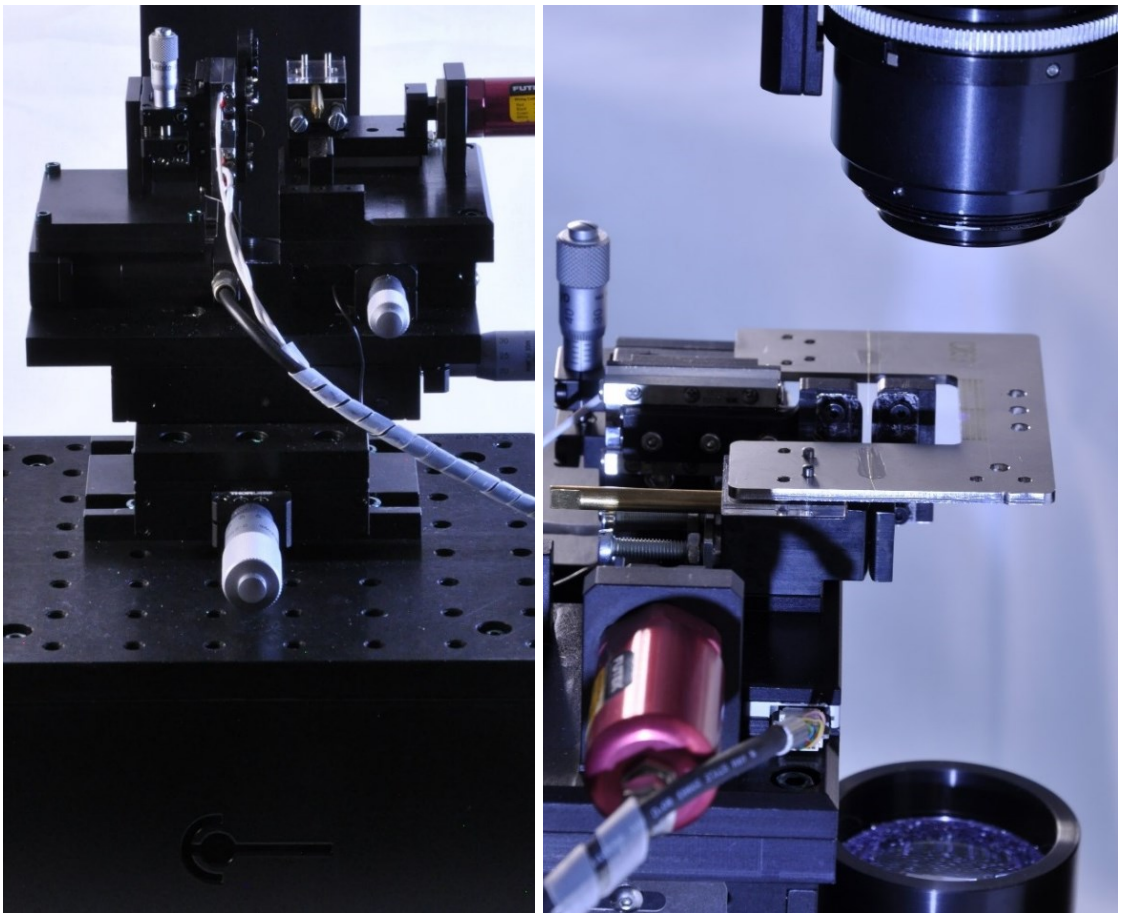

Figure 9. *The FIBRObond prototype instrument. Left: front view of the instrument, Right: attached sample holder and microvise blades.*

The blades responsible for gripping the resin droplet during the test have their own control to ensure a minimal gap is left between the fibre surface and the contact point of the blade to the fibre surface. Such a gap would alter the stress distribution inside the resin droplet resulting in a non–uniform stress distribution in the resin and compressive stresses at the interface. Together these factors cause the force to increase and therefore, unless the contribution of these effects can be accurately analysed, an overestimation of the IFSS result. (Chou et al. 1994)

Test data analysis for the microbond test include determination of the contact area for each droplet ($A_{embedded}$), requiring accurate determination of both the fibre diameter and the embedded length from optical microscope images. The IFSS in MPa is calculated from the maximum force (F_{max}) during the measured simply as:

$$IFSS = \frac{F_{max}}{A_{embedded}}. \qquad (1)$$

The other alternative is, as previously mentioned, determination of the IFSS from the slope of the load–area curve.

4. RESULTS

This chapter presents the results from the various methods used to examine the ageing for the different parts in a PMC. Only the results needed to reach the observations made during analysis of the results are presented. Further results are collected in appendices 1–3, to support the observations made in this chapter.

4.1 Weight change of the resin

The changes in resin sheet weights are presented graphically in figures 10, 11 and 12. Charts with the actual weights of the sheets at specific time points are presented in appendix 1. In figure 10, the weight change at 672 hours is not depicted for the 3mm sheet. This is because the value is above the upper limit selected for the graph and clearly erroneous, as is the corresponding 5 mm sheet value. This is likely caused by improper drying of the sheet surface before weighing.

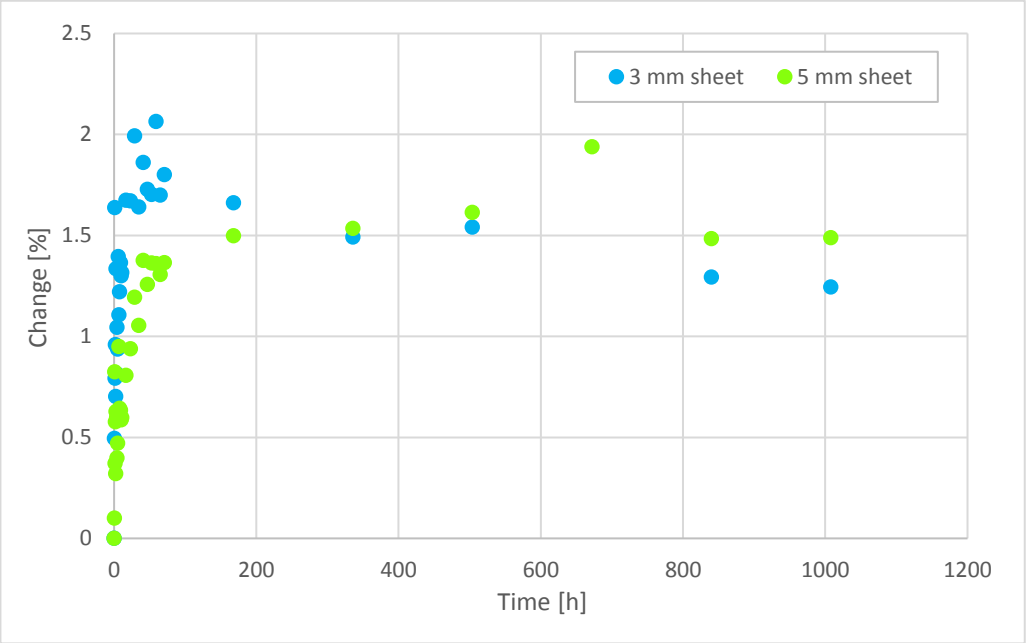

Figure 10. *Change in VE resin weight in deionized water.*

It is important to note that the changes are given as relative changes to the initial sheet weight. As expected, the diffusion of the solution into the sample resembles Fickian behaviour. However, as can be seen in figure 10 and even better in figure 11, the thinnest samples reaches the saturation quite quickly and subsequently starts to lose weight. This type of weight decrease in a solution environment is likely the result of the extraction of volatiles from the resin as reported by for example by Ashbee and Wyatt (1969) and Fraga et al. (2003).

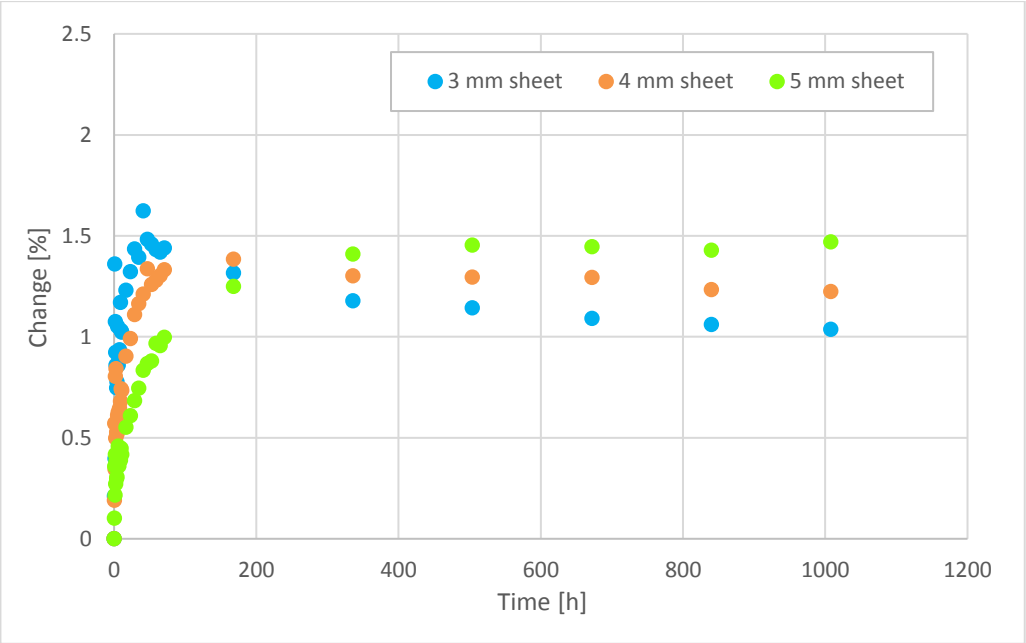

Figure 11. *Change in VE resin weight in 50 g/dm^3 sulphuric acid solution.*

Interesting observation can be made from figure 11. Both the total weight increase and the rate of that increase seem to be lesser than with deionized water. One possible explanation is that the acidic nature of the solution causes material loss immediately starting from the sample surface and therefore the total weight change seen in figure 11 is a combination on weight increase from solution diffusing into the sample and material loss from degradation caused by the acidic nature of the solution and the extraction of volatiles. It is also possible that the slower diffusion of the hydronium ions and conjugate bases hinders the total diffusion rate of the solution into the material. For example, Ehrenstein and Pongratz (2013 p. 710) have listed sulphuric acid as an acid which diffuses in polymers very weakly if at all. Selective diffusion of water molecules would lead to a change in the solution pH via sulphuric acid concentration and therefore osmosis could act as an opposing force for the water diffusion leading to slower diffusion and a lesser weight increase. Further evidence of the previous assessments are seen in figure 12.

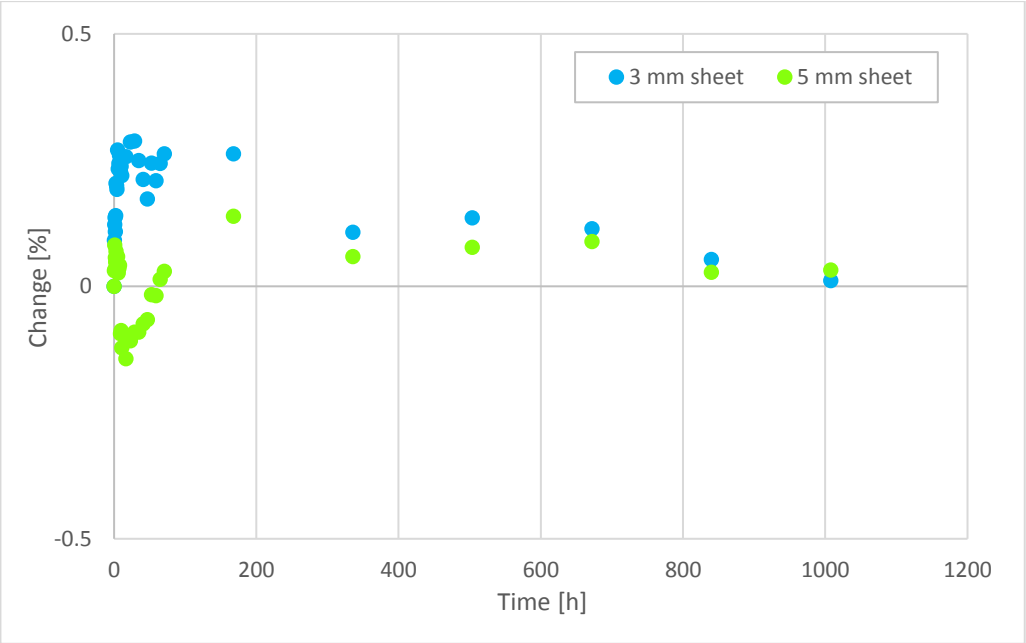

Figure 12. *Change in VE resin weight in 500 g/dm^3 sulphuric acid solution.*

In figure 12, the weight of the sample is not significantly increased at any point of the exposure and for a time the observed weight change is initially negative for the thicker sample. Overall, the sample weight examination shows clear trends towards lesser weight gain and greater material loss with more aggressive sulphuric acid environments.

4.2 Thermal properties of the resin

Figure 13 presents an overview of the DMTA results. The almost identical modulus values are one indication of successful sample preparation and reliability of the test procedure.

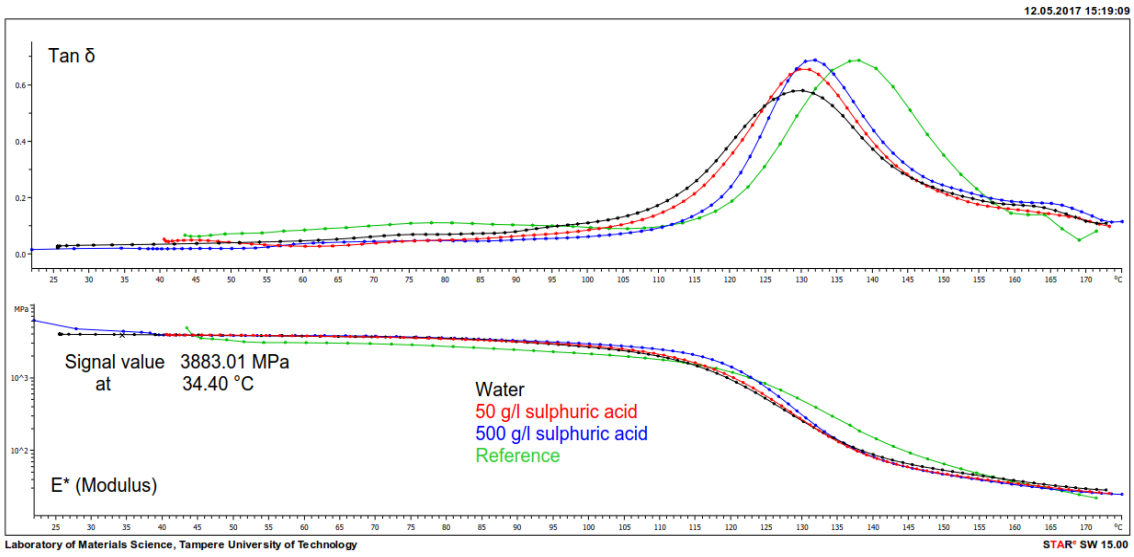

Figure 13. *Overview of the DMTA test results.*

Resin datasheet (Derakane® 2009) presents the flexural modulus of the material as 3400 MPa, based on ISO 178: Plastics. Determination of flexural properties. The different

modulus can be due to the differences between the testing methods as the ISO 178 standard uses a flexural test with linear unidirectional movement (EN ISO 178 2003). Some of the difference could also be from post-curing and removal of volatiles during ageing. This is supported by the modulus value measured for the unaged reference sample during the temperature settling before the measurement. During the pre-test settling, the DMTA measured the complex modulus of the reference as little above 3300 MPas. However due to an unknown error at the start of the test the device starts measuring only after the heating has advanced to 40 °C and overshoots the modulus value significantly. The early section of the complex modulus curve presented in figure 13 corresponds to the above-mentioned modulus value.

A more detailed overview of the measurement results are given in figure 14 and table 3. The moduli are presented separately as storage and loss modulus to make the determination of the glass transition temperature easier. The detailed views for other than the unaged sample are not presented separately, as the behaviour is very similar. All relevant observations can be made based on figures 13 and 14, and the values presented in table 3. The glass transition temperatures are determined from loss modulus peaks: both because it corresponds well with glass transition temperatures determined with DSC and because it corresponds to the start of significant decrease in (storage) modulus signifying the onset of "softening." (Ehrenstein et al. 2004 p. 239)

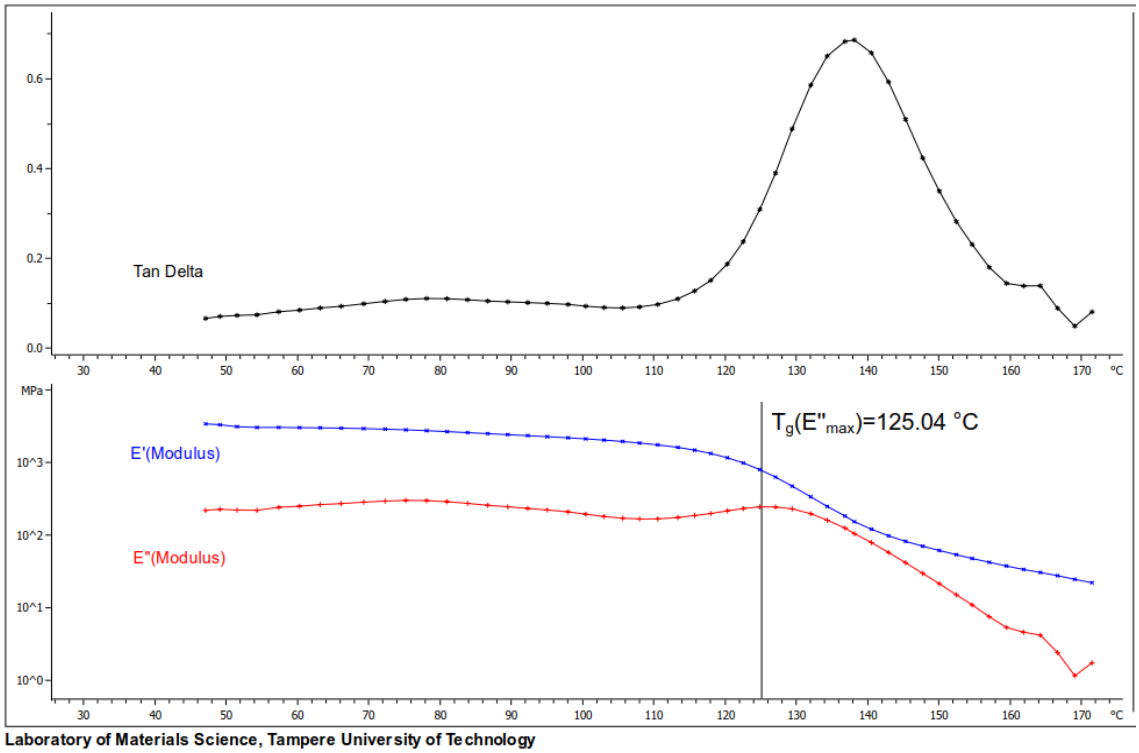

Figure 14. *DMTA of unaged, "clear cast" VE resin.*

The datasheet presents the glass transition temperature, determined with thermomechanical analysis accordingly to the ISO 11359-2 standard, as 135 °C (Derakane® 2009). Analysis of the loss factor (tan δ) peak shown in figure 14 gives the

glass transition of 138.7 °C, which is quite similar to the datasheet value. The glass transition temperatures determined from the loss modulus peaks are presented in table 3.

Table 3. *VE resin glass transition temperatures, $T_g(E''_{max})$, determined from the DMTA analysis.*

Environment	Deionized water	50 g/dm³ sulphuric acid	500 g/dm³ sulphuric acid
$T_g(E''_{max})$ [°C]	116.80	118.80	121.60

There is a significant decrease in glass transition temperature between the unaged sample and the aged samples. The moduli also respond to the temperature differently. As can be seen from figure 13, there is a clear shift in the behaviour of the material between the water and sulphuric acid aged samples. The glass transition temperature is 2 °C higher and the behaviour of the material, most easily evident from the peak shape of the loss factor curve in figure 13, is different. Ageing in sulphuric acid solution results in a higher glass transition temperature and narrower loss factor peak compared to the water-aged sample. The loss factor peak is similar for water-aged and unaged samples, indicating that the narrowing of the peak – resulting from different modulus response to temperature – is a result of interaction with the sulphuric acid.

With few notable exceptions, the results from the DSC analysis agree with the results from DMTA. Figure 15 presents the two DSC heating cycles for the unaged resin.

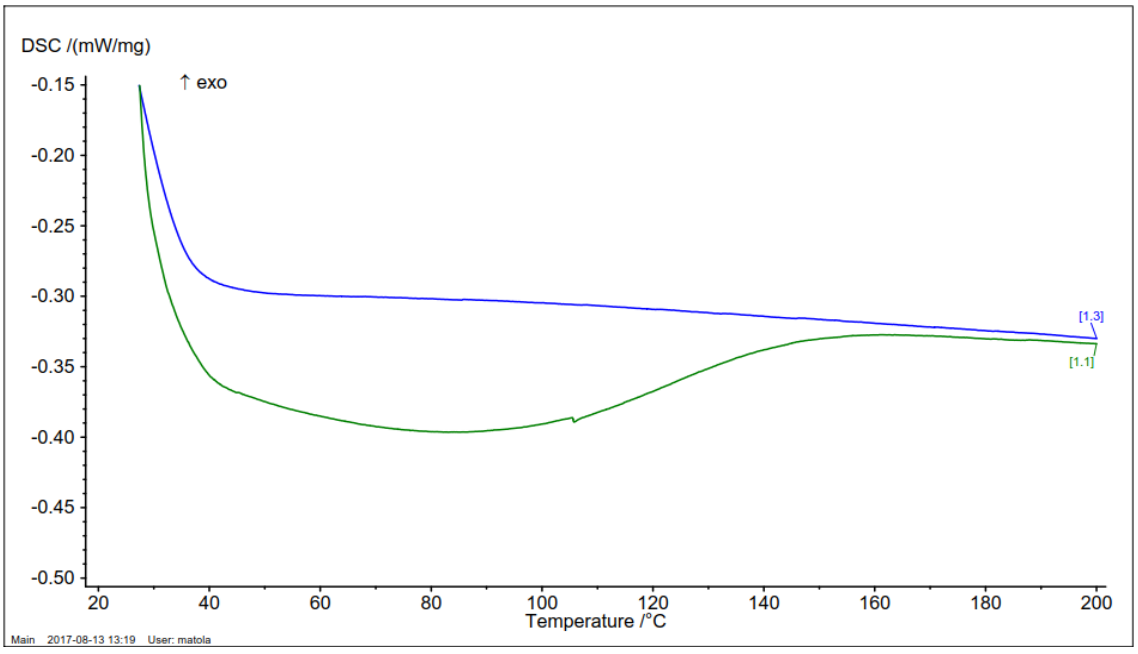

Figure 15. *DSC heating cycles of unaged VE resin. Green curve is first heating and blue second heating.*

Analysis of the DSC curve for the unaged resin sample is problematic. In the first heating cycle, an exothermic shift begins around 90 °C. This is likely the result of significant

post-curing, which could also obscure the glass transition of the material. In the second heating, the curve is more or less smooth, with no peaks or transitions observable, yet because no other significant peaks of shifts are observed, a glass transition should be clearly visible. No definitive explanation for this behaviour can be given based on the data available. Figure 16 presents the deionized water aged sample DSC heating cycles.

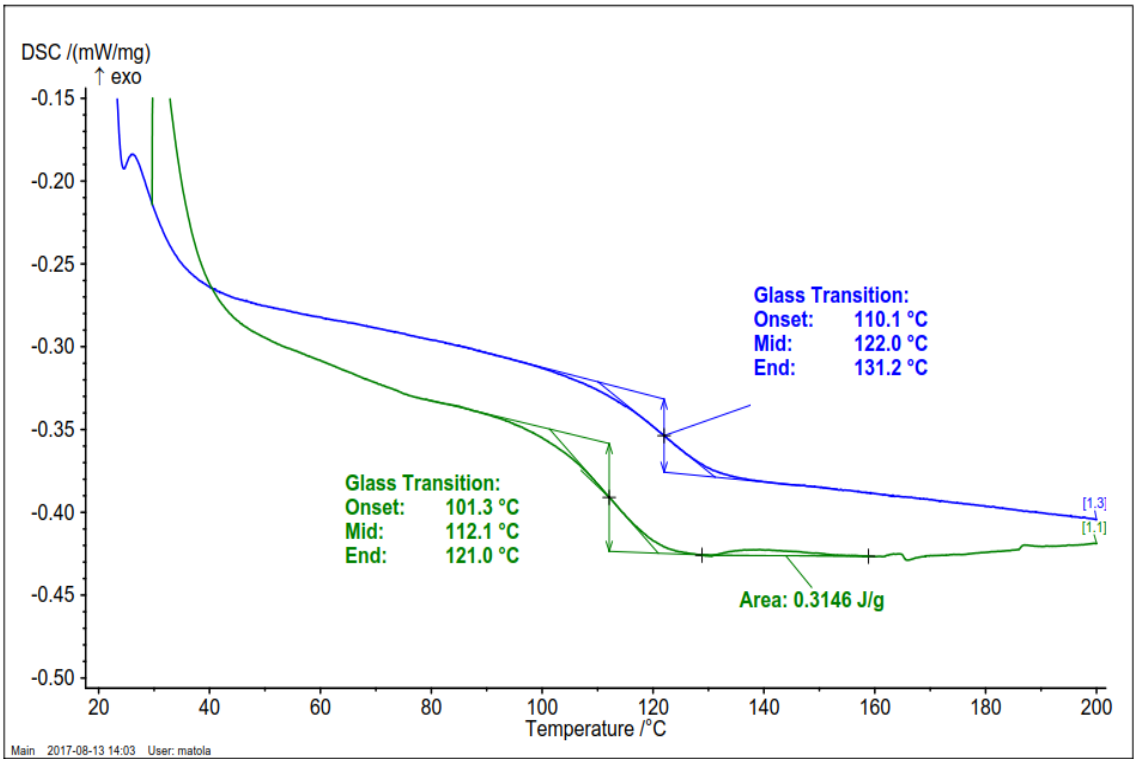

Figure 16. *DSC heating cycles of the VE resin after 1008 hours in 95 °C deionized water. Green curve is first heating and blue second heating.*

In the water-aged sample, the glass transition is clearly observable from the DSC results. The glass transition temperature is comparable; if slightly lower than the glass transition temperature determined from the loss modulus peak in DMTA. This can be a result from the significantly larger sample size, or the relative high heating rate used in the DMTA. Comparison of the two heating curves indicates slight post-curing in the first heating cycle. The post-curing reaction is also indicated by the small reaction peak around 140 °C. The DSC results for the 50 g/dm^3 sulphuric acid solution aged sample is presented in figure 17.

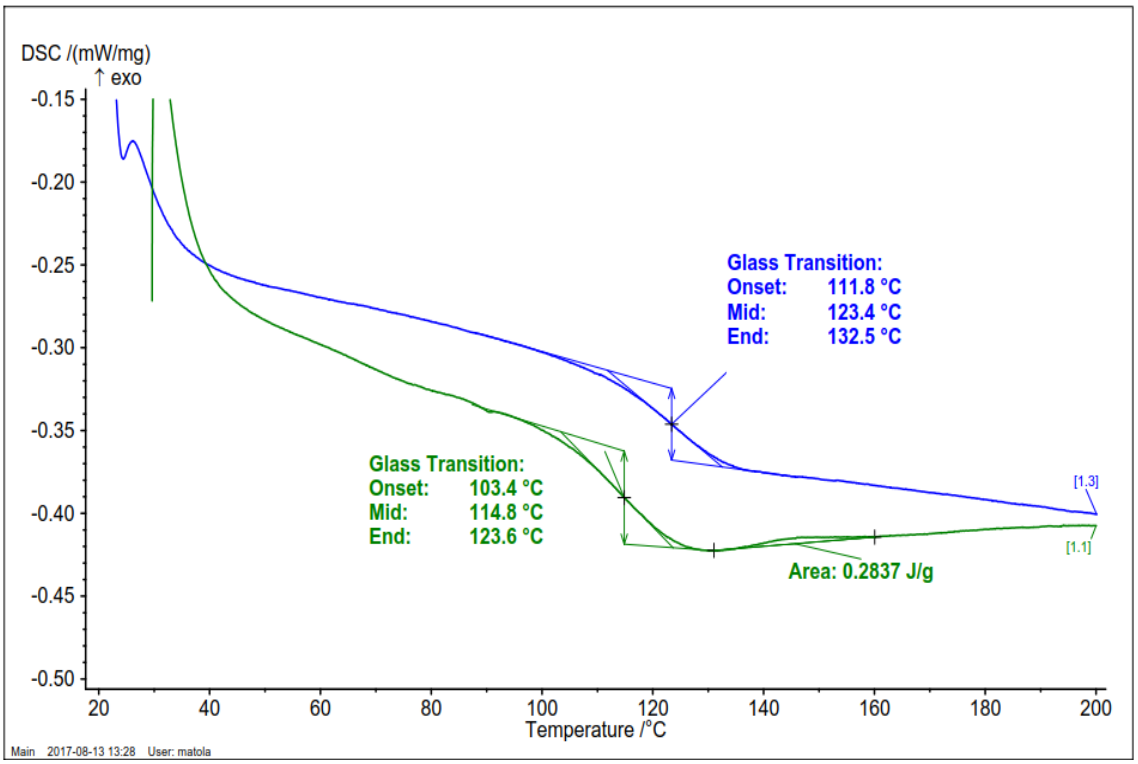

Figure 17. *DSC heating cycles of the VE resin after 1008 hours in 95 °C 50 g/dm^3 sulphuric acid solution. Green curve is first heating and blue second heating.*

The results for 50 g/dm^3 sulphuric acid are similar to those for deionized water. The glass transition temperature is however slightly higher, which is in agreement with the DMTA results. A small reaction peak is also visible in these results. There is less post-curing in in the 50 g/dm^3 sulphuric acid solution aged sample than in the sample aged in deionized water. This is indicated by both the slightly smaller peak energy and increase in the glass transition temperature. Figure 18 presents the DSC results for the 50 g/dm^3 sulphuric acid solution aged sample.

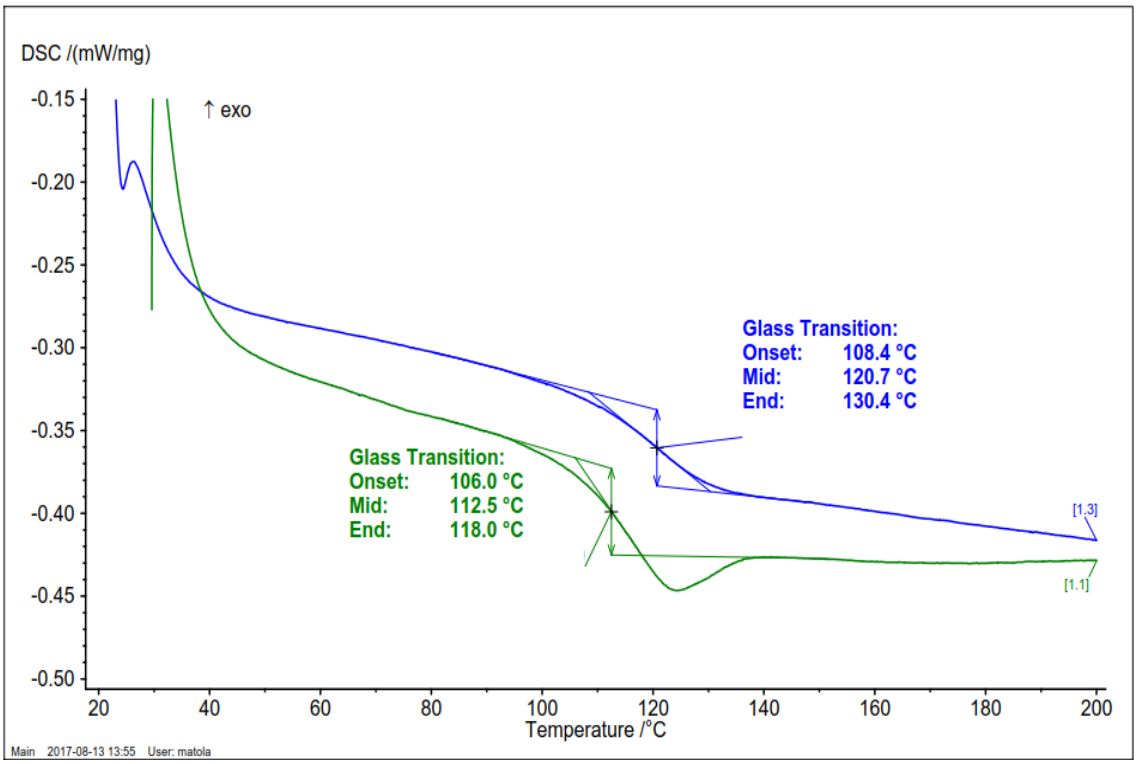

Figure 18. *DSC heating cycles of the VE resin after 1008 hours in 95 °C 500 g/dm^3 sulphuric acid solution. Green curve is first heating and blue second heating.*

The glass transitions show a similar shift as before, indicating post-cure reactions. The reaction peak observed in other aged samples is however not clearly observable. The region between 120 and 140 °C shows an endothermic peak, probably caused by mechanical action during sample preparation (Ehrenstein et al. 2004 pp. 35-36). Because of the endothermic peak, the reaction peak cannot be reliably evaluated. The endothermic peak also affects the analysis of the glass transition, which could cause the deviation from the trend observed in DMTA results and between the deionized water and 50 g/dm^3 environments in DSC, where higher sulphuric acid concentration aged samples exhibit higher glass transition temperatures.

4.3 Visible defects caused by ageing

The outer surfaces of the resin sheets are presented in figure 19. The aged resin sheets have undergone the previously described 1008 hours of ageing and complete drying before the examination. The slight colour differences in the samples are not indicative of ageing and are caused by the individual adjustment of the camera parameters during the imaging.

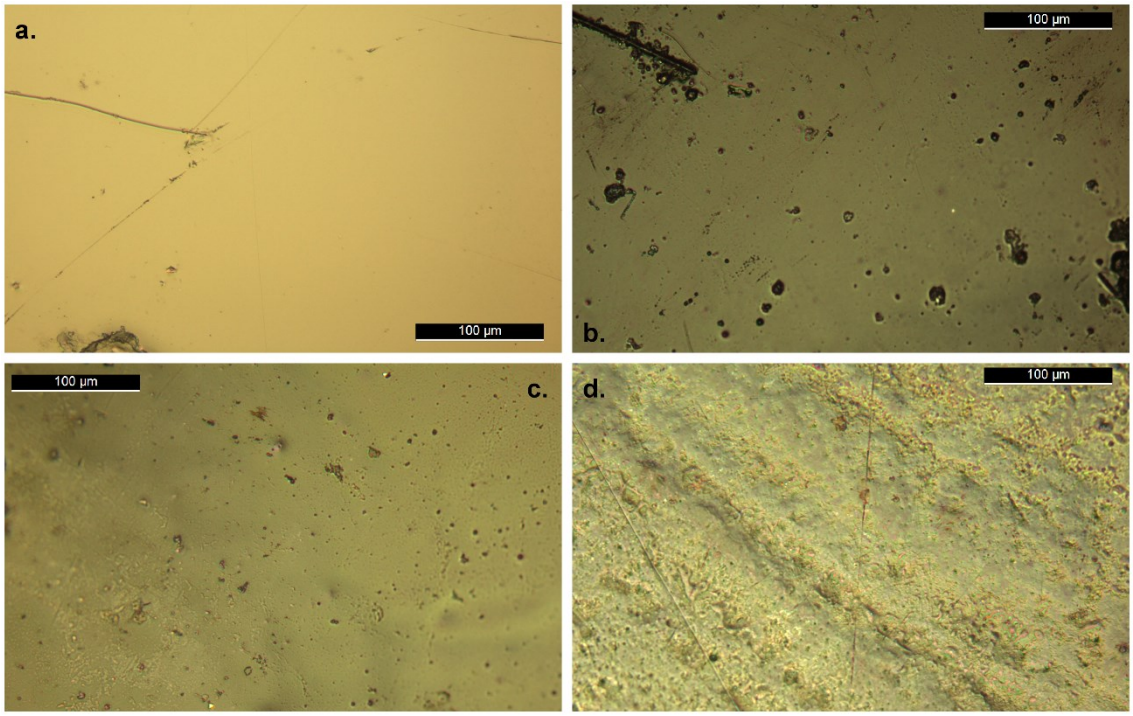

Figure 19. *VE sheet surfaces viewed with a 20× objective: a) unaged, b) deionized water, c) 50 g/dm^3 sulphuric acid and d) 500 g/dm^3 sulphuric acid.*

In the unaged sample, an almost even surface with very few defects can be observed. It is clear that more severe ageing environments result in surface damage and especially with the 500 g/dm^3 solution, significant surface degradation has occurred. It should be noted that no vacuum or other aid were used in the processing of the unaged resin sheet, which would explain the surface quality compared to the other samples. Therefore, the poor surface quality can be attributed to the ageing.

Changing the light source of the microscope to one below the resin sheet and adjusting the focus enables observation of defects inside the transparent resin sheets. Figure 20 presents such images for the unaged sample and the samples aged for 1008 hours in deionized water and 50 g/dm^3 sulphuric acid solution. An image for 500 g/dm^3 solution aged resin sheet is not presented, because no defects were found and taking an image without anything to focus the image to is not worthwhile.

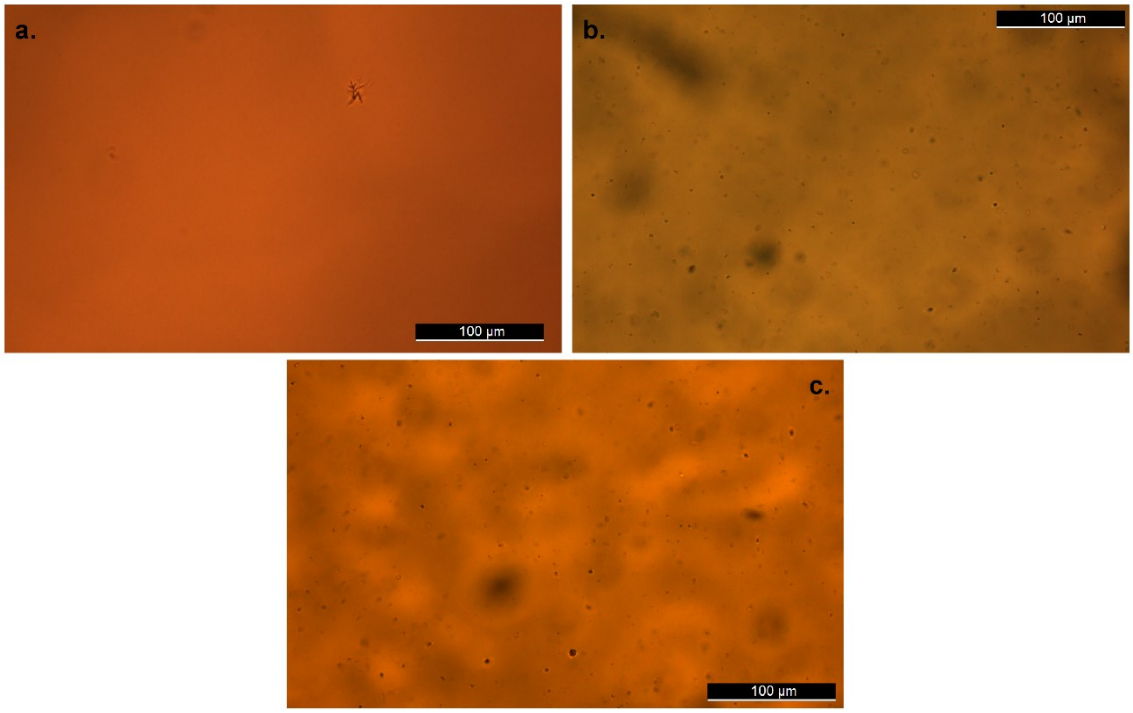

Figure 20. *Transillumination images from the VE sheets, viewed with a 20x objective: a) unaged, b) deionized water and c) 50 g/dm^3 sulphuric acid.*

Even without any aids to remove air bubbles from the resin during the cure, almost no defects can be observed inside the unaged sample. However, in both the water and the 50 g/dm^3 sulphuric acid aged samples a significant amount of small defects can be observed. The result of not finding any defects in the 500 g/dm^3 solution aged sample is therefore interesting.

Because of their significantly smaller size, changes in glass fibre surfaces were examined with SEM. Figure 21 presents two reference images for the Jushi E6CR glass fibres.

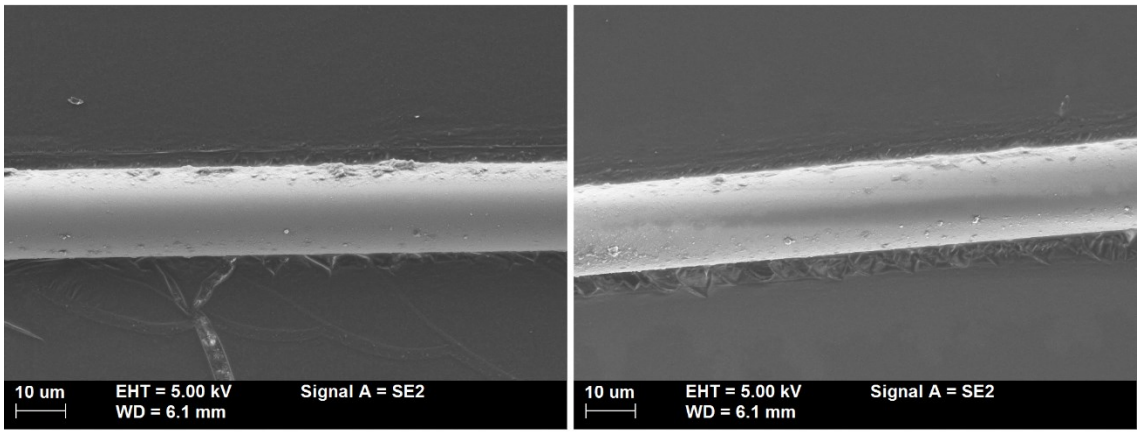

Figure 21. *SEM images of unaged Jushi E6CR fibres.*

The apparent uneven surface in the rightmost picture of figure 21 is likely caused by the sizing on the fibre surface. This can be from uneven thickness of the sizing or even atomic number contrast because the sizing is missing from part of the fibre surface. Overall, the

unaged fibres have almost no surface defects and most of the surface roughness visible at the edges is likely caused by the carbon tape the fibre is attached on for imaging. Figure 22 presents the first aged ECR-glass samples. The images in figure 22 are taken from fibres aged in deionized water heated to 95 °C.

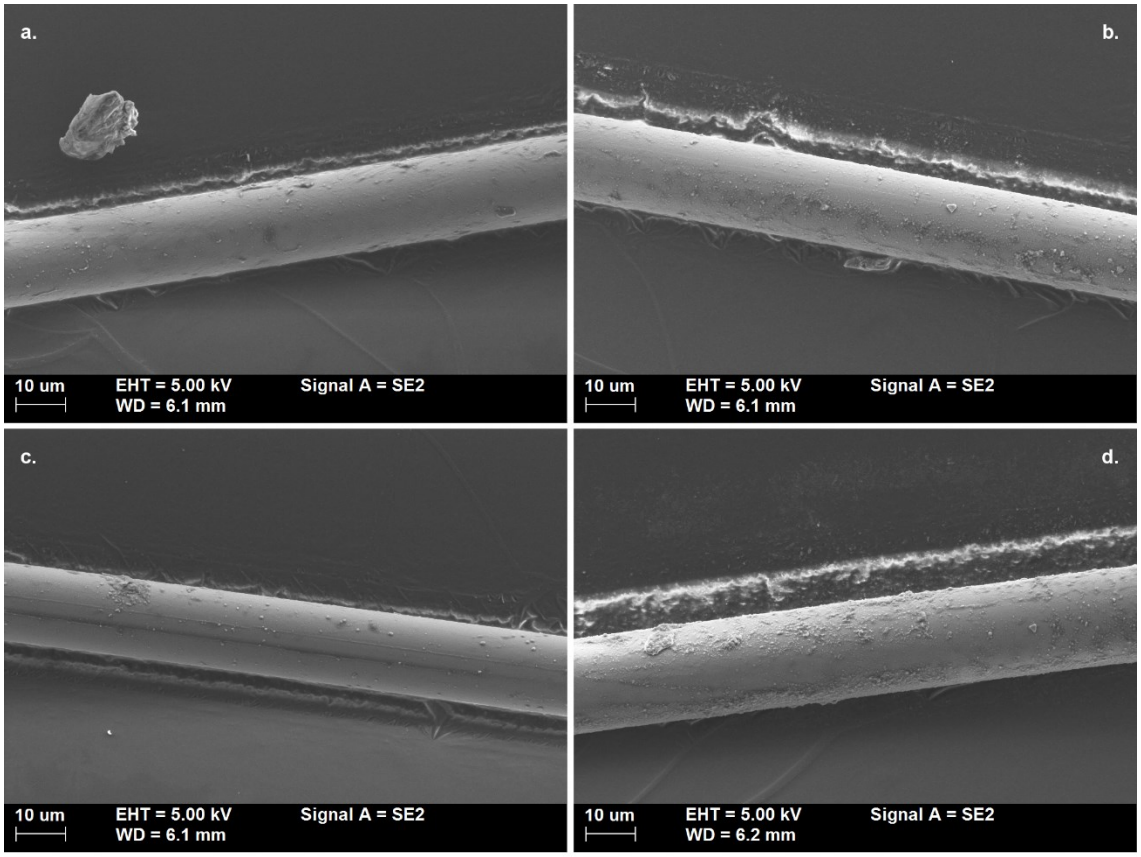

Figure 22. *SEM images of Jushi E6CR aged in 95 °C deionized water for a) 1 day, b) 2 days c) 1 week and d) 2 weeks.*

The deionized water aged samples show very little visible changes. Some interaction between the solution and the sizing is however likely. The axial texture visible in figure 22c, which is taken from a fibre aged for one week, is one possible indication of this. The differences in fibre diameter, most significant with the two weeks aged sample in figure 22d, are small enough to be normal variation in glass fibre diameter. Images of ECR fibres aged in 1 g/dm^3 sulphuric acid solution at 95 °C are presented in figure 23.

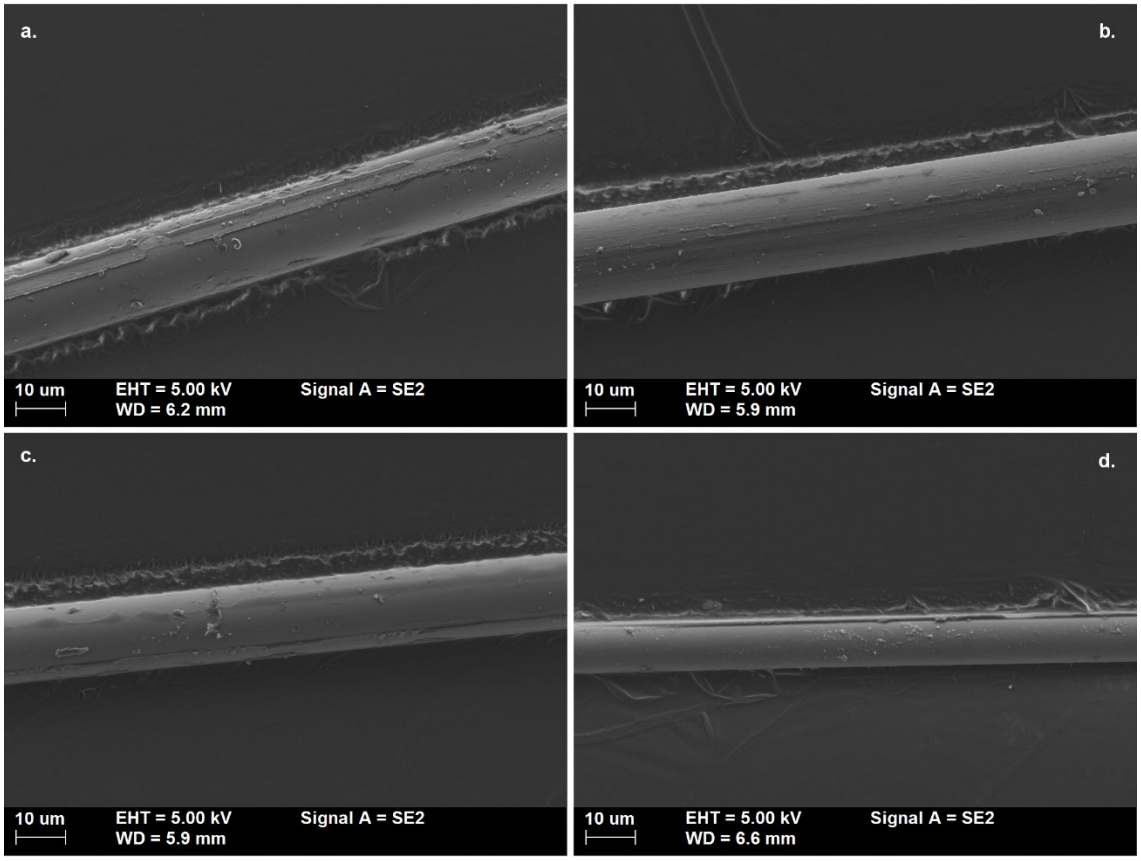

Figure 23. *SEM images of Jushi E6CR aged in 95 °C 1 g/dm^3 sulphuric acid solution for a) 1 day, b) 2 days c) 1 week and d) 2 weeks.*

Similar axial texture as observed in one image of the water-aged samples is visible in all of the images in figure 23. There also appears to be some reduction in the sample diameter, which is significant enough that it cannot be fully attributed to normal variation. For example, comparison to the scale bar gives the fibre in figure 23d a diameter of 9.7 micrometres. The ECR fibre is reported to be 17 micrometres in average and varies in the range of 16.5–21 micrometres, based on fibre diameter measurements made in the course of this work. Based on these observations and the images in figure 23 at least majority of the sizing and even some of the material was removed during the process of ageing, washing and transportation of the glass fibres. Images for the last ageing environment, 50 g/dm^3 sulphuric acid solution are presented in figure 24.

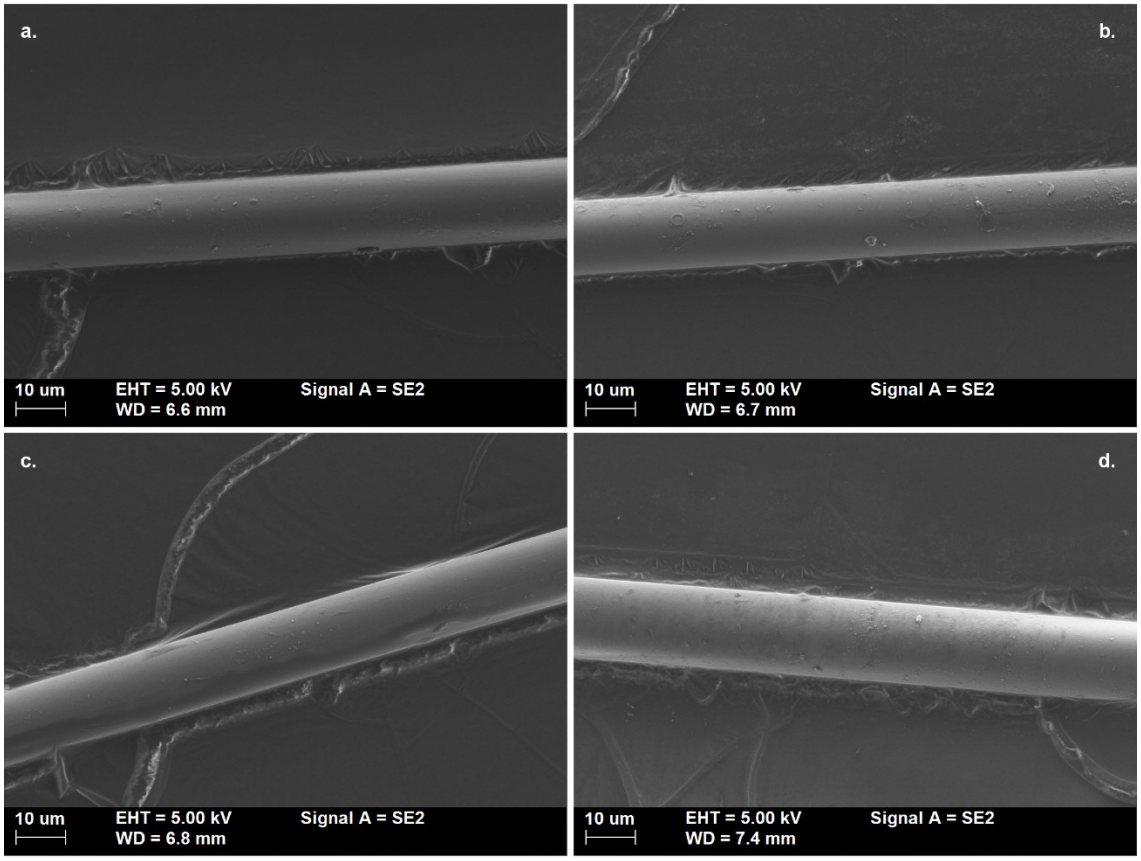

Figure 24. *SEM images of Jushi E6CR aged in 95 °C 50 g/dm^3 sulphuric acid solution for a) 1 day, b) 2 days c) 1 week and d) 2 weeks.*

Figure 24a shows a one day aged ECR glass fibre, which has surface defects indicative of the onset of corrosion. However due to the size of the picture this is not possible to observe from figure 24a. A larger version of the picture is presented in appendix 2 along with larger versions of all other SEM images. The images of fibres aged for two days and one week appear mostly unaffected to visual inspection. Some surface texture is observable in the lower edge of the fibre in figure 24c. The image presented in figure 24d was selected due to the interesting contrast on the fibre surface, which has no clear shape related reason. It is possible that a significant difference in chemical composition causes observable atomic number contrast. For atomic number contrast to be this clear in secondary electron image however, the compositional difference would have to be significant. This could be possible if an altered layer has formed on the glass fibre surface because of ageing and/or leached glass constituents have been deposited on the fibre surface from the solution.

Similar images were taken from the Ahlstrom R338 glass fibres aged in similar solution environments. The 95 °C ageing is expected to cause severe corrosion of these E-glass fibres, which should be observable in SEM images as well. Figure 25 shows two images of unaged fibres.

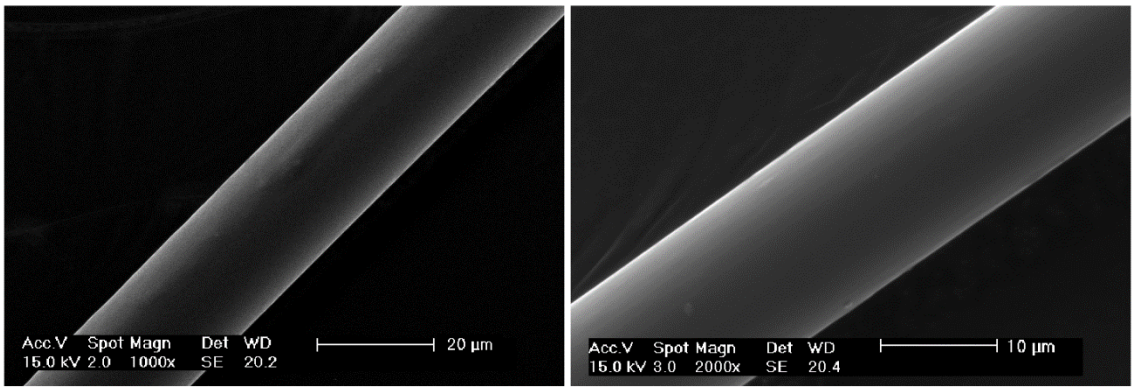

Figure 25. *SEM images of unaged Ahlstrom R338 E-glass fibres.*

Like with the ECR glass, there is very little of note in the unaged fibre SEM images. Uneven surface can be observed in the left side image of figure 25, again likely caused by the sizing applied to the glass fibre surface. Figure 26 presents the heated deionized water aged E-glass fibres.

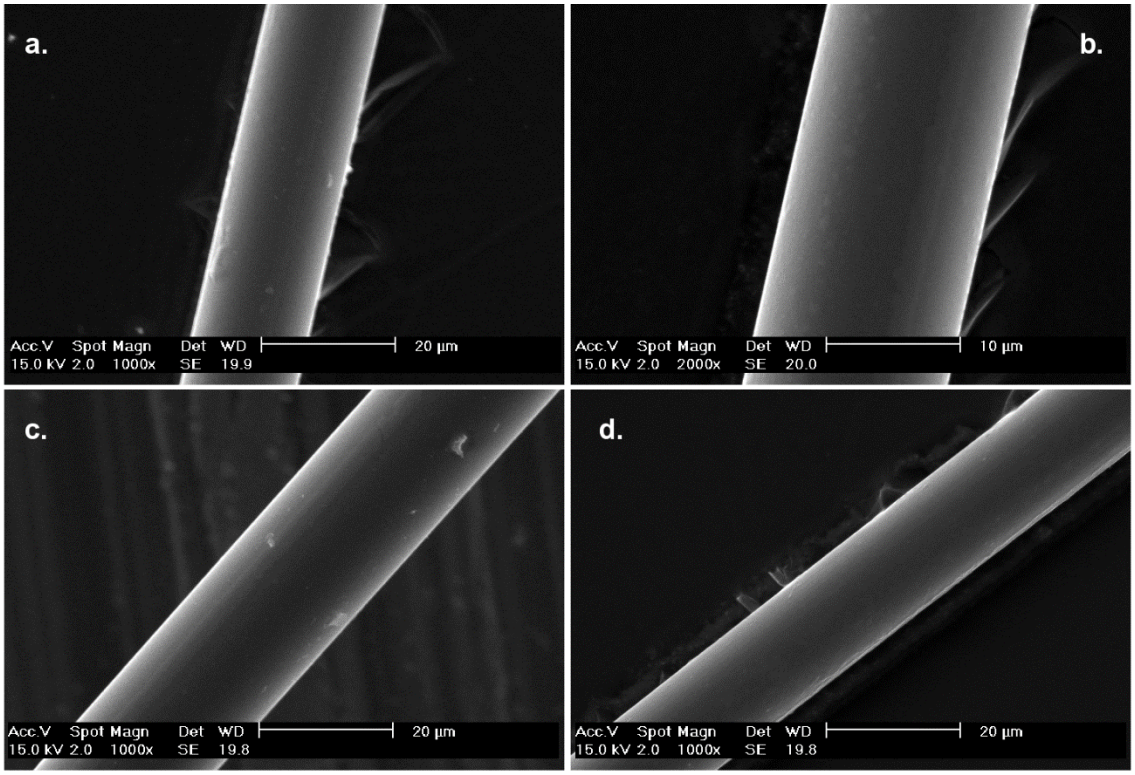

Figure 26. *SEM images of Ahlstrom R338 aged 95 °C in deionized water for a) 1 day, b) 2 days c) 1 week and d) 2 weeks.*

Similar lengthwise surface texture can be observed in figures 26a–c, which is also similar to what was observed in figure 22c. The explanation is likely the same: the texture is caused by sizing interaction with the solution environment. Figure 26d however resembles more the observations made from figure 23, which could indicate removal of sizing. The quality of the images is however worse than for the ECR images, which makes comparison difficult. Figure 27 shows images of the 1 g/dm^3 sulphuric acid solution aged fibres.

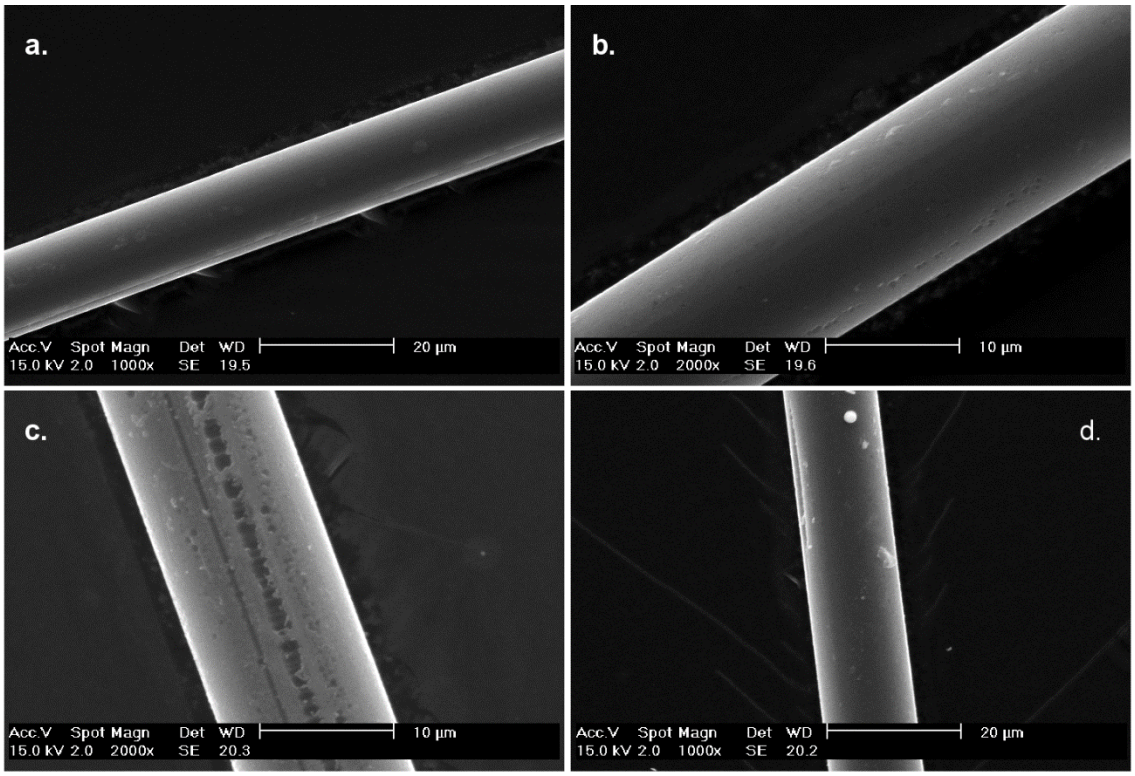

Figure 27. *SEM images of Ahlstrom R338 aged in 95 °C 1 g/dm^3 sulphuric acid solution for a) 1 day, b) 2 days c) 1 week and d) 2 weeks.*

The formation surface cracks in glass fibres aged in acidic environments is visible in the images of figure 27. It is in many cases however quite localized, which is clear from the severity of the effects, which does not appear to be determined by ageing time, as one would expect. Figure 28 presents two additional images from the heated 1 g/dm^3 solution ageing fibres.

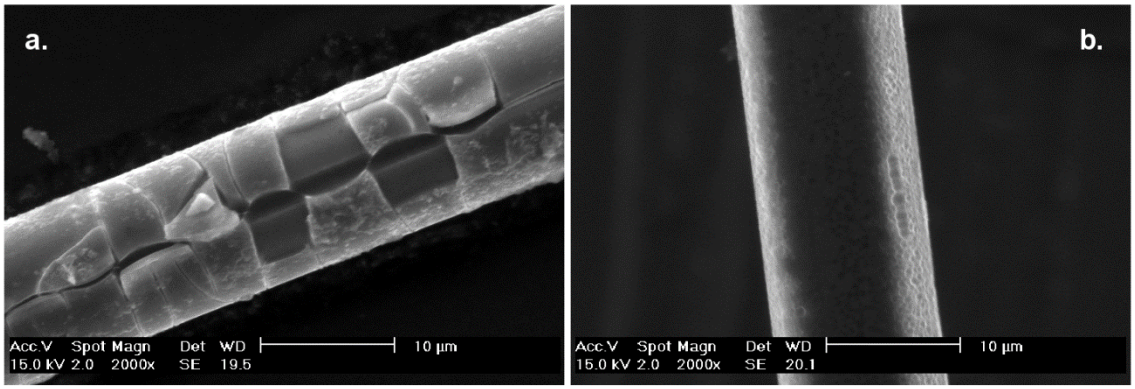

Figure 28. *SEM images of severe ageing phenomena found at specific locations in 95 °C 1 g/dm^3 aged fibres. Pictures from a) 1 day, b) 2 weeks aged samples*

Figure 28a clearly shows the core–shell structure, discussed widely in the literature presented in chapter 2. Interestingly it also presents the only noted instance of radial cracks on the fibre surface. The two weeks aged sample presented in figure 28b in turn shows an interesting pitting type corrosion behaviour throughout the fibre surface. Overall, the ageing of the E-glass appears to be localized with areas, which appear almost

unaffected to visual inspection whereas other areas have been severely affected even after very short ageing times. Figure 29 includes similar images from the E-glass fibres aged in heated 50 g/dm^3 sulphuric acid solution.

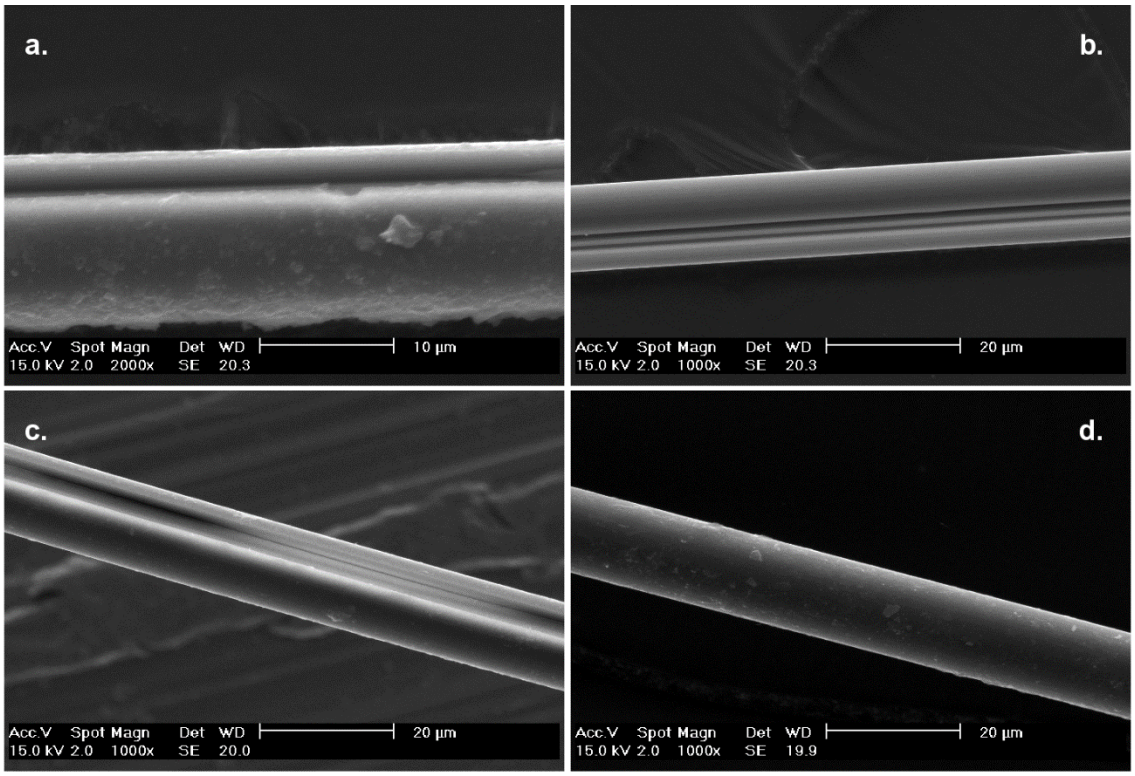

Figure 29. *SEM images of Ahlstrom R338 aged in 95 °C 50 g/dm^3 sulphuric acid solution for a) 1 day, b) 2 days c) 1 week and d) 2 weeks.*

Figure 29a–c show distinctive axial cracks, which are present in all images taken from samples that have undergone similar ageing treatment. Figure 29d is however interesting as no cracks are observed even though the other images of the same ageing environment prove the significant effect the environment has on the fibre. One possible explanation is that the altered outer layer of the fibre has detached from the fibre surface. Comparison to the scale bar reveals that the diameter of the fibre in figure 29d is approximately 15.6 micrometres, whereas the diameters of the unaged fibres have been observed between 18 and 22.5 micrometres. For comparison, the room temperature aged glass fibres are presented in figure 30. Only fibres aged for two weeks were available for study.

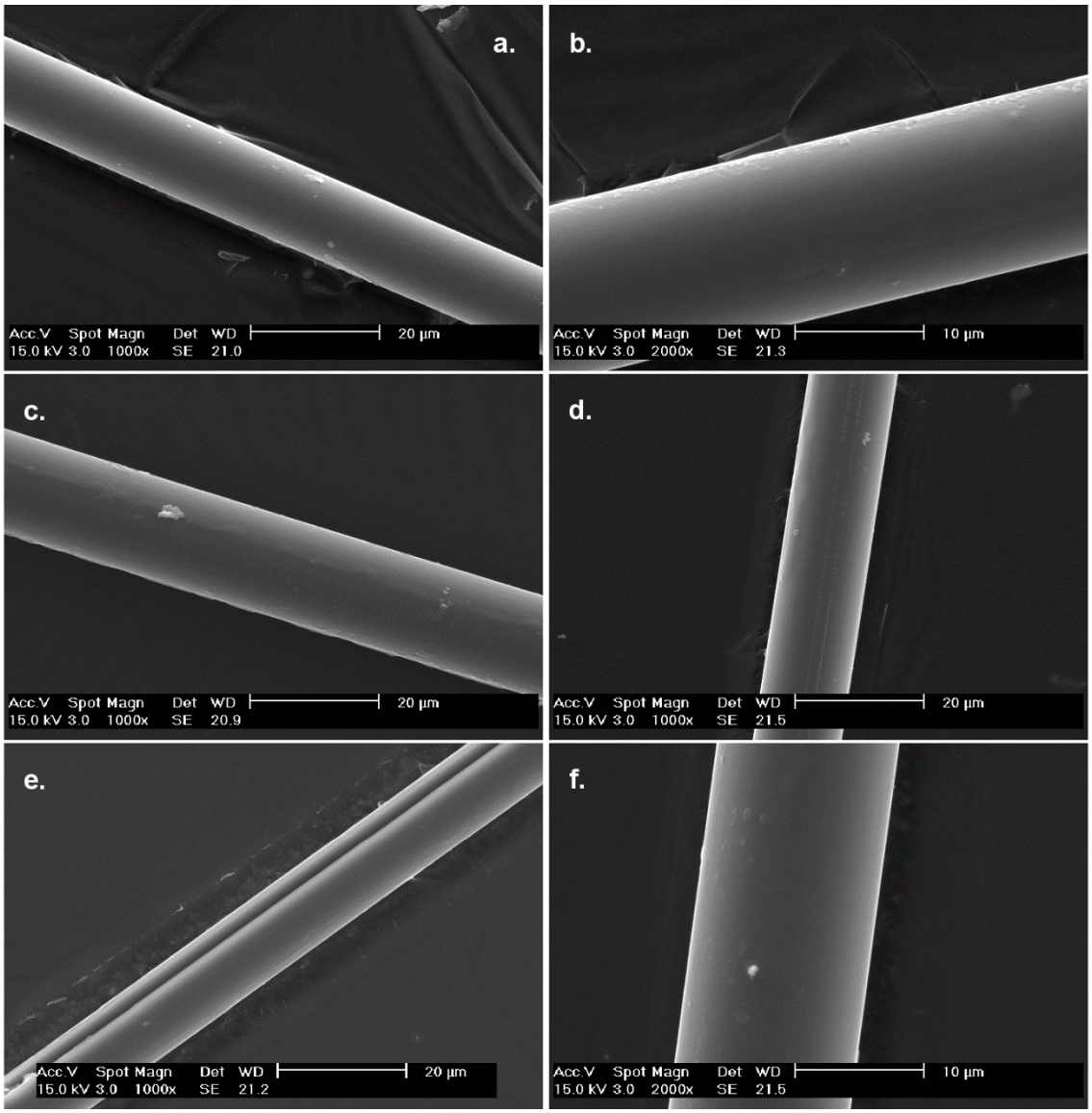

Figure 30. *SEM images of room temperature aged glass fibres. Left side: Ahlstrom R338 a) deionized water, c) 1 g/dm^3 sulphuric acid solution and e) 50 g/dm^3 sulphuric acid solution. Right side: Jushi E6CR b) deionized water, d) 1 g/dm^3 sulphuric acid solution and f) 50 g/dm^3 sulphuric acid solution.*

No severe visual markers of corrosion except in figure 30e, which depicts the 50 g/dm^3 sulphuric acid aged E-glass fibre. A clear axial crack can be observed and during imaging, it was noted to be present through the whole length of the fibre. Some surface changes can be observed in 1 g/dm^3 solution aged samples from both glass fibre grades. It is however unclear from SEM images whether the surface viewed in the image is the sizing applied on the fibre surface or the actual surface of the glass fibre.

4.4 Structural changes

Changes in resin and glass fibre chemical structures can be observed from the FTIR spectra. The results for VE resin sheets are presented in figure 31.

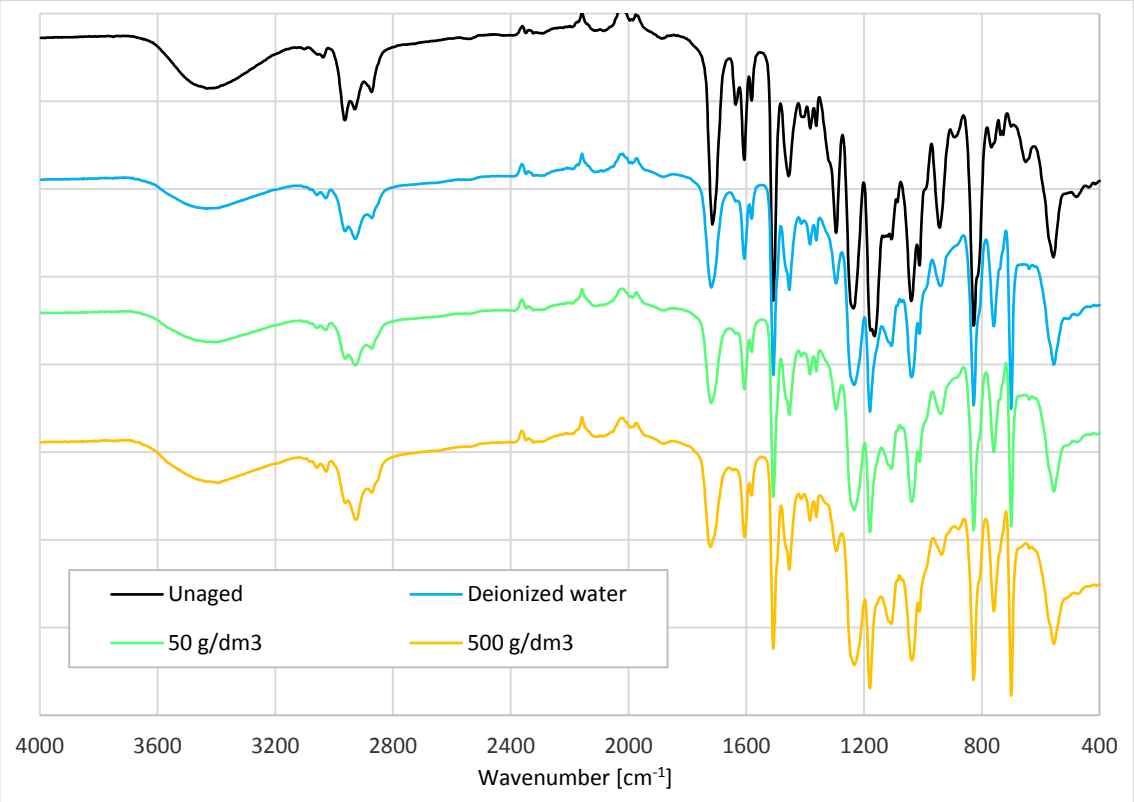

Figure 31. *FTIR spectra of the VE sheets. The vertical values have been shifted to ease observation.*

In figure 31, the notable differences are in the OH vibrations 3000–3600 cm^{-1} and in the C–H vibrations between 2800 and 3000 cm^{-1}. The latter consists in polymeric samples usually of the asymmetric and symmetric vibrations of CH_3 and CH_2 groups if present in the material. The amount of peaks is usually four in addition to which the combination vibrations of aromatic ring structures are slightly above this, as can also be seen as very weak peaks between the C–H group are and the broad OH peak in figure 31. Based on the wavenumbers of the peaks the CH group regions shows CH_3 and CH_2 asymmetric and CH_3 symmetric vibrations and the peak corresponding to CH_2 symmetric vibrations is obscured. (Silverstein et al. 1991 pp. 103,110) In the aged samples, instead of the CH_3 asymmetric, the CH_2 asymmetric is the strongest peak. The wavenumber region from 2000 to 2400 cm^{-1}, with apparent negative absorption bands is due to air contamination in the background measurement. To better observe the differences at the lower wavenumbers a limited view from the wavenumber range of 400–2000 cm^{-1} is presented in figure 32.

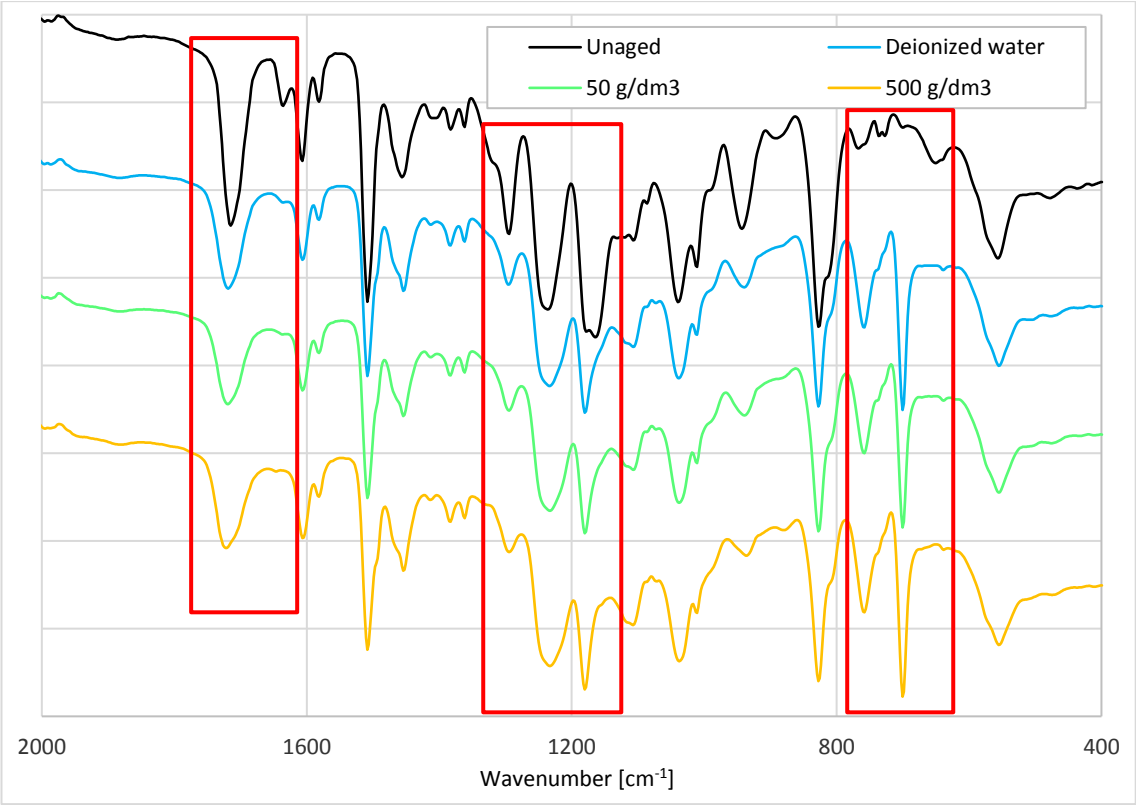

Figure 32. *The resin FTIR spectra in the range of 400-2000 cm^{-1}. Some significant regions are highlighted with rectangles.*

Some changes are also noticeable between the samples in the lower wavenumbers portion of the spectra. This region consists of most of the characteristic peaks corresponding to different polymer structures, but can be difficult to analyse correctly because of overlapping of the spectra of different structures. In the aged samples, relatively strong peaks at 700 and 760 cm^{-1} can be seen, which are not present in the unaged sample. In the aged samples, one peak at 1635 missing and the carbonyl peak at 1693 appears to be weaker compared to the unaged sample spectra. In the unaged sample a combination of two strong peaks at 1164 and 1171 cm^{-1} can be observed, while only a single peak with some shoulder is present in all aged sample spectra. The shoulder and peak intensity at 827 cm^{-1} are lower for the aged samples. It is important to note the similarity of all aged samples, despite very different ageing environments.

The glass fibre FTIR examination is aimed at observing changes in the bonding of the glass constituents, the most important being the Q_4 and Q_3 species of silica. The presence and subsequent leaching of boron in E-glass is also expected to present itself in the FTIR examination. Figures 33–37 present FTIR spectra from the glass fibre samples. In each figure, the reference spectra and aged sample spectra from two different time points – two days and two weeks – are presented. Because most of the relevant peaks in the glass spectra are observed at wavenumbers below 1500 cm^{-1} figures are limited to this region for easier observation.

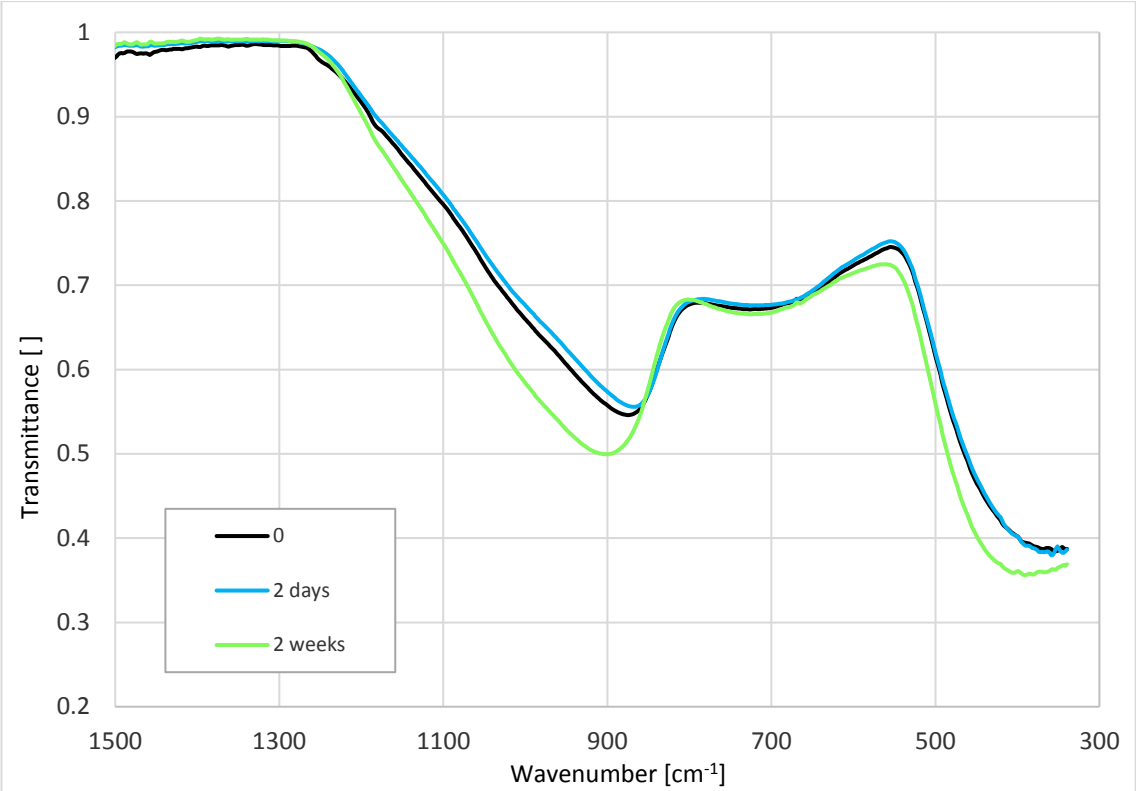

Figure 33. *FTIR spectra for Jushi E6CR glass fibres aged in deionized water.*

Three major peaks are evident in figure 33. However, the shoulder type region from below 900 to 1260 cm^{-1} suggests that several different vibrations contribute to the spectrum. Vitreous silica FTIR spectrum consists of Si–O–Si bending vibration between 400 and 500 cm^{-1} and usually more than one Si–O–Si stretching peaks between 1000 and 1300 cm^{-1} (Lynch et al. 2007). The composition of the sample however differs greatly from vitreous silica. It is possible that the presence of aluminium and network modifiers shifts the silica peaks closer together. IR spectroscopy studies to sol-gel mullite samples by Padmaja et al. (2001) assigned Si–O–Al vibrations also to this region. The maximum of the peak corresponds approximately to the wavenumber region commonly reported for Q_3 silica, meaning silica with a single NBO (Lynch et al. 2007; Khalil et al. 2008; Vidal et al. 2016). Analysis of sodium silicate solutions with FTIR conducted by Lucas et al. (2011) presents that the broad complex peak from 900 to 1200 cm^{-1} is a result of many Si–O–Si asymmetric vibrational modes while the Si–O–Si symmetric vibration band is around 768 cm^{-1}. The stretching modes of Al–O–Al linkages are however also in this region at 765 and 612 cm^{-1} (Padmaja et al. 2001). Other notable silicate vibrations reported are $Si–O^-$ stretching at 850 cm^{-1}, analogous to the Q_3 vibrations mentioned earlier, and O–Si–O bending vibration at 557 cm^{-1}, which is higher than what is reported elsewhere or observed in figure 33. (Lucas et al. 2011)

The changes caused by deionized water ageing consist of some increase in the intensity of these peaks and a slight shift observable for the 877 cm^{-1} peak maximum to approximately 900 cm^{-1} and for the 350 cm^{-1} maximum to 390 cm^{-1}. Rather similar results can be observed from the 1 g/dm^3 sulphuric acid solution ageing for the ECR glass fibres.

The ageing seems to be most evident in the Si–O–Si vibrations between 850 and 1100 cm^{-1} with the peak maxima shifting to a higher intensity and wavenumber. This result is similar to observations by Lynch et al. (2007) for the corrosion of glass surfaces. Interestingly however, both with the deionized water and with the 1 g/dm^3 sulphuric acid solution the ageing initially has the opposite effect as observable from the two day ageing spectrum. The spectra for ECR fibres aged in 50 g/dm^3 sulphuric acid solution are presented in figure 34.

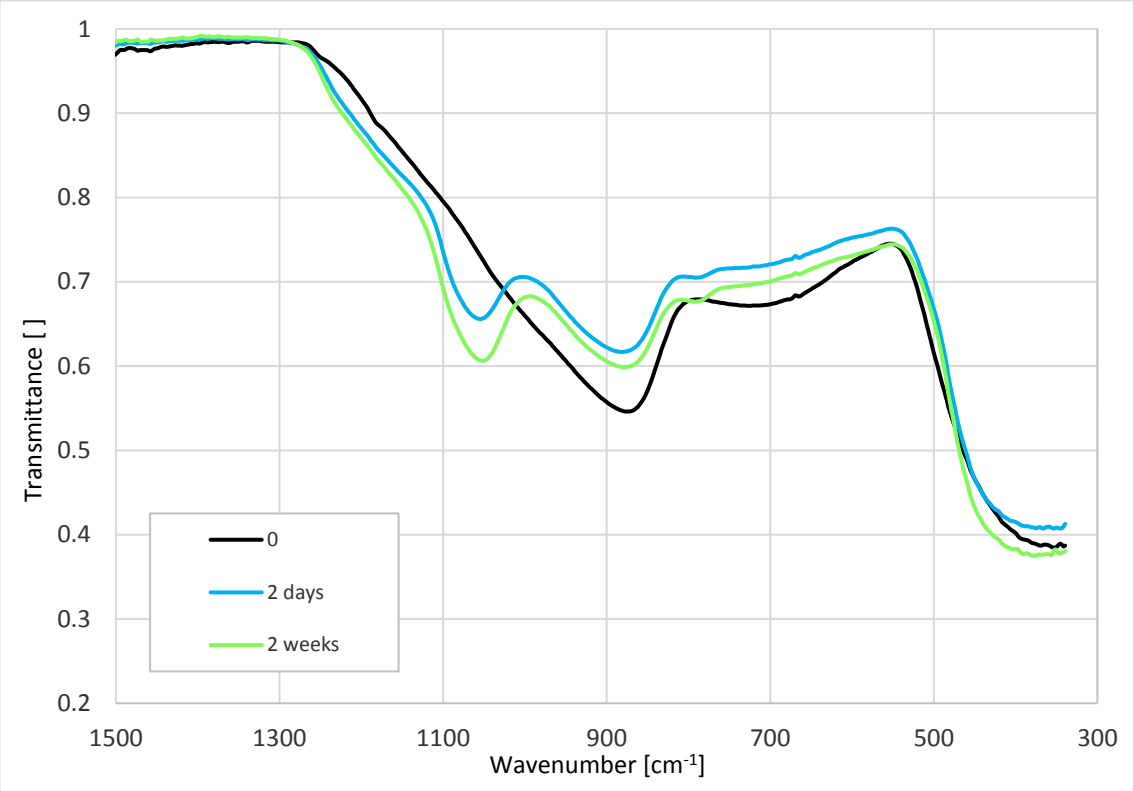

Figure 34. *FTIR spectra for Jushi E6CR glass fibres aged in 50 g/dm^3 sulphuric acid solution.*

The strongest acid environment appears to cause significant changes in the glass structure. The maximum above 700 becomes indistinctive from the surrounding spectrum, but a very small maximum can be seen at approximately 790 cm^{-1}. The region previously mentioned as most affected by ageing is significantly altered. The initially single broad peak is replaced by two distinctive peaks with a broad shoulder extending all the way to 1260 cm^{-1}. The first of the two maxima corresponds well with the maxima from the unaged sample. The second peak maximum is at 1055 cm^{-1} after two days and at 1050 cm^{-1} after two weeks of ageing. One significant change is not visible in figure 34. A broad peak around 3000–3600 cm^{-1} indicates the presence of OH groups in the sample. Complete spectra from the glass FTIR measurements are collected in appendix 3. The peak is rather weak compared to the major peaks presented in figure 34 but the distinctive shape, wavenumber region and slight increase with ageing make the analysis reliable. Figure 35 presents the E-glass spectra comparable to the one presented for ECR in figure 33.

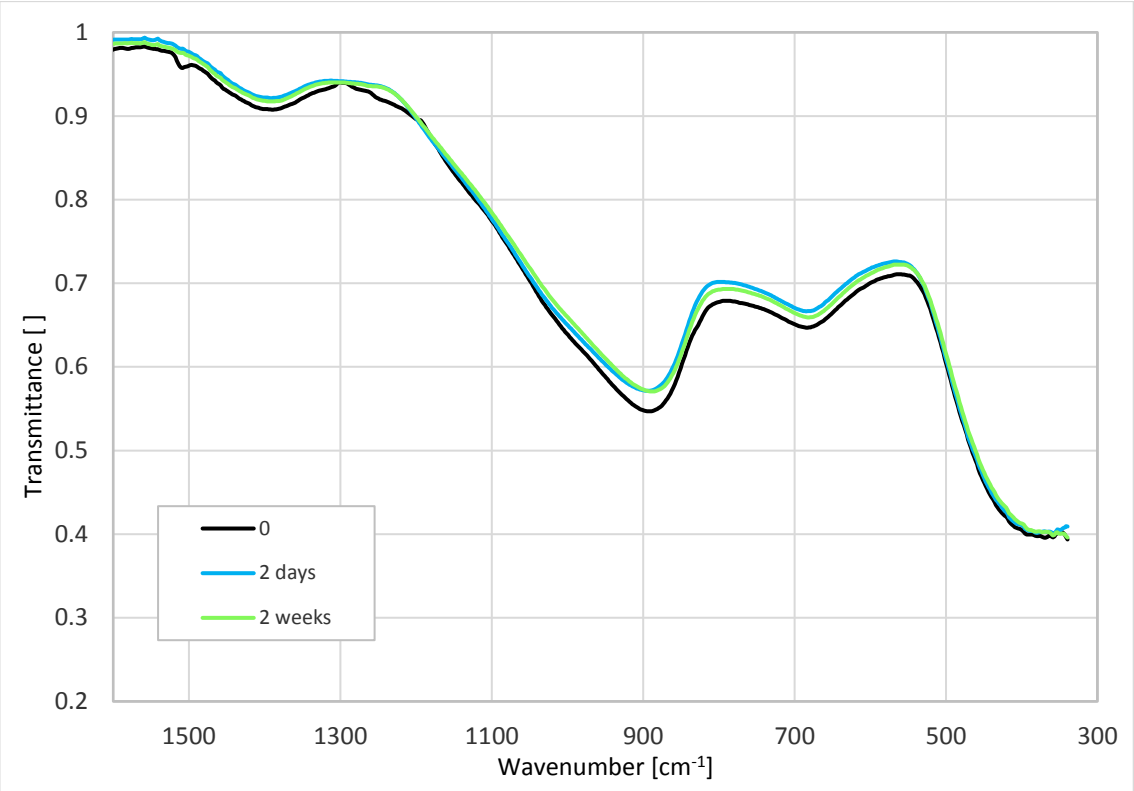

Figure 35. *FTIR spectra for Ahlstrom R338 glass fibres aged in deionized water.*

Notable differences to the ECR-glass include the broad absorption band at 1380 cm^{-1}, which was not present in previous figures and a slightly stronger and narrower peak in the 600–800 cm^{-1} region, which has the maximum absorption at 680 cm^{-1}. In literature regarding borate glasses, both of these regions are presented as characteristic of the borate structure. The narrow peak at 680 is in the region of B–O–B bending vibration and the higher wavenumber broad absorption around 1380 is in the range of B–O and $B–O^-$ bond vibrations of BO_3 type structures. In their study, Ali et al. (2017) assigned the $B–O^-$ bond vibration at 1368–1311 $cm^{-1,}$ which is close to the observed absorption maxima in the E-glass sample and the B–O vibration at 1220–1052 cm^{-1}. (Yiannopoulos et al. 2001; Ali et al. 2017)

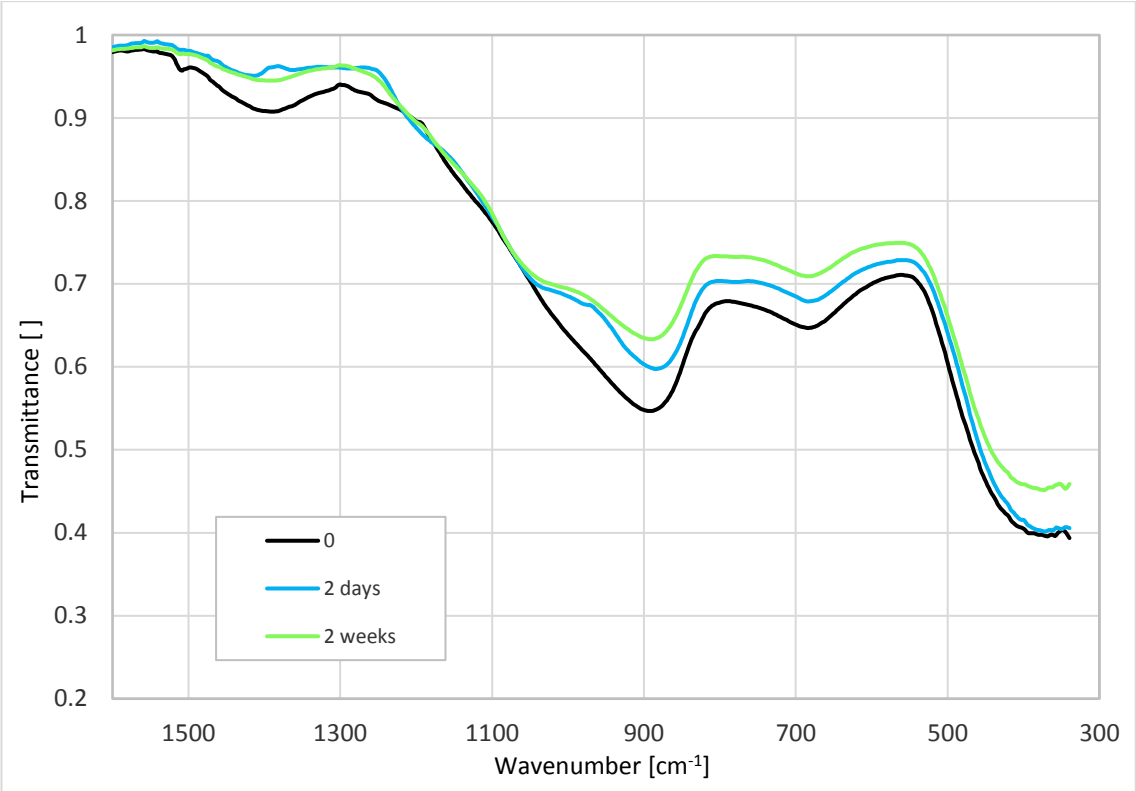

Figure 36. *FTIR spectra for Ahlstrom R338 glass fibres aged in 1 g/dm^3 sulphuric acid solution.*

A notable trend in 1 g/dm^3 sulphuric acid ageing is the decreasing intensity of the absorption with ageing time. It is however possible that some of the change in intensity is caused by different sample contact between the samples, as the baseline position for the unaged and the aged fibres are slightly different. The Si–O–Si and Si–O–Al vibration region at 850–1200 cm^{-1} shows similar response to ageing which was observed for ECR glass with the 50 g/dm^3 sulphuric acid solution. The changes are however less significant. The absorption band expected to correspond to borate structures at approximately 1400 cm^{-1} loses intensity significantly even after two days of ageing, whereas the low wavenumber region below 400 cm^{-1} is almost unchanged after two days. Also like to the ECR-glass aged in 50 g/dm^3 sulphuric acid solution, the 3000–3600 cm^{-1} has the broad and weak OH vibration band.

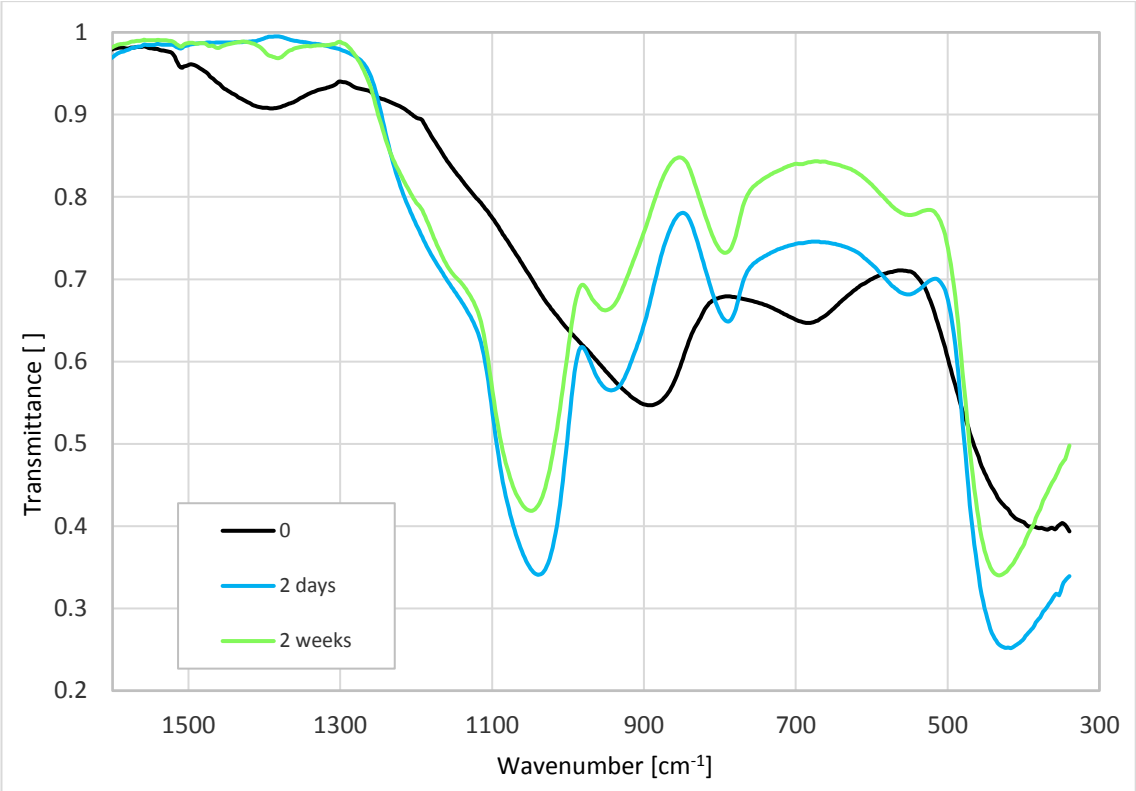

Figure 37. *FTIR spectra for Ahlstrom R338 glass fibres aged in 50 g/dm^3 sulphuric acid solution.*

As with the ECR glass the FTIR spectrum of the glass changes significantly when aged in the 50 g/dm^3 sulphuric acid solution. The absorption peaks previously speculated as resulting from borate structures at 1380 and 680 cm^{-1} are no longer present. However, the intensity of the remaining absorption bands is increased significantly and their narrow shape is an indication of the purity of the sample. Strong absorption bands are detected at 430, 550, 790, 950 and 1050 cm^{-1} with a shoulder towards higher wavenumbers. The changes in chemical structure appear to penetrate quickly into the glass structure as the spectrum has the final absorption bands only after two days of ageing. Subsequent ageing result only in decreased intensity of the measured spectrum.

4.5 Tensile properties of glass fibres

The tensile testing of glass fibres does not include glass fibres aged in 50 g/dm^3 sulphuric acid. These samples were excluded as the properties of the Ahlstrom R338 fibres aged for more than two days, had decreased too significantly to withstand the required handling. This is however, an interesting result in itself and will be noted when changes in glass fibre mechanical properties are discussed. Figure 38 presents an example of the test results. The figure depicts measured force versus test time for unaged and 2 weeks in 1 g/dm^3 sulphuric acid solution aged ECR-glass fibres.

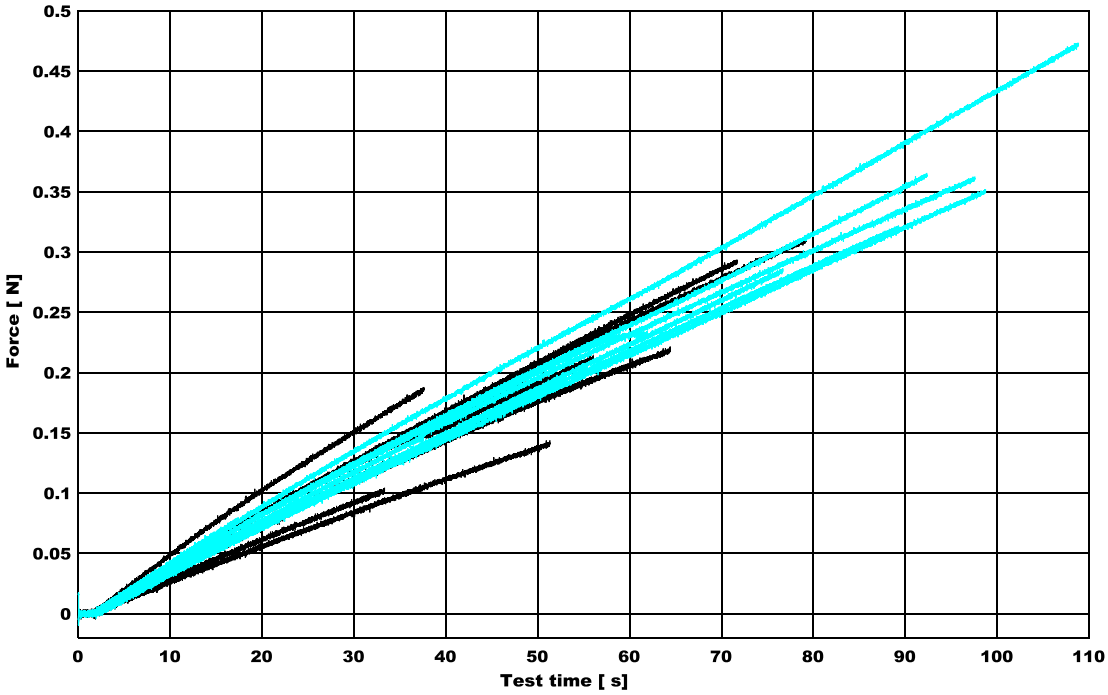

Figure 38. *ECR-glass fibre tensile test results for unaged (cyan) and 2 weeks in 1 g/dm^3 sulphuric acid aged samples (black).*

The average maximum force measured decreases significantly for the aged fibres. The scattering of the curves is also more pronounced for the aged samples. It needs to be noted however that the presentation of the results in figure 38 does not account for the diameters of the fibres, which were noted to vary significantly. Especially with the E-glass fibres, a notable difference in the fibre diameters is observable with different ageing environments. The average diameters with standard deviations of the tested glass fibres are presented in table 4.

Table 4. *Average diameters (in micrometres) of the glass fibres selected for mechanical testing.*

Fibre	Unaged	Deionized water	1 g/dm^3 sulphuric acid
E-glass [µm]	19.3 ± 2.5	17.4 ± 2.0	14.6 ± 1.0
ECR-glass [µm]	16.9 ± 1.1	15.6 ± 1.3	16.7 ± 1.8

Some samples also broke prematurely because of additional stresses caused by impurities or the slight impact from the grips of the device closing. Such samples were excluded from further analysis. The average tensile strengths of the tested fibres are presented in figure 39. The error bars represent standard deviations.

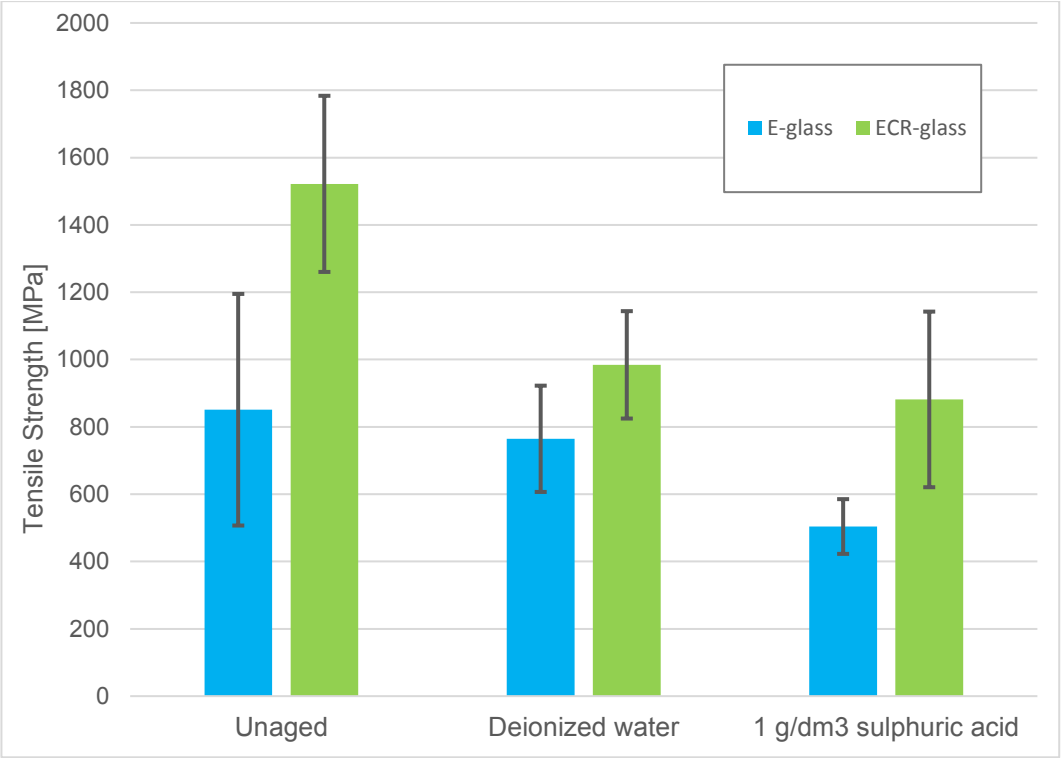

Figure 39. *Tensile test results of glass fibres aged for two weeks in 95°C, deionized water. Error bars represent the standard deviations.*

Figure 39 shows changes in the mechanical properties of the fibres with the ageing environments. After two week in deionized water, the tensile strengths of the ECR-glass is approximately 35 % lower than for the unaged sample. The significant difference in the tensile strengths of the unaged fibres is an interesting result, as comparative values for E-glass and its boron free variants – such as ECR-glass – are presented in literature (Wallenberger et al. 2001). The number of parallel samples in the examination is however too small to make definitive conclusions on the behaviour of the samples. Qualitatively, the effect of ageing on the mechanical properties appears significant.

To evaluate the difference in behaviour without the strain-measurement, relative modulus values were formed from the ratio of the average slopes of the stress-time curve to the highest slope observed during the measurements. These results are presented in figure 40.

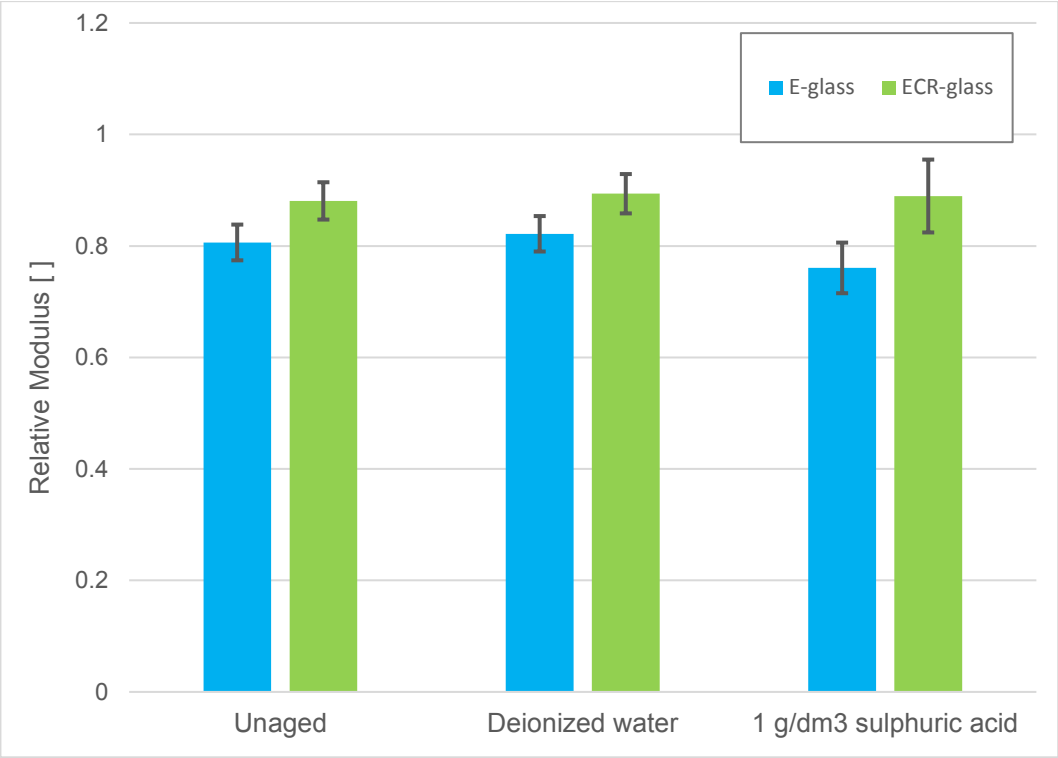

Figure 40. *Tensile test results of glass fibres aged for two weeks 95°C, 1 g/dm³ sulphuric acid solution.*

This part of the mechanical behaviour appears practically unaffected for the ECR-glass. A slight decrease in the slope can in turn be observed for the sulphuric acid solution aged E-glass fibres. The role of ageing in the decreasing of glass fibre mechanical properties would seem to present mostly in the tensile strength, while the modulus remains unaffected. This result should however be confirmed with a similar high accuracy measurement device, which also has the required tools for strain evaluation.

4.6 Surface composition of glass fibres

The data from the EDS analysis has significant contributions from oxygen, arising from the oxide nature of the compounds in the glass and from the carbon surface used to prevent charging of the sample surface during SEM imaging. Both of these are excluded from the presented results as they are of little relevance to the glass behaviour. The results presented are modified as fractions of the specified element from the sum of the atomic percentages of relevant elements. Relevant elements in this case are sodium, magnesium, aluminium, silicon, potassium and calcium. This way the results of for example the reference samples are in the same range as the corresponding oxide contents in table 1. Very low contents are however excluded from view, as the accuracy of the method is limited. Because of this only aluminium, calcium and silicon fractions are presented. EDS results of both glass fibre types in deionized water are presented in figure 41.

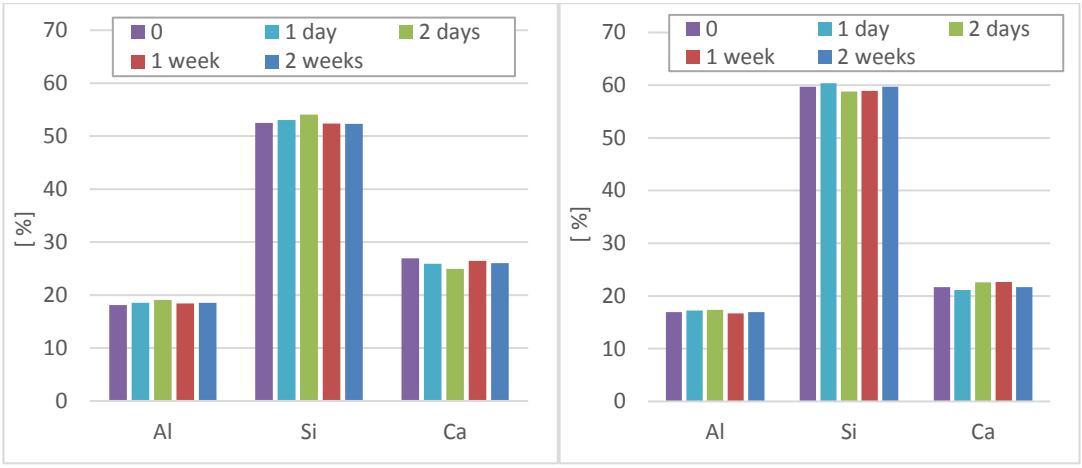

Figure 41. *EDS analysis of the glass fibres aged in 95 °C deionized water. Left) E-glass, right) ECR-glass.*

The EDS reveals no significant changes in the glass composition because of the ageing. Some variation can be expected from the measurement itself and the differences observed are likely mostly because of this inaccuracy. Figure 42 presents a similar overview of the 1 g/dm^3 sulphuric acid aged glass fibres.

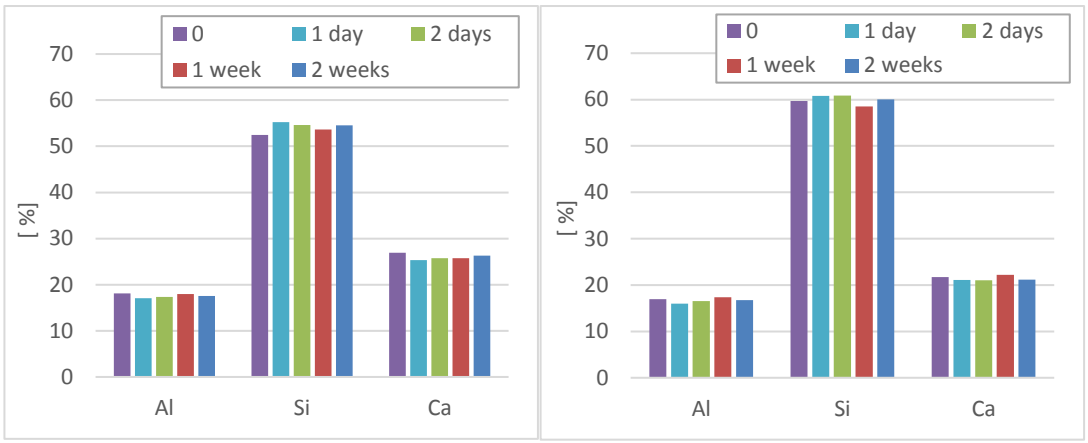

Figure 42. *EDS analysis of the glass fibres aged in 95 °C 1 g/dm^3 sulphuric acid solution. Left) E-glass, right) ECR-glass.*

Like the previous results for deionized water, the results of the EDS analysis of 1 g/dm^3 sulphuric acid solution aged glass fibres show no significant compositional changes. Some trend towards higher silicon and lower aluminium and calcium can be observed, but in terms of significance, this in the range of experimental variation and thus is not sufficient to indicate ageing. Figure 43 presents the overview of 50 g/dm^3 sulphuric acid aged samples.

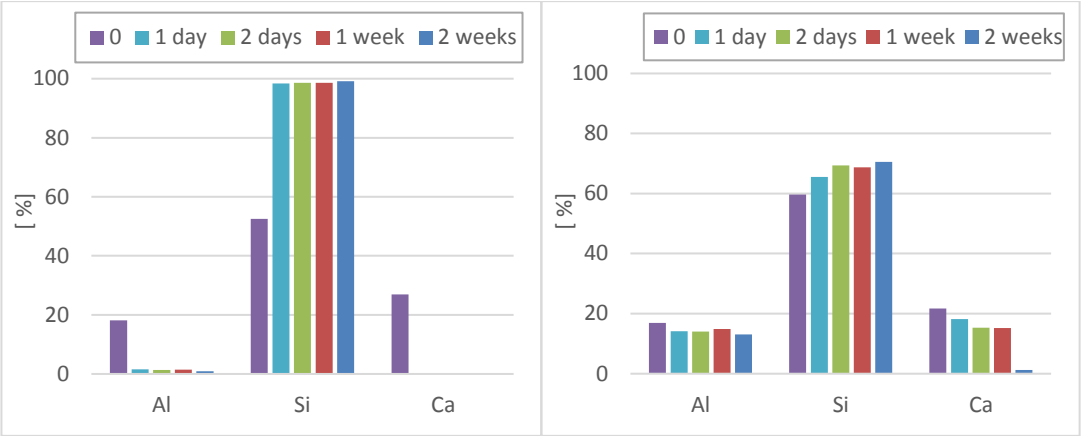

Figure 43. *EDS analysis of the glass fibres aged in 95 °C 50 g/dm^3 sulphuric acid solution. Left) E-glass, right) ECR-glass*

The difference in behaviour between the two glass fibre grades is evident from figure 43. After one day of ageing the interaction with the sulphuric acid solution has caused a silica right layer to form on the E-glass surface. This layer comprises only of silica and trace amounts of aluminium oxide. Calcium appear to be complete depleted from the observed depth of the sample. The ECR-glass shows similar behaviour, but significant calcium depletion is observed only after two weeks of exposure and a significant amount of aluminium oxide is present even then.

4.7 Leaching results

ICP-MS analysis of the glass fibre ageing solutions was done to determine the presence and abundance of the leached glass constituents. The test offers significant information on the differences between solution-temperature combinations and their effect on glass fibres. Figure 44 presents ICP-MS results from the deionized water ageing.

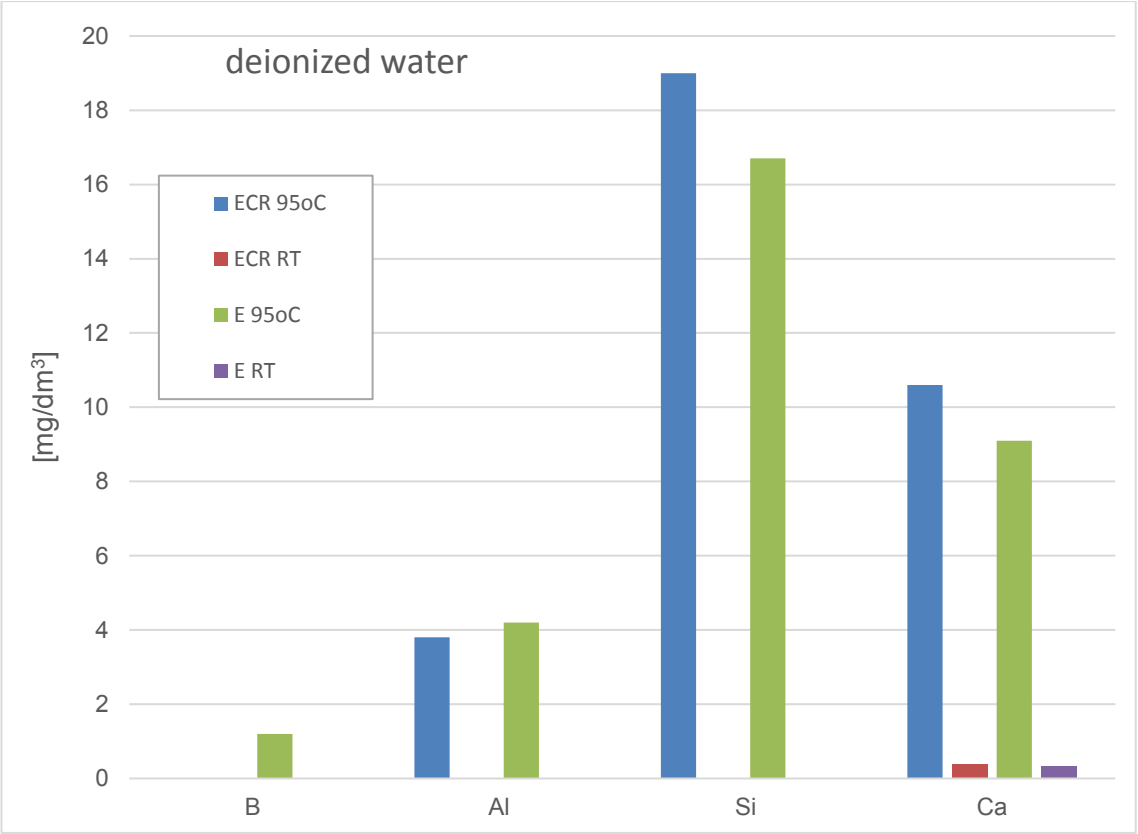

Figure 44. *ICP-MS of the deionized water used to age the glass fibres for two weeks. Only for qualitative purposes.*

No significant leaching products are observed in room temperature ageing. From notable leaching products, only trace amounts of calcium are present in the solution. In the more aggressive environment of 95 °C during ageing, all major leaching products are present in the solution. Silicon most likely in the form of some silanol-type hydrolysis product is the most significant. Calcium and aluminium as the next two most abundant glass constituents are present in concentrations roughly corresponding to the actual glass composition. From the E-glass ageing solution, also a significant amount of boron can be observed. The small amount of boron is significant as the relative amount of boron in the glass is low. Table 1 in chapter 2.2 (page 12) presents the usual glass composition ranges, which are useful for comparison. The ICP-MS results from the 1 g/dm^3 sulphuric acid solutions are presented in figure 45.

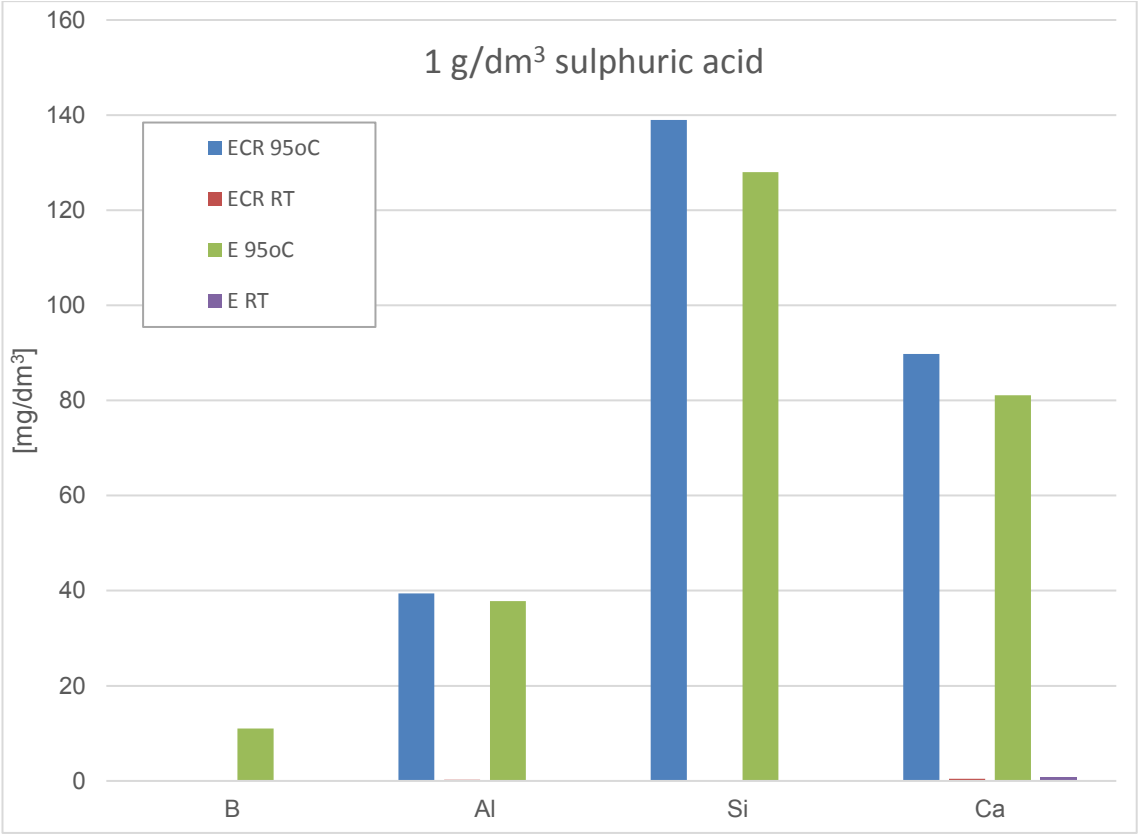

Figure 45. *ICP-MS of the 1 g/dm^3 sulphuric acid solution used to age the glass fibres for two weeks. Only for qualitative purposes.*

The relative concentrations of different constituents in the 1 g/dm^3 sulphuric acid are similar to those in deionized water. However, it is important to note that the actual concentration values are approximately ten times higher than in the previous figure for deionized water. The phenomena is however not present in the room temperature results. The calcium concentrations in the 1 g/dm^3 ageing solution is roughly twice the calcium concentration in the corresponding deionized water solution. The results from the higher sulphuric acid concentration 50 g/dm^3 are presented in figure 46.

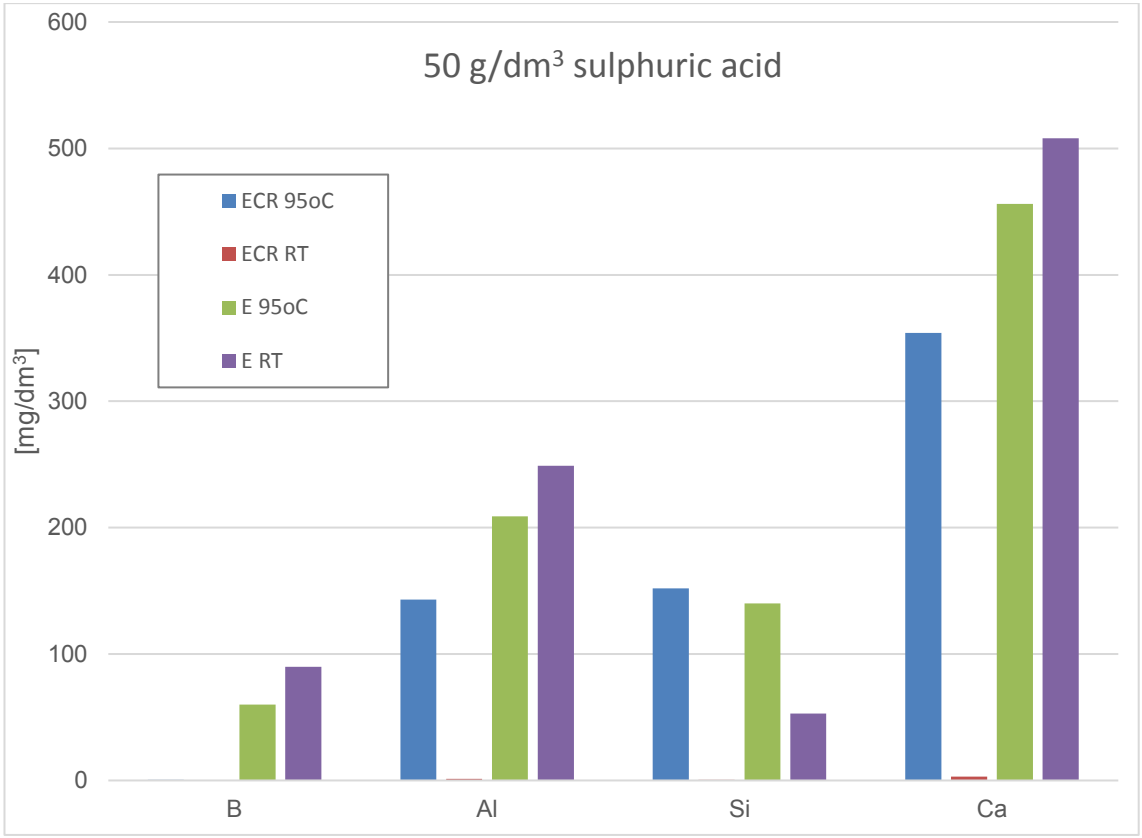

Figure 46. *ICP-MS of the 50 g/dm^3 sulphuric acid solution used to age the glass fibres for two weeks. Only for qualitative purposes*

When comparing figure 46 to the previous two figures, major changes in relative concentrations of the glass constituents can be observed. Silicon is no longer the most abundant glass constituent found in the solution. Calcium is leached in very significant concentrations and in the E-glass ageing solutions, aluminium also is present in higher concentrations than silicon. A significant result is also the very low concentrations in room temperature ECR ageing solution. The highest concentration, which is calcium for ECR in room temperature as well, is approximately 3 mg/dm^3. The differences in E-glass behaviour with ageing temperature are noteworthy, as the hydrolysis of the silica network appears dependant on the ageing temperature.

4.8 Interfacial properties

Because of scheduling limitations only a part of the results are presented in this work. The rest of the microbond test results including more environments and several parallel samples from all conditions will be presented elsewhere. Figure 47 presents deionized water aged microbond samples from the ECR–epoxy combination.

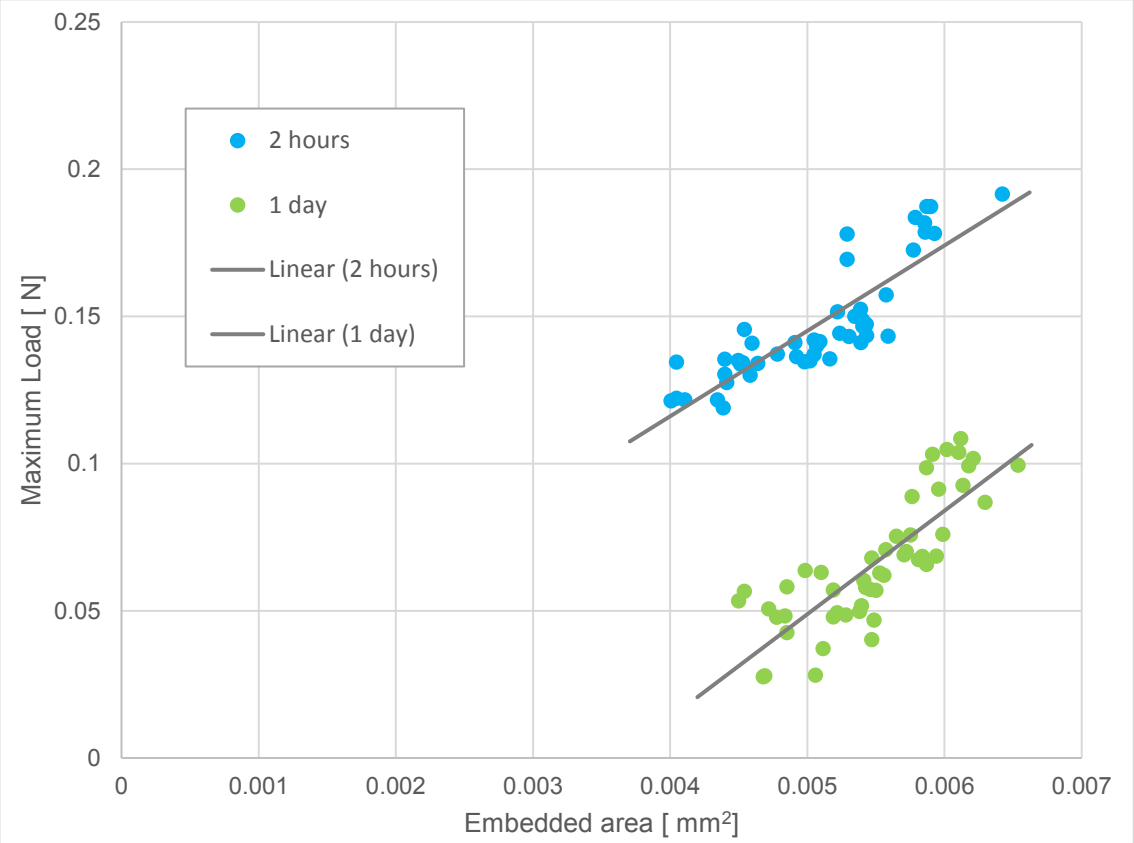

Figure 47. *Microbond test results for water aged Jushi E6CR fibres with droplets made from EPON 828 epoxy resin. Linear regression parameters for the linear fits: 2 hours) slope = 29.017 N/mm^2, R^2 = 0.7423, 1 day) slope = 35.155 N/mm^2, intercept = -0.1269 N, R^2 = 0.6666.*

The results show significant decrease of the interfacial shear strength. The IFSS calculated for the samples with equation (1) are 29.03 ± 1.93 MPa and 11.85 ± 3.07 MPa, for the 2 hours and 1 day aged samples, respectively. The slope of the load–area curve should correspond with the IFSS, which is however not the case with the 1 day sample. The cause of this is unclear. Figure 48 presents the microbond test results for the E-glass–epoxy combination.

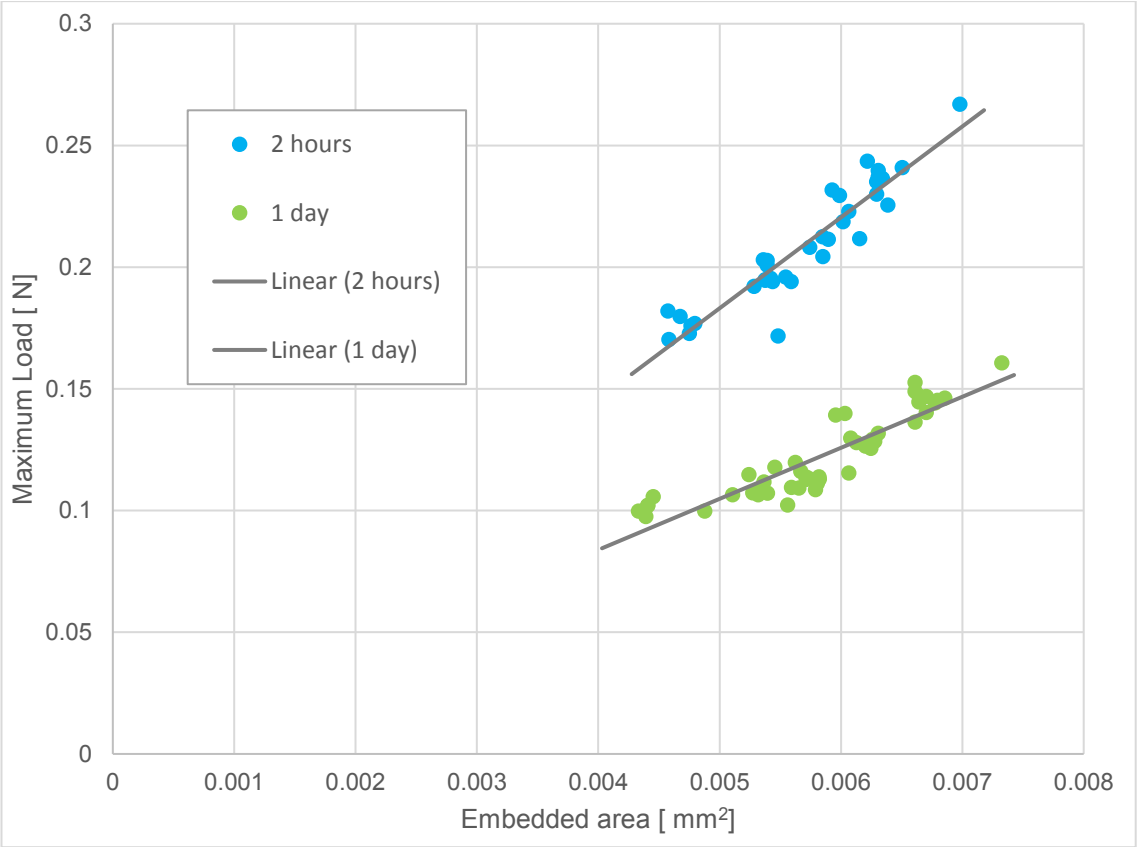

Figure 48. *Microbond test results for water aged Ahlstrom R338 fibres with droplets made from EPON 828 epoxy resin. Linear regression parameters for the linear fits: 2 hours) slope = 37.347 N/mm^2, intercept = 0.0036 N, R^2 = 0.8686, 1 day) slope = 20.961 N/mm^2, R^2 = 0.8073.*

E-glass fibres show a similar trend of lower IFSS with longer ageing time. The IFSS results for the 2 hours and 1 day aged E-glass fibres are 36.71 ± 1.57 MPa and 21.59 ± 2.37 MPa, respectively. The 1 day aged E-glass fibres exhibits significantly greater interfacial properties than the similar ECR-glass fibre. One should however note that these are singular fibre samples and complete characterization of the fibre properties would require significantly larger test series.

5. DISCUSSION

A variety of testing methods has revealed significant changes in the properties of the different materials present in glass fibre reinforced PMCs. As in the literature review part of the work, chapter 2, the ageing effects are discussed separately for the matrix resins, glass fibre reinforcements and the interface between the two. The last of these is also indicative of the composite as a whole, so analysis of the importance of the other results for the composite as a whole are included in chapter 5.3 as well.

5.1 Changes in the resin matrix

Most of the resin testing was limited to a VE resin because of its significance as the chemically resistant thermosetting polyester resin and the limited schedule of the work. The weight of resin sheets with different thicknesses was observed as the ageing progressed and the diffusion of the solution environment followed Fickian behaviour reasonably well. However, with the sulphuric acid environments a sulphuric acid concentration related negative weight change was also observed. Because of the ester groups in the resin, acid catalysed hydrolysis likely at least contributes to this phenomenon. It is also likely that the concentration difference created by the faster diffusion of water molecules, compared to the larger acidic constituents, hinders the diffusion of water into the material because of osmosis (Ehrenstein & Pongratz 2013, p. 710; Zumdahl 2009 pp. 867–868). Overall, the observed maximum weight increase shows a clear trend with sulphuric acid concentration. It should be noted that the sulphuric acid concentrations used, 50 and 500 g/dm^3 of solution are very severe environments even without the relatively high temperature. Based on the data received from Outotec, the pH values for these environments at 95 °C are 0.40 and -0.36, respectively.

In an effort to observe chemical changes in the resin, FTIR spectra from the aged resin sheets and a reference sheet from the same material were measured. The most significant peaks are collected in table 5 and most the absorption bands are identified for vibrations of certain chemical structures present in the VE. It is recommended to keep in mind the chemical structure of the resin as depicted in figure 2, and the nature of the crosslinking reaction advancing from the unsaturated carbon–carbon bonds.

Table 5. *Analysis of the major peaks in the FTIR spectra of VE sheets.*

Peak [cm^{-1}]	Comment	Peak identification	Ref.[a] page
3429	broad	ν O–H, Hydrogen bonded	p.110
3024, 3060	weak	ν C–H, Aromatic	p.108
2962		ν_{as} CH_3	p.103
2925		ν_s CH_3	
2871	2850 shoulder in 500 g/dm^3	ν_{as} CH_2 (ν_s CH_2)	
1712	strong	ν C=O	pp.113–114
1637		ν C=C, vinyl group	p.106
1606, 1581		ν C=C, ring	p.108
1508	strong		
1456		δ_s CH_2, scissoring δ C–O–H	p.104 p.118
1294		ν C–O, ester	Ahmad et al. (2005)
1234		ν_{as} C–O–C	p.112–113
1163, 1170	1170 shoulder in unaged sample 1170 peak value for aged samples	C–(C=O)–O	p.120
1107	shoulder in unaged sample	C–C–O, ester	
1037		C–C–O, alcohol ν_s C–O–C	p.120 pp.112-113
1010			
943	weak in aged		
827	strong	δ(oop) =C–H, para.	p.109
757	weak in unaged		
736, 727	weak, obscured by the 757 cm^{-1} peak in aged samples	ρ CH_2, doubled for solid sample	p.104
700	strong, not present in unaged	δ C=C, ring	p.109
649	Broad, weak not present in aged samples		
555			

[a] Peak identification based on Silverstein et al. (1991).

Based on the analysis of the absorption bands, some of the observations made from the spectra can be explained with changes in the chemical structure of the resin. The unsaturated carbon–carbon absorption band of vinyl groups, at 1637 cm^{-1}, is weak but observable in the unaged resin and is not observed in the aged samples. Vinyl groups can be found in unreacted crosslinking sites in the vinyl ester resin and the absence of the peak in aged samples indicates fewer unreacted chain ends. The reason for this can be

either removal of unreacted resin or post-curing reactions. The wavenumber region at approximately 1000–1300 cm^{-1}, with several absorption peaks characteristic to the ester groups in the resin, also changes significantly with ageing. This means some chemical changes, likely from hydrolysis of the ester structures. Unfortunately, an unambiguous peak allocation for some of the most significant changes in the spectra such as the peaks at 700, 757 and 943 cm^{-1}, that would also agree with the known chemical structure of the resin, was not found.

Visual changes caused by ageing were also observed under an optical microscope. The quality of the surface deteriorates significantly with all ageing environments, though likely for slightly different reasons. With the deionized water and 50 g/dm^3 sulphuric acid solution, which underwent notable weight increase due to water diffusion into the material, the swelling of the material is one possible explanation for the observed change in surface quality. For the 500 g/dm^3 solution aged sample, the more likely reason is chemical degradation of the resin by the acid. This explanation agrees with the weight change results, which indicate some material loss in the sample. The defects noted inside the water and 50 g/dm^3 solution samples could be extensions of the phenomena causing the surface defects as well. Osmotic pressure from the solution and volatiles and the possible defects it causes is presented as one of the significant ageing phenomena for thermosetting polyester resins (Boinard et al. 2000; Gautier et al. 2000).

Thermal analysis of the resin is in agreement with the previous results. The DSC analysis of the unaged resin shows significant post-curing in the resin, but some post-curing appears to happen even in the aged samples. Analysis of the loss factor peak in DMTA, shows a clear behavioural difference between samples that have and have not been in contact with sulphuric acid solutions. The glass transition temperatures also show a trend with higher glass transition temperatures when aged in sulphuric acid solutions. DMTA results, however, show the highest glass transition temperature for the unaged sample. The rest of the samples follow the previously mentioned trend. It is possible that a measuring error causes some of this behaviour, for example, the placement of the thermocouple responsible for sample temperature measurement was slightly misadjusted. The behaviour could also be a result of the slightly different processing of the samples, which unfortunately cannot be elucidated further as the samples are made from different resin batches and by different personnel. The flexural modulus, approximated from the complex modulus of the DMTA measurements was almost unchanged by ageing. A slight increase was noted when compared to the unaged sample, that is likely caused by post-curing. This result is interesting, as the modulus of the composite has been reported to decrease significantly with aqueous environment ageing (Fraga et al. 2003; Visco et al 2008). Some of the modulus change is however likely due to the plasticizing effect water in the resin structure has, which was excluded in this work by allowing the samples to dry before testing.

Overall, the results from various tests correspond well to those found in literature. Ageing in heated aqueous environments begins with diffusion of the solution into the sample. Water appear to be the most efficient in penetrating the structure, whereas the acidic constituents begin degrading the resin from the surface. The heated environment appears to result in post-curing and the acidic environment causes some change in the structure, based on the significantly different loss factor peak noted in the DMTA results. Interestingly, the differences between water and sulphuric acid solution aged samples in the FTIR spectra were not significant. Visible defects were formed inside the resin by water, likely due to the crazing phenomenon discussed in literature.

5.2 Changes in fibre reinforcements

A variety of methods was used to observe the changes caused by the solution environments to two grades of glass fibres. When analysing the results, one must keep in mind the accelerated nature of these ageing tests. In actual applications, the resin matrix surrounding the fibre reinforcements limits the access of the environment to the fibres significantly. However, as it has been shown in the resin tests the matrix will not prevent solution environment access to the fibres indefinitely, especially at application where the composite is under mechanical load. (Ehrenstein & Pongratz 2013; pp. 709-713,817 Li et al. 2013). Therefore, the fibre response to the environment as the major load-bearing component in the composite is of great importance to its durability.

Mechanical properties of both fibres were reduced with ageing in the selected environments. Most notable change is the catastrophic property loss exhibited by the E-glass in 50 g/dm^3 sulphuric acid solution. The chemical analysis consisting of FTIR, EDS and ICP-MS methods revealed the reason as acid catalysed hydrolysis of the glass network. However, the network does not degrade evenly. The ICP-MS of the ageing solutions shows clearly that the non–silica constituents of the glass are most abundant in the solution. Boron, even though only a minor component in the glass is relatively abundant in the solution. The aluminium, a four coordinated charged network former, is also effectively removed from the glass structure. Calcium is the most significant of the removed constituent and its removal helps partly to explain the loss of aluminium as the charged aluminium structure is stabilized by the Ca^{2+}-ion (Wu & Stebbins 2009). It could be argued that the charge of the $[AlO_4]^-$ group could be balanced by hydronium or hydrogen ions once the calcium is removed. Such a structure would still likely be significantly more vulnerable to hydrolysis than the silica network. Both the FTIR and EDS of the aged fibres show a clear change towards a pure silica structure with some silanol groups, with increasing ageing time in acidic environments (Lynch et al. 2007). The most significant difference from the hypothesis presented in chapter 2.2 was revealed by the FTIR examination of the Ahlstrom R338 E-glass fibre. A broad absorption band at 1380 cm^{-1} was allocated to the presence of boron for two separate reasons: it is not present in the Jushi E6CR spectrum and it corresponds to an absorption band in borate

structures. However, unlike presented in chapter 2.2, the borate structure in question is not BO_4^- but BO_3 or possibly even BO_2O^-, the latter meaning a three-coordinated boron with one NBO. (Yiannopoulos et al. 2001) The presence of a NBO is however not certain as the surrounding structure can shift the absorption band and determining the peak value for a weak and broad absorption band is not very accurate.

The mechanical properties of the glass in the less severe environments follow the expected trends reasonably well. The ECR-fibres retain somewhat better mechanical properties than E-glass in all environments. This result is supported by the FTIR, EDS and ICP-MS results, which show better retention of non–silica glass constituents. Even after the whole two weeks of ageing in 50 g /dm^3, both FTIR and EDS indicate that, a significant portion of the aluminium is retained in the sample. Unfortunately, FTIR studies on the presence of aluminium in silicate glass are scarce. Therefore, more data is required to evaluate whether the bonding of the aluminium is changed in the ageing. It is, however, known that the bonding of aluminium in aluminosilicate glasses can be significantly different based on the abundance of calcium and other network modifiers (Du & Stebbings 2005; Neuville et al. 2007).

The ICP-MS also results show a clear correlation between solution temperature and silica network hydrolysis. This can be expected to extend to the other network formers as well, but is most evident from the results for the 50 g/dm^3 E-glass ageing solution. Both room temperature and 95 °C ageing show quite comparable concentrations of boron, aluminium and calcium in the solution, but in the room temperature ageing solution the silicon concentration is less than half of the concentration in the 95 °C solution. The ICP-MS results also show an important aspect pf the greater resistance of the ECR-glass, because it shows definitive data on even quite small changes that apparently do not affect the properties of the fibre significantly. The 50 g/dm^3 room temperature ageing solution ICP-MS shows only a slight signal for calcium and no other leached species, which means that in low temperatures, the glass remains practically unaffected despite the high sulphuric acid concentration.

Based on these results the process proposed in chapter 2.2 for the ageing in glass fibres seems at least partially correct. The FTIR results however show that boron exists in three-coordinated form to a significant degree even with the abundance of network modifiers, which would enable the $[BO_4]^-$ structure. The reasons for the significantly more severe ageing, when comparing E to ECR or other boron free glass with otherwise similar composition, are therefore still unclear. The FTIR, however, showed promising results as a method for examining the ageing in glass fibres as it offers information on the bonding of the glass constituents, while being more accessible than an NMR. The role of boron, aluminium and other constituents in ageing could therefore be elucidated by FTIR and NMR examination of the ageing of self-made glass samples with similar compositions, while excluding one of the constituents.

5.3 Ageing of the composite

The FIBRObond instrument was used to characterise the interfacial properties between the glass fibre reinforcement and the resin matrix. Like in the glass fibre studies the ageing done to the samples should be considered accelerated ageing because of the small resin volume and available largely unprotected fibre surface. It has been reported that direct access of the environment to exposed fibre–matrix interface leads to rapid loss of properties in a composite (Ashbee & Wyatt 1969; Myers et al. 2007). Unfortunately, not all the intended samples were tested in the course of this work, so the data on loss of interfacial strength is limited. However, the deionized water samples show a clear correspondence between ageing time and interfacial strength. The older, Jushi E6CR sample exhibited greater loss of interfacial properties, which can be caused by the age of the sizing and the resulting difference in the interphase itself. Such changes could include for example lesser interpenetrating network between the silanes, films formers and the resin. It could be argued that such differences could account for similar interfacial properties before ageing, but result in worse resistance to aqueous environments. In the study by Thomason (1995a–c), it was shown that both ageing and removal of the sizing have a significant effect on the ILSS results of glass fibre PMCs. The study also showed for example that resin incompatible sizing can exhibit comparable interfacial strength to a compatible sizing, but such interface loses properties significantly faster than a compatible interface. Together these results hint at interesting phenomena at the interface and could offer an explanation to the behaviour of the samples in the IFSS results of this work. However as the composition of the sizing applied to the fibres tested in this work are not disclosed, meaning accurate analysis is not possible. Further testing should be conducted to elucidate the matter, with knowledge of the age and at least qualitative composition of the sizing.

The significantly different interfacial behaviour of the one day aged ECR–epoxy combination also presents an interesting question. Based on these results, it is difficult to determine the cause of the low interfacial strength but high slope exhibited by the test series. One possible explanation is that because of the ageing, the dimensions of the droplet do not correspond to the dimensions of the interface. This would mean that the ageing has caused some of the interface to debond prior to the testing. Based on this hypothesis, the results in figure 47 could also be presented as in figure 49.

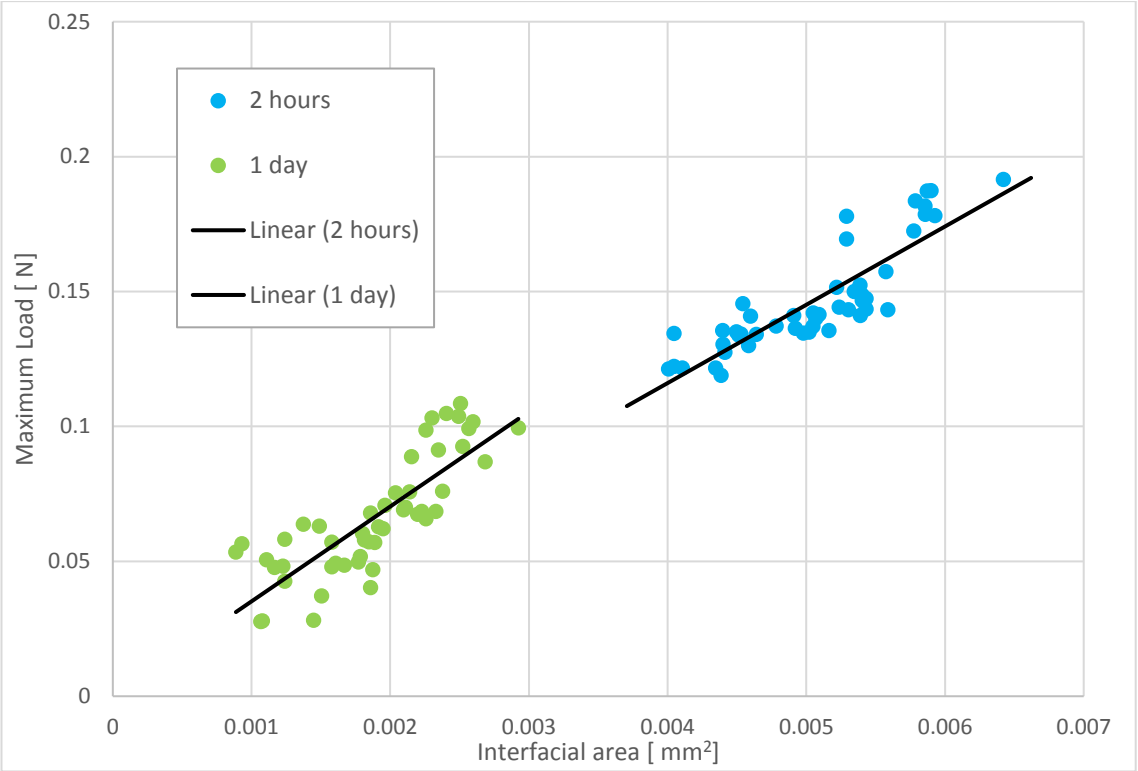

Figure 49. *Alternative presentation of the Jushi E6CR–EPON 828 microbond test results, based on the theory that the deionized water ageing has caused partial debonding by blister formation at the interface.*

In these results, the IFSS and the slope of the load–area curve correspond as in the other results. The interfacial area for the modified results is decreased by an average of 66.3 % compared to the embedded area measured from droplet dimensions. These results are however insufficient to determine the accuracy of the model. Simulations done to analyse the possibility of this kind of interfacial degradation, conducted by van der Wal (2006), however indicates, that in heated aqueous environment blister formation at the interphase is possible. It is also possible that some other phenomenon is causing the results exhibited by the sample and one must keep in mind that the results are for a single fibre sample and do not adequately represent the properties of the whole glass fibre batch. The cause for the phenomenon should be determined with further testing. Overall, the behaviour of the interface has proven interesting even based on these limited results. For example, the environment tested should not have a significant effect on the fibre properties, based on the fibre ageing tests done with deionized water and the short time of the ageing. The fibre grade, which has in almost every other test, exhibited superior properties – the Jushi E6CR – had somewhat lower interfacial shear strength and especially the significant decrease in interfacial properties between the 2 hour and 1 day time points is interesting.

The results for resin and glass fibre samples allow some prediction to their relevance for a composite material as well. The nature of the solution environment had a significant contribution to the diffusion and defect formation in the resin samples. The sample with most weight increase due to water in the structure was deionized water. These samples

also had significant defects caused by the ageing, but this effect appeared to be slightly more severe for the 50 g/dm^3 sulphuric acid environment. Overall, the diffusion and defect formation for these samples was similar and for these samples, solution access to fibre reinforcement can be expected to be significant as well. The 500 g/dm^3 sulphuric acid environment however appeared to diffuse poorly as could be expected based on literature and no defect formation was noted inside the resin. This environment however had a significant effect on the outer surface of the resin sample, which also explains the negative weight change at the end of the ageing period. Based on this result, the effect on fibre reinforcements could however be expected as minimal at least until the degradation of the resin surface exposes the reinforcements to the solution. Then significant ageing of the fibres will take place as indicated by the ageing results for unprotected glass fibres.

The effect the ageing of the glass fibre reinforcements has on the ageing is harder to evaluate based on just these results. Of course, one significant contribution to the composite properties with ageing is the mechanical properties provided by the glass fibres. If the glass fibre properties are significantly decreased, the properties of the composite as a whole are decreased and cases of failure can occur. (Myers et al. 2007; Ehrenstein & Pongratz 2013 pp. 709-713; Li et al. 2013) The removal of specific constituents from the glass structure has been shown in this work. The contribution of these constituents, along with the unreacted resin volatiles, to the debonding of the interface has been speculated as early as in the study be Ashbee and Wyatt (1969). This phenomenon has however been largely overlooked in recent studies and definitive information on its contribution is not available. Hydro- and hygrothermal ageing studies utilizing the microbond and other interfacial strength methods have mostly focused on the applicability of the method for such research and less on the ageing phenomena behind the observed changes in property (Gaur & Miller 1990; Gaur et al. 1994). A water diffusion and thermal analysis study of glass fibre–epoxy composites by Chateauminois et al. (1994), however, offered further insight into such behaviour. In the study, water diffusion and desorption together with dynamic mechanical behaviour indicate that once the water content in the resin reached saturation, increasing defect formation and interfacial debonding occurs as longer ageing times are used, which cannot be attributed to the ageing of the resin as unreinforced resin samples were used as reference for the composite samples. The role of glass constituents in causing the phenomenon was not discussed. (Chateauminois et al. 1994) The role of glass fibre in the ageing of the resin and the interface warrants further study, despite the difficulties, and definitive answer to the existence of such an effect would be of immense value to the total understanding of the ageing in glass fibre reinforced PMCs.

The role of stresses, both external and those created into the structure during processing have been shown as an important accelerating factor in loss of properties exhibited by aqueous environment aged glass fibre-composites (Megel at al. 2001; Kumosa et al. 2001; Myers et al. 2007; Li et al. 2013; Solis-Ramos & Kumosa 2017). An important aspect of

this phenomenon are for example the stresses caused by the resin to the glass fibres, which can cause stress corrosion cracking of the reinforcements even without external stresses (Megel et al. 2001). This examination was excluded in the practical portion of this work, in part due to the significant number of studies on the subject. One common attribute in many of these studies – and the main reason this phenomenon is excluded from this work – is that because of the complexity of the composite behaviour, the role of some of the ageing phenomena are discussed somewhat arbitrarily as the presence of stresses offers a simple explanation for the failure of the samples. This phenomenon is, however, an important part of the subject of ageing in glass fibre reinforced polymers.

6. CONCLUSIONS

Several, well documented ageing effects for glass fibre reinforced PMCs were found in literature. The ageing of the resin is a combination of physical and chemical ageing effects, such as the diffusion of water into the material, hydrolysis of vulnerable structural groups and post-curing reactions, which over time affect the whole composite. The high temperature ageing tests in water and strongly acidic environments show similar ageing effects as other research groups have reported for similar materials, but further testing is required to determine the severity of all the noted phenomena and to examine behavioural differences between different materials. An important result for composite applications is the apparently effective diffusion barrier for solution constituents larger than water, also reported elsewhere. Based on the weight change and optical microscopy examination of the aged resins, the very high concentration sulphuric acid solution interacts mostly with the resin surface allowing very little solution to diffuse through the material. This is a positive finding in terms of composite structures, where preventing water and acidic media access to the reinforcements embedded in the resin is important. The changes on the resin surface were however noted as significant as well, indicating that the material is gradually degraded from the surface. The flexural modulus of the resin remained unchanged by the ageing in all environments – except for a slight increase caused by post-curing – despite chemical changes noted in FTIR examination, which can be attributed to ester hydrolysis.

Should the acidic solution environment reach the glass fibre reinforcements, the results presented – in both literature and in this work – indicate severe loss of properties in the glass fibres. However, using more resistant glass grades offers significant advantages in terms of the durability of the reinforcement. The role of boron inside the glass structure appears to be a major weakness in terms of durability in sulphuric acid solutions. This is not a simple phenomenon and other aspects of the glass structure contribute to the chemical durability as well. The temperature of the environment also has a major effect to the durability of the fibres, especially in the terms of silica network hydrolysis, as shown by the ICP-MS results of leaching tests both in room temperature and in solutions heated to 95 °C.

The literature review part of this work elucidated the structure of the glass grades close to E-glass in composition, and based on the structural model a hypothesis of the advancement of ageing in glass fibres was presented. The severe ageing – exhibited by for example E-glass – is a result of preferred hydrolysis of non-siliceous species in the glass network, which can be, for example, charged structures weakened by the leaching of charge balancing network modifiers like calcium ions. The hydrolysis of the silica network is, however, the major reason in the loss of glass properties. The resistance to

ageing exhibited by ECR-glass is a result of the formation of a silica rich layer in which the silica network hydrolysis–repolymerization reaction reaches equilibrium. The ageing of E- and ECR-fibre grades tested in this work agrees with the presented hypothesis reasonably well, although the FTIR measurements indicate the proposed bonding of boron in the glass structure might not be entirely accurate. This needs to be investigated further, as the actual role of boron in the chemical durability of E-glass is of significant interest in the field of glass fibre composites. Mechanical testing of the glass fibres showed a decrease in properties for both glass grades in aqueous environment ageing.

The applicability of the microbond method was shown in the examination of changes in the interfacial properties of glass fibre reinforced PMCs. The preliminary testing conducted in the course of this work shows a decrease in the interfacial shear strength with increased ageing for both E- and ECR-glass-epoxy combinations. The results also hint at the role of the sizing in the durability of the interface, as the ECR-glass, which out-performed the E-glass in practically all ageing tests, experienced significantly more severe loss of interfacial properties. This is likely caused by differences in the sizing, meaning the sizing has aged more significantly or is less compatible with the used epoxy matrix.

The change in interfacial properties is behaviourally different with the two glass grades. The E-glass–epoxy combination exhibited a clear decrease IFSS indicated both by the calculated values for IFSS and the slope of the load–embedded area curve. The ECR-glass, in turn, has a similar slope for both ageing time points, but exhibits significantly lower calculated IFSS values for the 1-day ageing time point. The cause of this behaviour was proposed to be a result of defect formation or debonding at the interface, which causes the actual interfacial area to be lower. The actual strength of the still connected interface, however, remains unchanged as indicated by the slope. The repeatability of these results is however questionable, as the results are from individual fibres from both fibre grades. Further work on the subject has however been planned and more comprehensive results on the subject will be presented elsewhere.

This work has given further evidence of the role of the ageing of glass fibre and the sizing in the changes of the composite materials as a whole, where ageing in aqueous environments is considered. The chemical durability of the glass fibres is directly related to the structure of the glass, which should be understood in order to predict the behaviour of the composite. The role of sizing in the retention of interfacial properties is also discussed and appears significant, based on the presented results. The sizing compositions are, however, proprietary information of the fibre manufacturers, which hinders efforts in characterizing its role in the ageing of composites utilizing the glass fibres. This work represents an effort of gathering information on the different ageing phenomena and on methods available for examination of these phenomena, which should prove useful for further efforts in studying the ageing of glass fibre–reinforced polymer matrix composites.

REFERENCES

Ahmad, S. Ashraf, S.M. Hassan, S.N. Hasnat, A. 2005. Synthesis, Characterization, and Performance Evaluation of Hard, Anticorrosive Coating Materials Derived from Diglycidyl Ether of Bisphenol A Acrylates and Methacrylates. Journal of Applied Polymer Science, Vol. 95, Issue 3. Wiley. pp. 494–501.

Ali, A.A. Rammah, Y.S. El-Mallawany, R. Souri, D. 2017. FTIR and UV spectra of pentaternary borate glasses. Measurement, Vol. 105. Elsevier. pp. 72–77.

Angeli, F. Gaillard, M. Jollivet, P. Charpentier, T. 2006. Influence of glass composition and alteration solution on leached silicate glass structure: A solid-state NMR investigation. Geochimica at Cosmochimica Acta, Vol. 70, Elsevier. pp. 2577–2590.

Angeli, F. Gaillard, M. Jollivet, P. Charpentier, T. 2007. Contribution of ^{43}Ca MAS NMR for probing the ctructural configuration of calcium in glass. Chemical Physical Letters, Vol, 440, Issue 4-6. Elsevier. pp. 324–328.

Apicella A. Nicolais L. 1984. Role of Processing on the Durability of Epoxy Composites in Humid Environments, Industrial & Engineering Chemistry Product Research and Development. ACS Publications, Washington, DC. pp. 288–297.

Ashbee, K.H.G. Wyatt, R.C. 1969. Water damage in glass fibre/resin composites. Proceedings of the Royal Society A: Mathematical, Physical and Engineering Sciences, Vol. 312, Issue 1511. pp. 553–564.

ASTM D 3379-75. 1989. Standard Test Method for Tensile Strength and Young's Modulus for High-Modulus Single-Filament Materials (Withdrawn). ASTM International. USA. 5 p.

Boinard, E. Pethrick, R.A. Dalzel-Job J. MacFarlane C. 2000. Influence of resin chemistry on water uptake and environmental ageing in glass fibre reinforced composites-polyester and vinyl ester laminates. Journal of Materials Science, Vol. 35, Issue 8. Springer. pp. 1931–1937.

Carter, H.G. Kibler, K.G. 1978. Langmuir-Type Model for Anomalous Moisture Diffusion In Composite Resins. Journal of Composite Materials, Vol. 12, Issue 2. SAGE Publishing. pp. 118–131.

Chateauminois, A. Vincent, L. Chabert, B. Soulier, J.P. 1994. Study of the interfacial degradation of a glass–epoxy composite during hygrothermal ageing using water diffusion measurements and dynamic mechanical thermal analysis. Polymer, Vol 35, Issue 22. Elsevier. pp. 4766-4774.

Chou, C.T. Gaur, U. Miller, B. 1994. The effect of microvise gap width on microbond pull-out test results. Composites Science and Technology, Vol. 51, Issue 1. Elsevier. pp. 111–116.

Clayden, J. Greeves, N. Warren, S. Wothers, P. 2001. Organic Chemistry. Oxford University Press, New York. pp. 411-415, 434–435.

Dai, J. Yao, X. Liang, X. Yeh, H.Y. 2006. Experimental study of micro-cracks in stress corrosion of fiber reinforced composites. Polymer testing, Vol. 25, Issue 6. Elsevier. pp. 758–765.

Day, R.J. Cauich-Rodrigez, J.V. 1998. Investigation of the micromechanics of the microbond test. Composites Science and Technology, Vol. 58, Issue 6. Elsevier. pp. 907–914.

Derakane® 441-400 Epoxy Vinyl Ester Resin Datasheet. 2009. Document 1767 V1 F2. Ashland Inc. 5p. Available: http://addresins.com/technical-literature/DERAKANE_441-400_TDS%20(2).pdf. Accessed: 7.6.2017

Dey, M. Deitzel, J.M. Gillespie, J.W. Schweiger, S. 2014. Influence of sizing formulations on glass/epoxy interphase properties. Composites: Part A, Vol. 63. Elsevier. pp. 59–67.

Dirand, X. Hilaire, B. Soulier, J.P. Nardin, M. 1996. Interfacial Shear Strength in Glass-fiber/Vinylester-resin Composites. Composite Science and Technology, Vol. 56, Issue 5. Elsevier. pp. 533–539.

Du, L.-S. Stebbins, J.F. 2005 Network connectivity in aluminoborosilicate glasses: A high-resolution ^{11}B, ^{27}Al and ^{17}O NMR study. Journal of Non-crystalline Solids, Vol. 351. Elsevier. pp. 3508–3520.

Ehrenstein, G.W. Riedel, G. Trawiel, P. 2004. Thermal Analysis of Plastics - Theory and Practice. Hanser Publishers. pp. 236–294. Limited availability: https://app.knovel.com/web/toc.v/cid:kpTAPTP003/viewerType:toc/. Accessed: 20.7.2017

Ehrenstein G.E. Pongratz S. 2013. Resistance and Stability of Polymers, Carl Hanser Verlag, Munich, Germany. 1436 p.

EN ISO 178. 2003. Plastics – Determination of flexural properties (ISO 178:2001). European Committee for Standardization. 19 p.

Epikote™ Resin 828 Technical data sheet. Hexion Inc. 3 p. Available: http://www.hexion.com/products/technicaldatasheet.aspx?id=4364. Accessed: 7.6.2017

Fraga, A.N. Alvarez, V.A. Vázquez A. 2003. Relationship Between Dynamic Mechanical Properties and Water Absorption of Unsaturated Polyester and Vinyl Ester Glass Fiber Composites. Journal of Composite Materials, Vol. 37, Issue 17. SAGE Publishing. pp. 1553–1574.

Fried, J.R. 2003. Polymer Science and Technology. 2nd Edition. Prentice Hall PTR. USA. pp. 271-273, 379–380.

Gaur, U. Miller, B. 1990. Effects of Environmental Exposure on Fiber/Epoxy Interfacial Shear Strength. Polymer Composites, Vol. 11, Issue 4. Society of Plastics Engineers/ Wiley. pp. 217–222.

Gaur, U. Chou, CT. Miller, B. 1994. Effect of hydrothermal ageing on bond strength. Composites, Vol. 25, Issue 7. Elsevier. pp. 609–612.

Gautier, L. Mortaigne, B. Bellenger, V. Verdu, J. 2000. Osmotic cracking nucleation in hydrothermal-aged polyester matrix. Polymer, Vol. 41, Issue 7. Elsevier. pp. 2481–2490.

Guzman, V.A. Brøndsted, P. 2015. Effects of moisture on glass fibre-reinforced polymer composites. Journal of Composite Materials, Vol. 49, Issue 8. SAGE Publishing. pp. 911–920.

Haynes, W.M. (ed), CRC Handbook of Chemistry and Physics, 97th Edition (Internet Version 2017), CRC Press/Taylor & Francis, Boca Raton.

Ignatyev, I.S. Partal, F. Lopéz-González, J.J. 2003. Condensation reactions in silanol-water clusters. Chemical Physics Letters, Vol. 368, Issues 5-6. Elsevier. pp. 616–624.

Jeffamine® D-230 Polyetheramine Technical Bulletin. Hunstman Corporation. 2 p. Available: http://www.huntsman.com/. Accessed: 7.6.2017

Jégou, C. Gin, S. Larché , F. 2000. Alteration kinetics of simplified nuclear glass in an aqueous medium: effects of solution chemistry and of protective gel properties on diminishing alteration rate. Journal of Nuclear Materials, Vol 280, Issue 2. Elsevier. pp. 216–229.

Johansson, O.K. Stark, F.O. Vogel, G.E. Fleischmann, R.M. 1967. Evidence for Chemical Bond Formation at Silane Coupling Agent Interfaces. Journal of Composite Materials, Vol. 1, Issue 3. SAGE Publishing. pp. 278–292.

Jones, R.L. 2006a. Chemical corrosion of E-Glass Fibers in Oxalic and Other Organic Acids. Journal of the American Ceramic Society, Vol. 89, Issue 1. The American Ceramic Society. pp. 20–23.

Jones, R.L. 2006b. The role of boron in the corrosion of E-glass fibres. Glass Technology - European Journal of Glass Science and Technology part A, Vol. 47, Issue 6. Society of Glass Technology. pp. 167–171.

Jones, R.L. Stewart, J. 2010. The kinetics of corrosion of e-glass fibres in sulphuric acid. Journal of Non-Crystalline Solids, Vol. 356. Elsevier. pp. 2433–2436

Khalil, E.M.A. Elbatal, H.A. Hamdy, Y.M. 2008. Investigation of Bioactivity of Silicate Glass-Ceramics in the System SiO_2-Na_2O-CaO-P_2O_5 Containing MgO and TiO_2. Transactions of the Indian Ceramic Society, Vol. 67, Issue 3. The Indian Ceramic Society. pp. 119–128.

Kiczenski, T.J. Du, L.-S. Stebbins, J. 2005. The effect of fictive temperature on the structure of E-glass: A high resolution, multinuclear NMR study. Journal of Non-crystalline Solids, Vol. 351. Elsevier. pp. 3571–3578.

Kumosa, L. Armentrout, D. Kumosa, M. 2001. An evaluation of the critical conditions for the initiation of stress corrosion cracking in unidirectional E-glass/polymer composites. Composites Science and Technology, Vol. 61, Issue 4,

Ledieu, A. Devreux, F. Barboux, P. Sicard, L. Spalla, O. 2004. Leaching of borosilicate glasses. I. Experiments. Journal of Non-Crystalline Solids, Vol. 343, Issues 1–3. Elsevier. pp. 3-12.

Lindgren, M. Bergman, G. Kakkonen, M. Lehtonen, M. Jokinen, J. Wallin, M. Saarela, O. Vuorinen, J. 2015. Failure analysis of a leaching reactor made of glass-fiber reinforced plastic. Engineering Failure Analysis, Vol. 60. Elsevier. pp. 117–136.

Lucas, S. Tognonvi, M.T. Gelet, J-L. Soro, J. Rossignol, S. 2011. Interactions between silica sand and sodium silicate solution during consolidation process. Journal of Non-Crystalline Solids, Vol. 357. Elsevier. pp. 1310–1318.

Lynch, M.E. Folz, D.C. Clark, D.E. 2007. Use of FTIR reflectance spectroscopy to monitor corrosion mechanisms on glass surfaces. Journal of Non-Crystalline Solids, Vol. 353, Issue 27. Elsevier. pp. 2667–2674.

Li, H. 1998. Synthesis, Characterization and Properties of Vinyl Ester Matrix Resins, dissertation. Virginia Polytechnic Institute and State University Publication. Virginia, USA. pp. 1–29.

Li, H. Gu, P. Watson, J. Meng, J. 2013. Acid corrosion resistance and mechanism of E-glass fibers: boron factor. Journal of Materials Science, Vol. 48, Issue 8. Springer. pp. 3075–3087.

Marzouk, S.Y. 2010. Ultrasonic, FTIR and thermal investigations of SiO_2–Na_2O–CaO–P_2O_5 glasses doped with CeO_2. Philosophical Magazine, Vol. 90, Issue 33. Taylor & Francis. pp. 4393–4407.

Megel, M. Kumosa, L. Ely, T. Armentrout, D. Kumosa, M. 2001. Initiation of stress-corrosion cracking in unidirectional glass/polymer composite materials. Composites Science and Technology, Vol. 61, Issue 2. Elsevier. pp. 231–246.

Miller, B. Muri, P. Rebenfeld, L. 1987. A Microbond Method for Determination of the Shear Strength of a Fiber/Resin Interface. Composites Science and Technology. Vol. 28, Issue 1. Elsevier. pp. 17–32.

Myers, T.J. Kytömaa, H.K. Smith, T.R. 2007. Environmental stress corrosion cracking of fiberglass: Lessons learned from failures in the chemical industry. Journal of Hazardous Materials, Vol. 142, Issue 3. Elsevier. pp. 695–704.

Neuville, D.R. Cormier, L. Montouillout, V. Massiot, D. 2007. Local Al site distribution in aluminosilicate glasses by ^{27}Al MQMAS NMR. Journal of Non-crystalline Solids, Vol. 353. Elsevier. pp. 180–184.

Padmaja, P. Anilkumar, G.M. Mukundan, P. Aruldhas, G. Warrier, K.G.K. 2001. Characterization of stoichiometric sol-gel mullite by fourier transform infrared spectroscopy. International Journal of Inorganic Materials, Vol. 3, Issue 7. Elsevier. pp. 693–698.

Pandey, G. Kareliya, C.H. Singh, R.P. 2011. A study of the effect of experimental test parameters on data scatter in microbond testing. Journal of Composite Materials, Vol. 43, Issue 3. SAGE Publications, pp. 275–284.

Pape, P.G. 2017. 25 – Adhesion Promoters: Silane Coupling Agents. In: Kutz, M. Applied Plastics Engineering Handbook - Processing, Materials, and Applications, 2nd Edition. Elsevier. pp. 555–559. Limited availability: https://app.knovel.com/web/toc.v/cid:kpAPEHPMA5/. Accessed: 13.4.2017

Pitaressi, G. Scafidi, M. Alessi, S. Di Filippo, M. Billaud, C. Spadaro, G. 2015. Absorption kinetics and swelling stresses in hydrothermally aged epoxies investigated by photoelastic image analysis. Polymer Degradation and Stability, Vol. 111. Elsevier. pp. 55–63.

Plonka, R. Mäder, E. Gao, S.L. Bellman, C. Dutschk, V. Zhandarov, S. 2004. Adhesion of epoxy/glass fibre composites influenced by aging effects of sizings. Composites, Part A: applied science and manufacturing, Vol. 35, Issue 10. pp. 1207–1216.

Reilly, S.P. Thomason, J.L. 2010. Effects of silane coating on the properties of glass fibre reinforced epoxy resin. In: 14th European Conference on Composite Materials, ECCM14, 7-10 June 2010, Budapest, Hungary. 10 p.

Rudzinski, S. Häussler, L. Harnisch, Ch. Mäder, E. Heinrich, G. 2011. Glass fibre reinforced polyamide composites: Thermal behaviour of sizings. Composites, Part A, Vol. 42. Elsevier. pp. 157–164.

Scheer, R.J. Nairn, J.A. 1995. A Comparison of Several Fracture Mechanics Methods for Measuring Interfacial Toughness with Microbond Tests. The Journal of Adhesion, Vol. 53, Issue 1-2. Taylor & Francis. pp. 45–68.

Scheetz, B.E. Freeborn, W.P. Smith. D.K, Anderson, C. Zolensky, M. White, W.B. 1985. The Role of Boron in Monitoring the Leaching of Borosilicate Glass Waste Forms. MRS Proceedings, Vol. 44. pp.129–134.

Schrader, M.E. 1974. Radioisotope studies of coupling agents at the interface. In: Plueddemann, E.P. (editor), Composite Materials, Vol. 6: Interfaces in Polymer Matrix Composites, Academic Press, New York, 1974, pp. 109–129.

Schutte, C.L. 1994. Environmental durability of glass-fiber composites. Materials Science and Engineering: R: Reports, Vol 13. Issue 7. Elsevier. pp. 265-323.

Sethi, S. Ray, B.C. 2015. Environmental effects of fibre reinforced polymeric composites: Evolving reasons and remarks on interfacial strength and stability. Advances in Colloid and Interface Science, Vol. 217. Elsevier. pp. 43–67.

Shelby, J.E. 2005. Introduction to Glass Science and Technology. 2nd Edition. Royal Society of Chemistry. pp. 72–100. Limited availability: https://app.knovel.com/web/toc.v/cid:kpIGSTE002/. Accessed: 7.3.2017

Silverstein, R.M. Bassler, G.C. Morrill, T.C. 1991. Spectrometric identification of organic compounds, 5th Edition. USA. John Wiley & Sons. pp. 102–121.

Solis-Ramos, E. Kumosa, M. 2017. Synergistic effects in stress corrosion cracking of glass reinforced. Polymer Degradation and Stability, Vol. 126. Elsevier. pp. 146-157.

Sugiman, S. Putra, I.K.P. Setyawan, P.D. 2016. Effects of media and ageing condition on the tensile properties and fracture toughness of epoxy resin. Polymer Degradation and Stability, Vol. 134. Elsevier. pp. 311–321.

Thomason, J.L. 1995a. The interface region in glass fibre-reinforced epoxy resin composites: 1. Sample preparation, void content and interfacial strength. Composites, Vol. 26, Issue 7. Elsevier. pp. 467–475.

Thomason, J.L. 1995b. The interface region in glass fibre-reinforced epoxy resin composites: 2. Water absorption, voids and the interface, Vol. 26, Issue 7. Elsevier. pp. 477–485.

Thomason, J.L. 1995c. The interface region in glass fibre-reinforced epoxy resin composites: 3. Characterization of fibre surface coatings and the interphase, Vol. 26, Issue 7. Elsevier. pp. 487–498.

Toscano, A. Pitaressi, G. Scafidi, M. Di Filippo, M. Spadaro, G. Alessi, S. 2016. Water diffusion and swelling stresses in highly crosslinked epoxy matrices. Polymer Degradation and Stability, Vol. 133. Elsevier. pp. 255–263.

Qiu Q. Kumosa M. 1996. Corrosion of E-glass Fibers in Acidic Enviroments, Composites Science and Technology, Vol. 57. Elsevier. pp. 497–507.

Vidal, L. Joussein, E. Colas, M. Cornette, J. Sanz, J. Sobrados, I. Gelet, J-L. Absi, J. Rossignol, S. 2016. Controlling the reactivity of silicate solutions: A FTIR, Raman and NMR study. Colloids and Surfaces A: Physicochemical and Engineering Aspects, Vol. 503. Elsevier. pp. 101–109.

Visco, A.M. Brancato, V. Campo, N. 2011. Degradation effects in polyester and vinyl ester resins induced by accelerated aging in seawater. Journal of Composite Materials, Vol. 46m, Issue 17. SAGE Publications. pp. 2025–2040.

Visco, A.M. Calabrese, L. Cianciafara, P. 2008. Modification of polyester resin based composites induced by seawater absorption. Composites, Part A: applied science and manufacturing, Vol. 39, Issue 5. Elsevier. pp. 805–814.

Wallenberger, F.T. Watson, J.C. Li, H. 2001. Glass Fibres. In: Miracle, D.B. Donaldson, S.L. (ed.) ASM Handbook Volume 21: Composites. ASM International. pp. 27–34.

van der Wal, J.S. 2006. Water Resistance of Glass Fibre Reinforced Epoxy (GFRP) and Carbon Fibre Reinforced Epoxy (CFRP) Composite. Diffusion-polymers.com (Composite Agency). 6 p. Available: http://www.composite-agency.com/archive/Osmosis-in-Composite-Materials.pdf. Accessed: 18.8.2017

Wang, M. Xu, X. Ji, J. Yang, Y. Shen, J. Ye, M. 2016. The hygrothermal ageing process and mechanism of the novolac epoxy resin. Composites, Part B: Engineering, Vol. 107. pp. 1–8.

Wu, J. Stebbins, J.F. 2009. Effects of cation field strength on the structure of aluminoborosilicate glasses: High-resolution ^{11}B, ^{27}Al and ^{23}Na MAS NMR. Journal of Non-crystalline Solids, Vol. 355. Elsevier. pp. 556–562.

Yiannopoulos, Y.D. Chryssikos, G.D. Kamitsos, E.I. 2001. Structure and properties of alkaline earth borate glasses. Physics and Chemistry of Glasses, Vol. 42, Issue 3. Society of Glass Technology. pp. 164–172.

Zumdahl, S.S. 2009. Chemical Principles, 6th Edition. International edition. Brooks/Cole, USA. pp. 867–868.

APPENDIX 1: RESIN WEIGHT DURING AGEING

The VE sample weights, measured at Outotec Research Center during the ageing of the samples, are presented in table 6.

Table 6. *VE sheet weights during the ageing for all sheets.*

Environment	Deionized water		50 g/dm^3 H2SO4			500 g/dm^3	
Approx. sample thickness [mm]	3	5	3	4	5	3	5
Time [h]	**Mass [g]**						
0	31.624	62.01	33.003	48.265	74.004	34.328	64.849
0.5	31.782	62.072	33.073	48.357	74.079	34.360	64.869
1	32.151	62.526	33.459	48.543	74.27	34.370	64.902
1.5	31.877	62.241	33.135	48.432	74.164	34.375	64.871
2	31.931	62.37	33.362	48.656	74.314	34.366	64.886
2.5	31.848	62.209	33.311	48.507	74.206	34.377	64.88
3	32.052	62.402	33.289	48.675	74.29	34.399	64.894
3.5	31.884	62.384	33.252	48.522	74.226	34.397	64.87
4	31.958	62.258	33.262	48.516	74.232	34.394	64.877
5	31.923	62.303	33.354	48.562	74.292	34.421	64.887
6	32.072	62.389	33.290	48.570	74.345	34.408	64.866
7	31.978	62.605	33.303	48.567	74.272	34.412	64.872
8	32.015	62.412	33.315	48.579	74.291	34.418	64.876
9	32.062	62.406	33.394	48.596	74.293	34.406	64.788
10	32.041	62.376	33.347	48.626	74.337	34.410	64.792
11	32.046	62.383	33.344	48.622	74.314	34.404	64.77
17	32.163	62.515	33.414	48.705	74.415	34.417	64.756
23	32.162	62.598	33.446	48.749	74.458	34.427	64.779
29	32.267	62.759	33.484	48.807	74.514	34.427	64.79
35	32.152	62.671	33.470	48.833	74.56	34.414	64.79
41	32.224	62.875	33.548	48.857	74.626	34.401	64.801
47	32.181	62.8	33.500	48.919	74.652	34.388	64.806
53	32.172	62.867	33.492	48.881	74.661	34.412	64.838
59	32.29	62.865	33.483	48.891	74.727	34.400	64.837
65	32.171	62.831	33.479	48.903	74.718	34.412	64.858
71	32.204	62.868	33.486	48.916	74.75	34.419	64.868
168	32.159	62.953	33.444	48.943	74.94	34.419	64.939
336	32.103	62.976	33.397	48.902	75.062	34.365	64.887
504	32.119	63.027	33.385	48.899	75.096	34.375	64.899
672	32.443	63.236	33.368	48.898	75.090	34.367	64.907
840	32.039	62.944	33.357	48.868	75.077	34.347	64.867
1008	32.023	62.947	33.349	48.863	75.107	34.332	64.870

APPENDIX 1: GLASS FIBRE SEM IMAGES

Scanning electron microscope images taken from aged glass fibres are presented here in a larger scale for ease of observation. For the findings made while observing the images see chapter 4.4 in the text. Unaged and room temperature aged samples are excluded as the scale in chapter 4.4 is sufficient for the required observations.

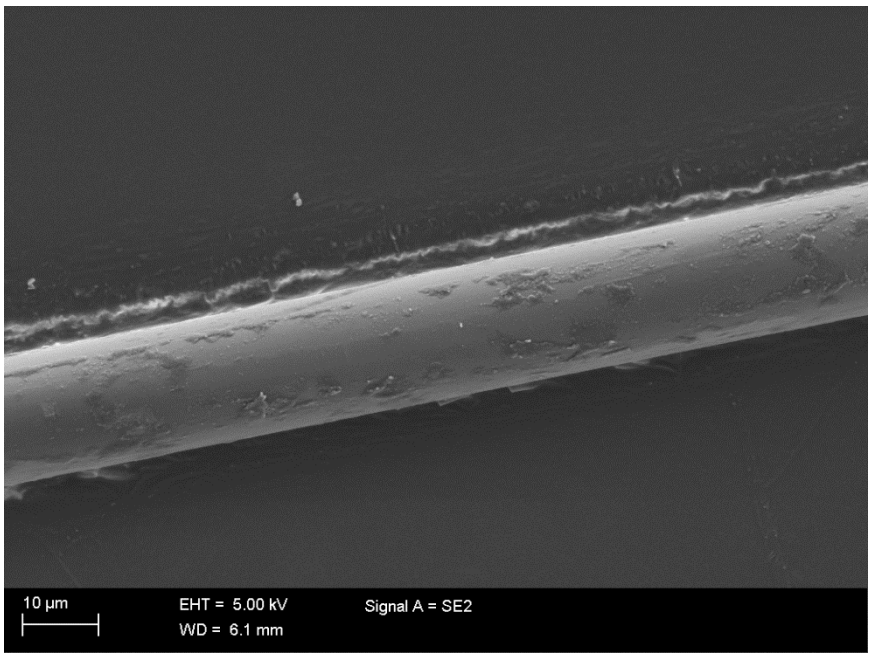

Figure 50. *SEM image of a Jushi E6CR fibre aged for 1 day in 95 °C deionized water.*

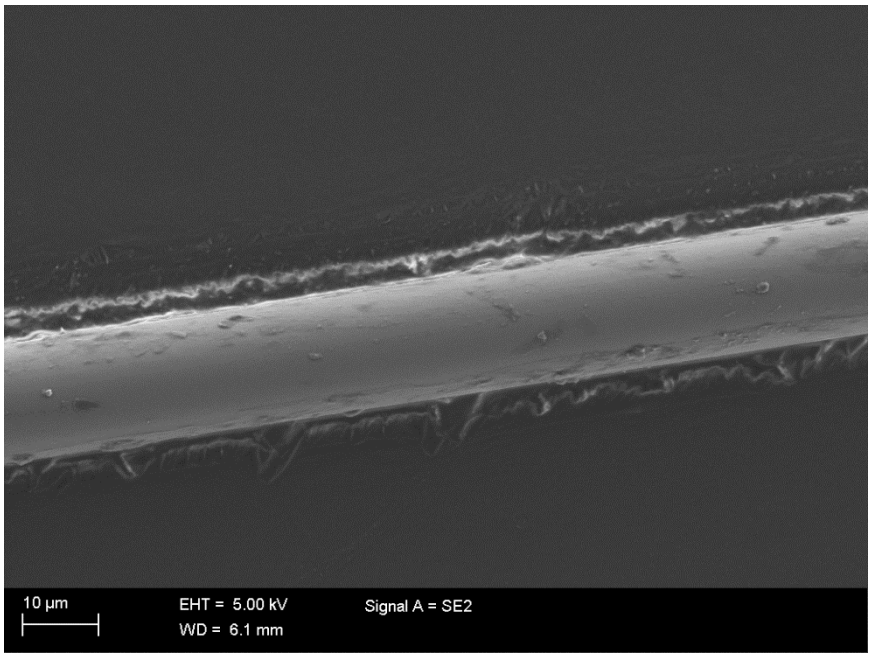

Figure 51. *SEM image of a Jushi E6CR fibre aged for 1 day in 95 °C deionized water.*

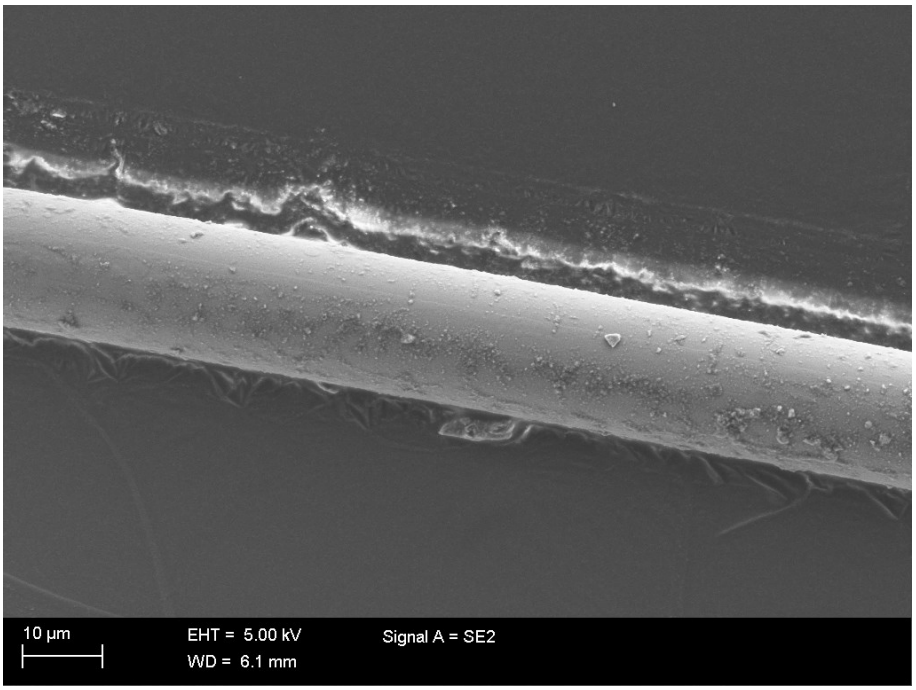

Figure 52. *SEM image of a Jushi E6CR fibre aged for 2 days in 95 °C deionized water.*

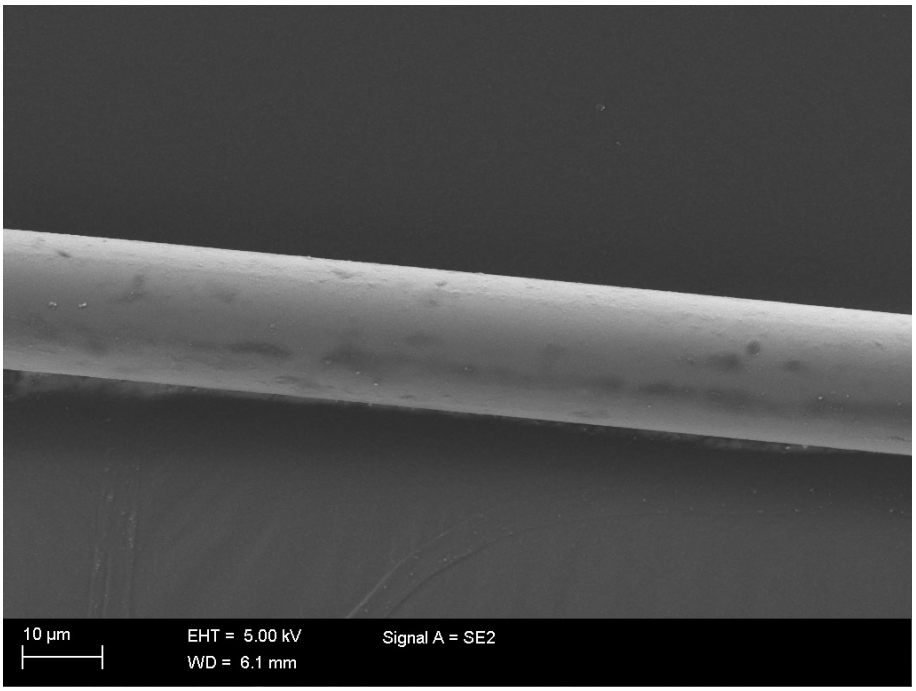

Figure 53. *SEM image of a Jushi E6CR fibre aged for 2 days in 95 °C deionized water.*

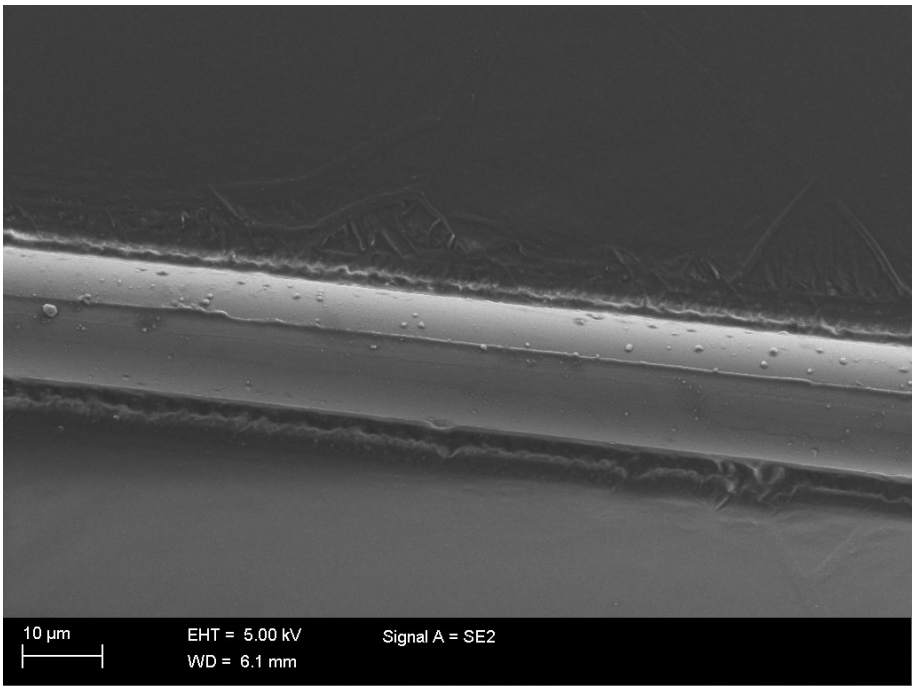

Figure 54. *SEM image of a Jushi E6CR fibre aged for 1 week in 95 °C deionized water.*

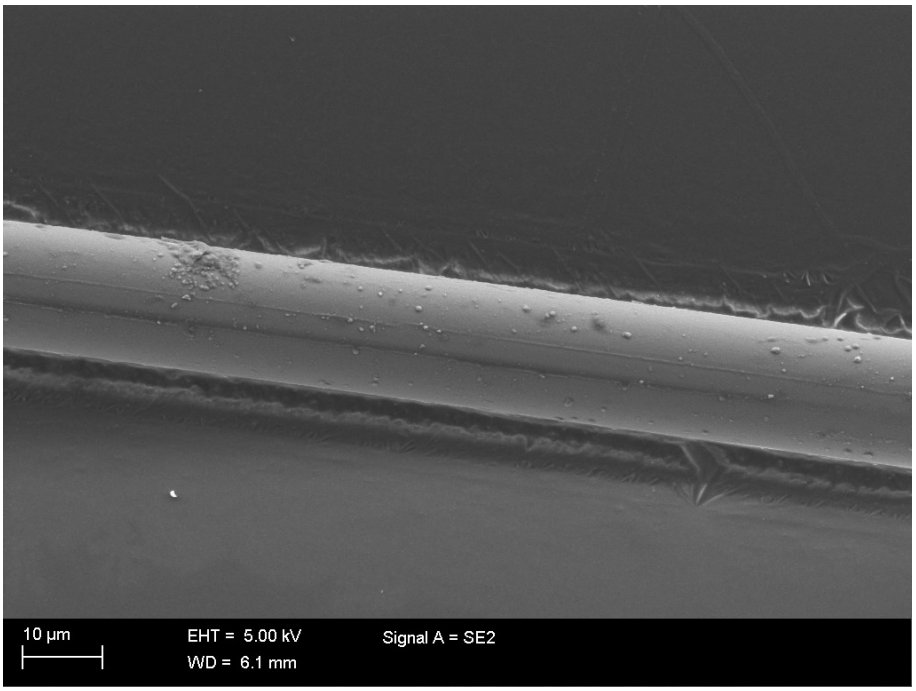

Figure 55. *SEM image of a Jushi E6CR fibre aged for 1 week in 95 °C deionized water.*

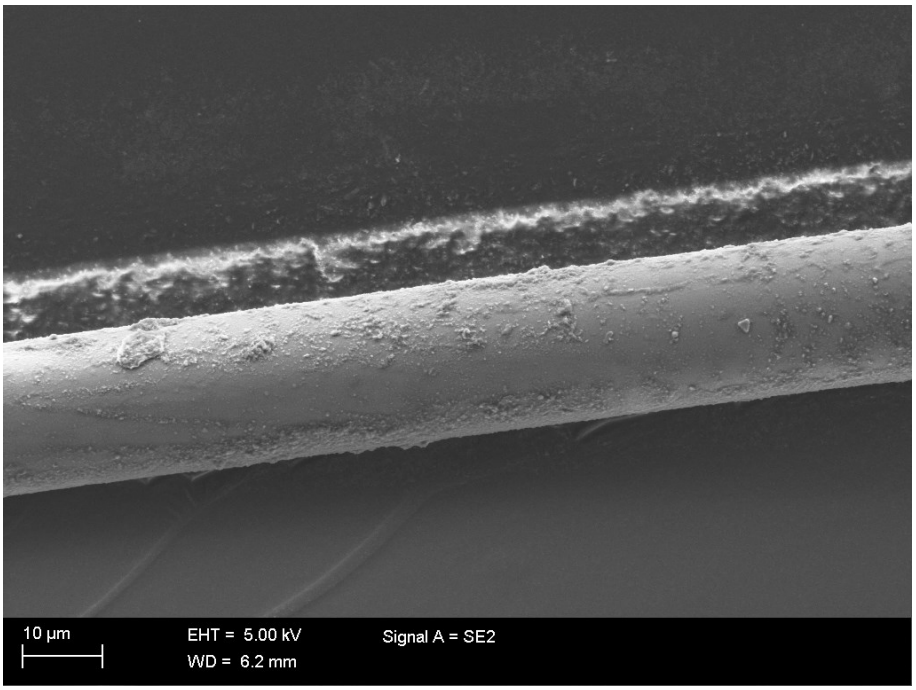

Figure 56. *SEM image of a Jushi E6CR fibre aged for 2 weeks in 95 °C deionized water.*

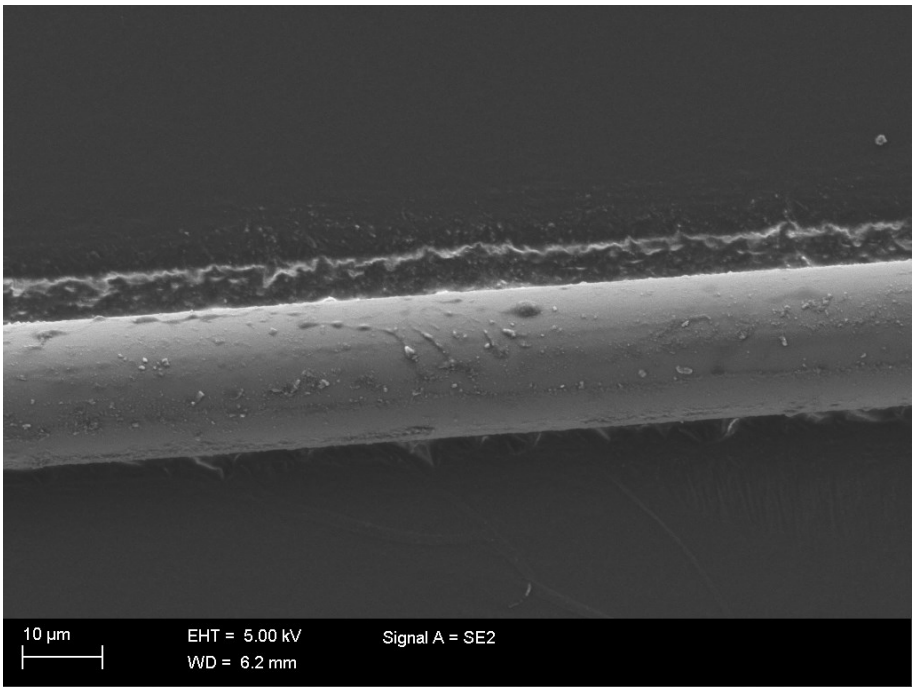

Figure 57. *SEM image of a Jushi E6CR fibre aged for 2 weeks in 95 °C deionized water.*

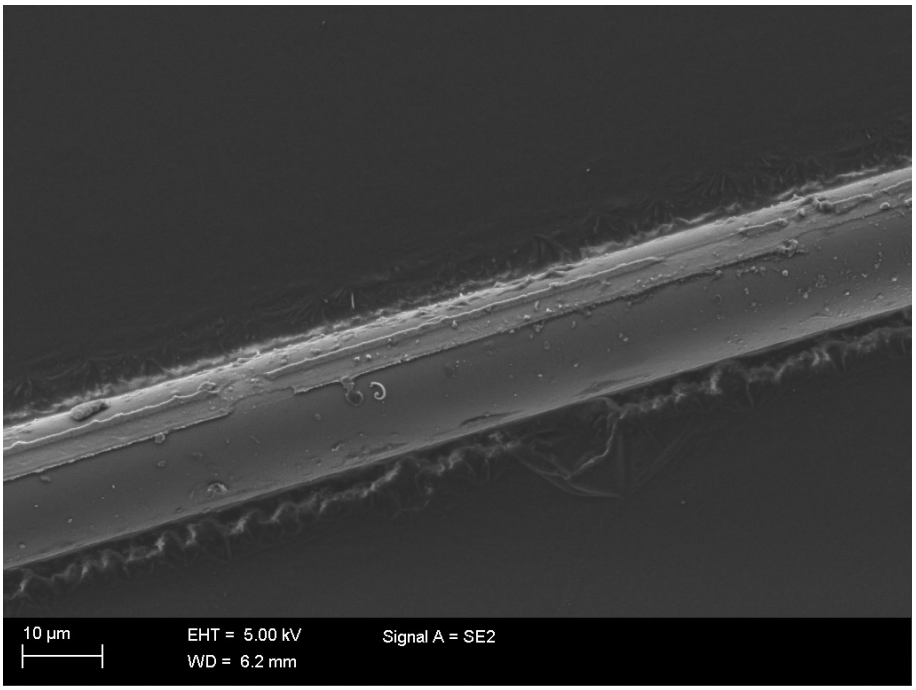

Figure 58. *SEM image of a Jushi E6CR fibre aged for 1 day in 95 °C 1 g/dm^3 sulphuric acid solution.*

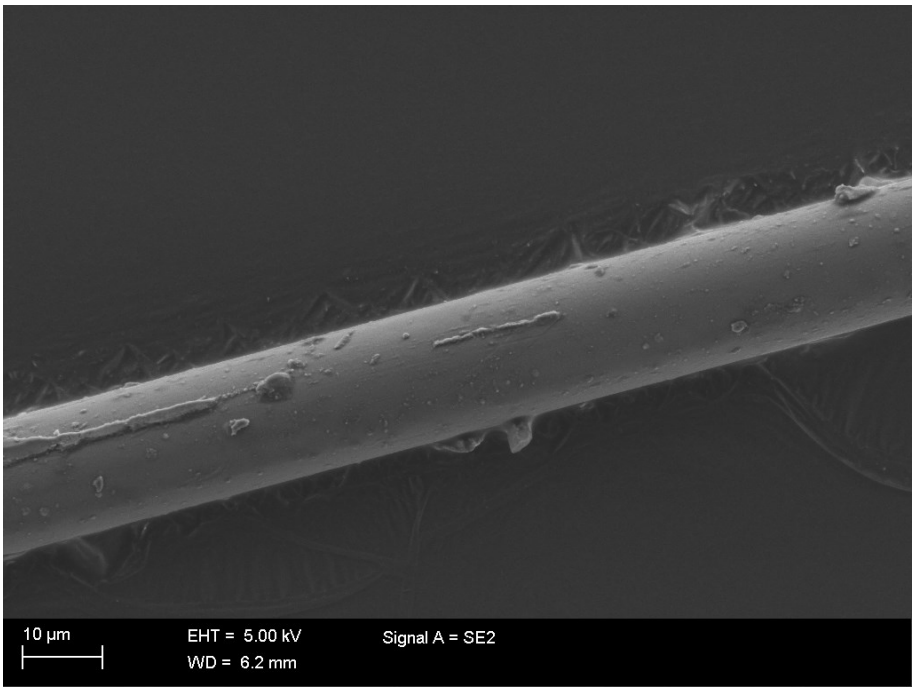

Figure 59. *SEM image of a Jushi E6CR fibre aged for 1 day in 95 °C 1 g/dm^3 sulphuric acid solution.*

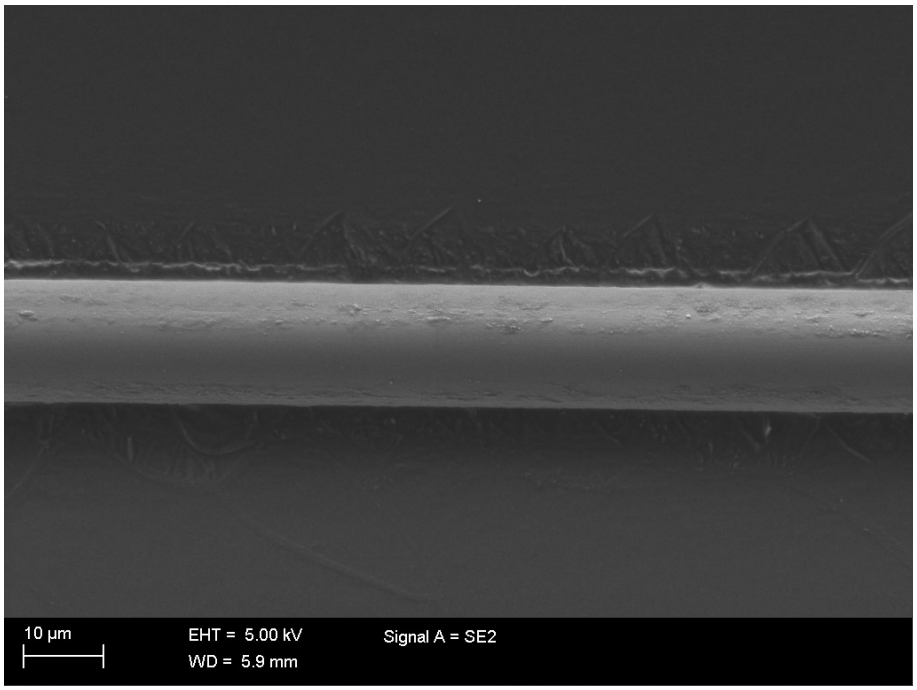

Figure 60. *SEM image of a Jushi E6CR fibre aged for 2 days in 95 °C 1 g/dm^3 sulphuric acid solution.*

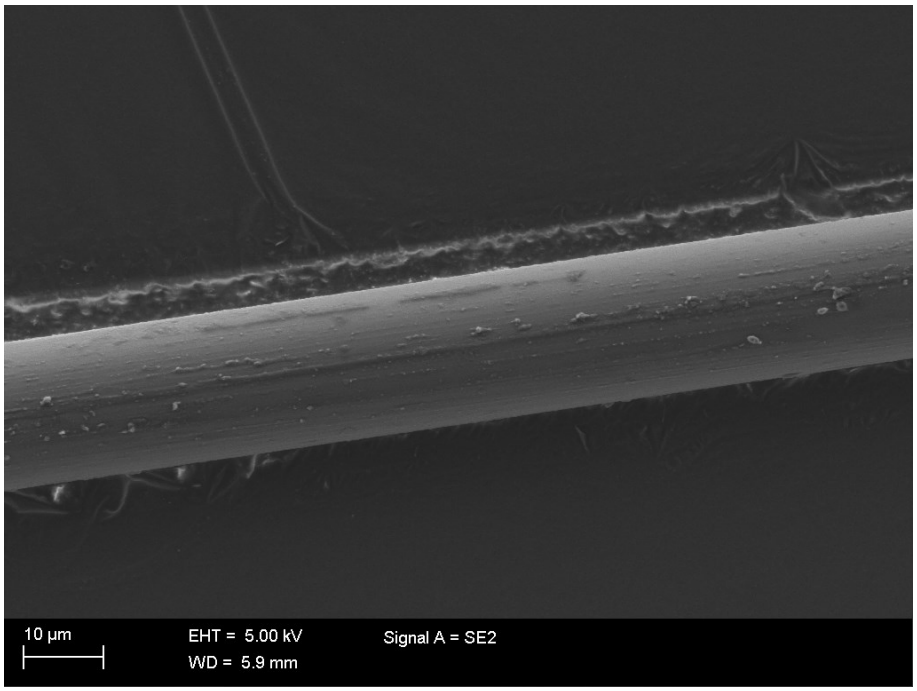

Figure 61. *SEM image of a Jushi E6CR fibre aged for 2 days in 95 °C 1 g/dm^3 sulphuric acid solution.*

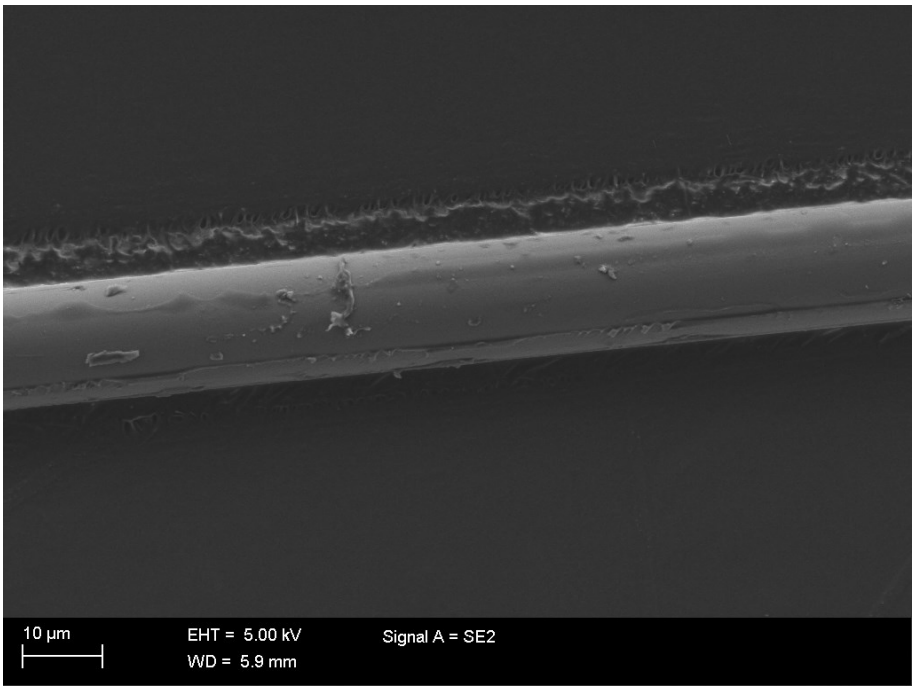

Figure 62. *SEM image of a Jushi E6CR fibre aged for 1 week in 95 °C 1 g/dm^3 sulphuric acid solution.*

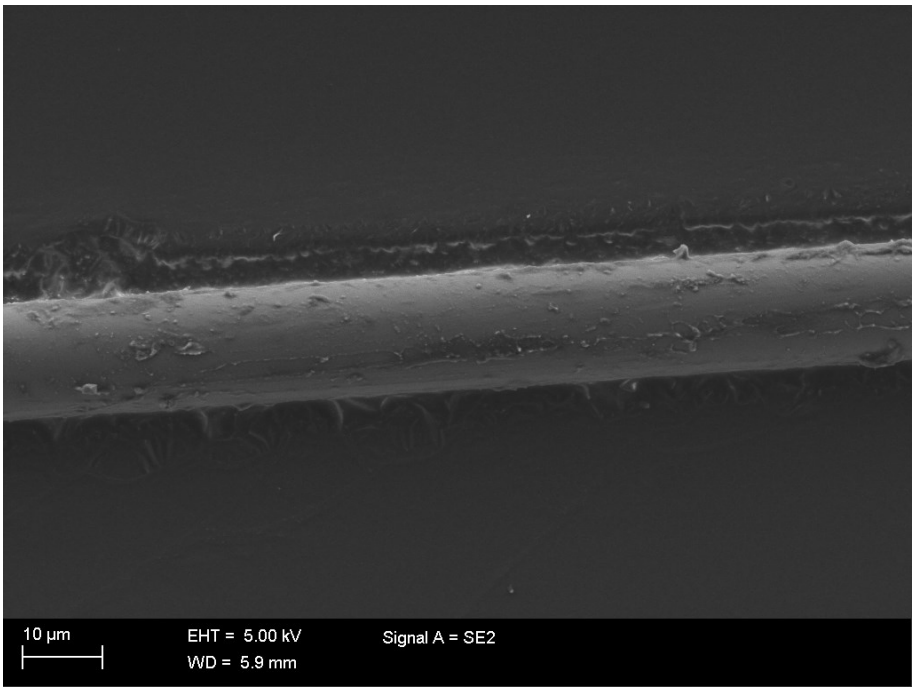

Figure 63. *SEM image of a Jushi E6CR fibre aged for 1 week in 95 °C 1 g/dm^3 sulphuric acid solution.*

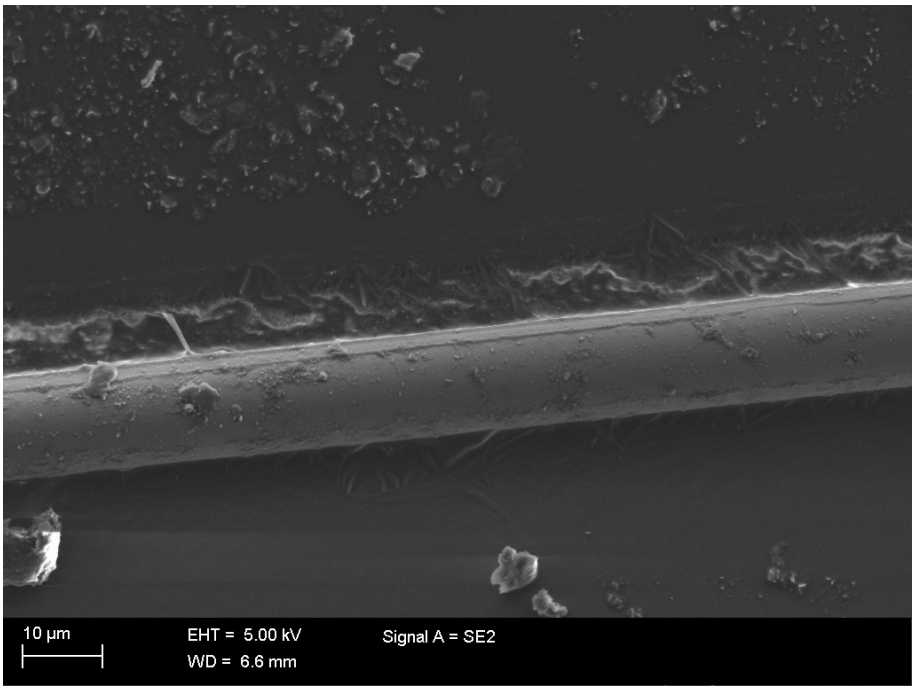

Figure 64. *SEM image of a Jushi E6CR fibre aged for 2 weeks in 95 °C 1 g/dm^3 sulphuric acid solution.*

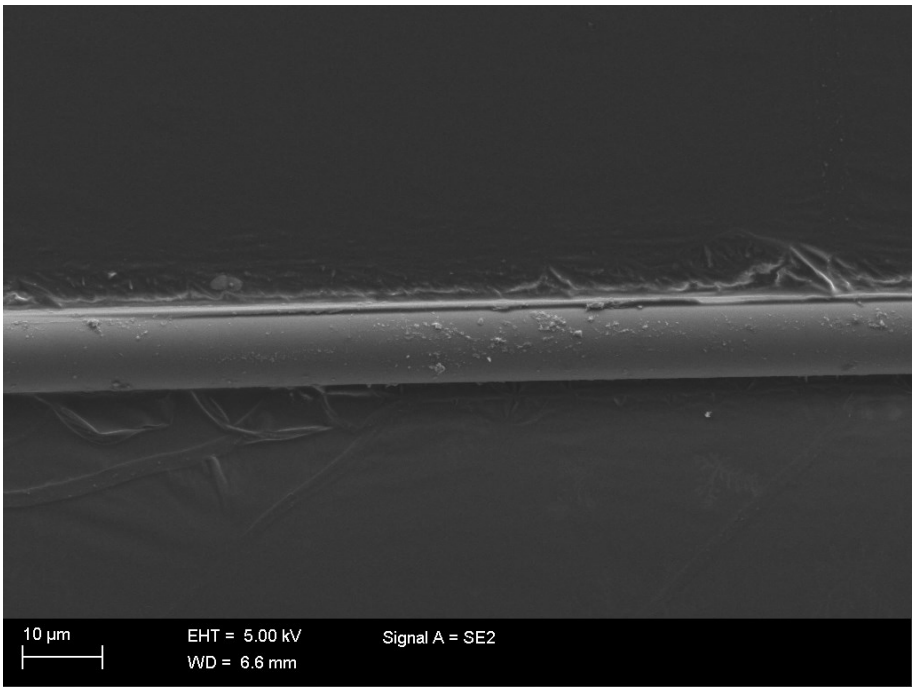

Figure 65. *SEM image of a Jushi E6CR fibre aged for 2 weeks in 95 °C 1 g/dm^3 sulphuric acid solution.*

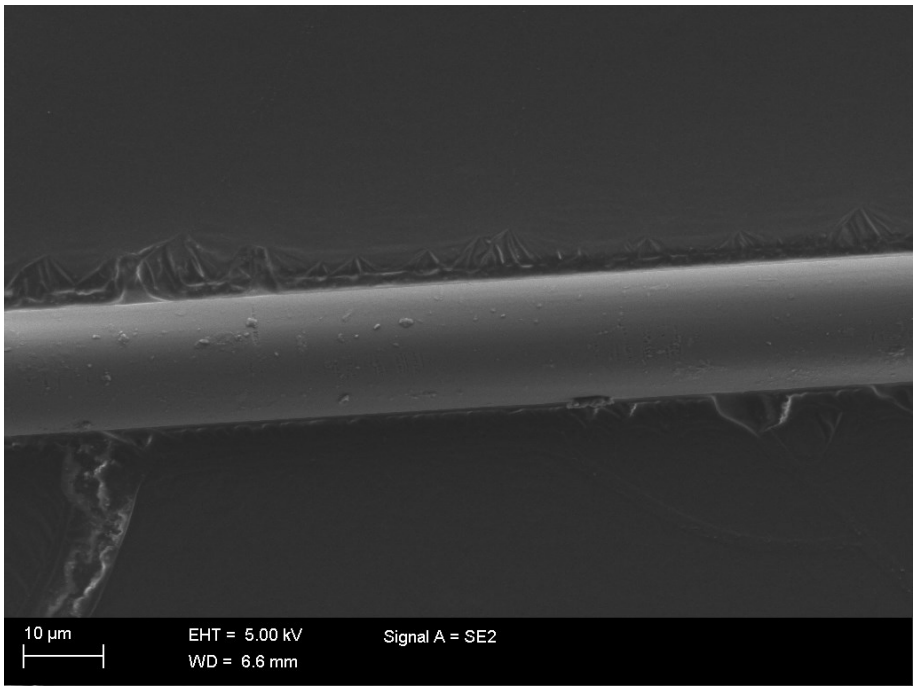

Figure 66. *SEM image of a Jushi E6CR fibre aged for 1 day in 95 °C 50 g/dm^3 sulphuric acid solution.*

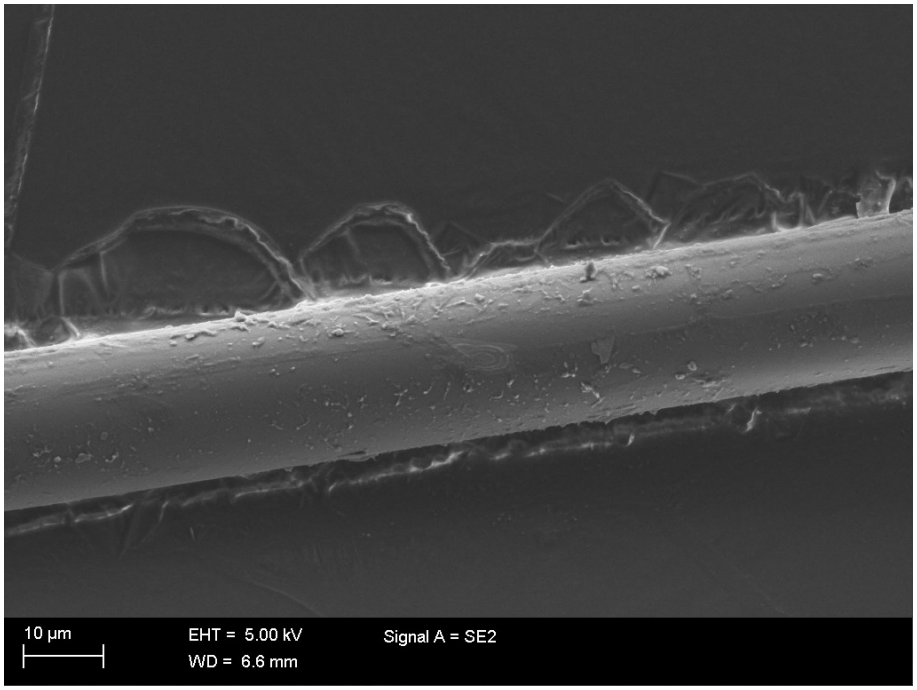

Figure 67. *SEM image of a Jushi E6CR fibre aged for 1 day in 95 °C 1 g/dm^3 sulphuric acid solution.*

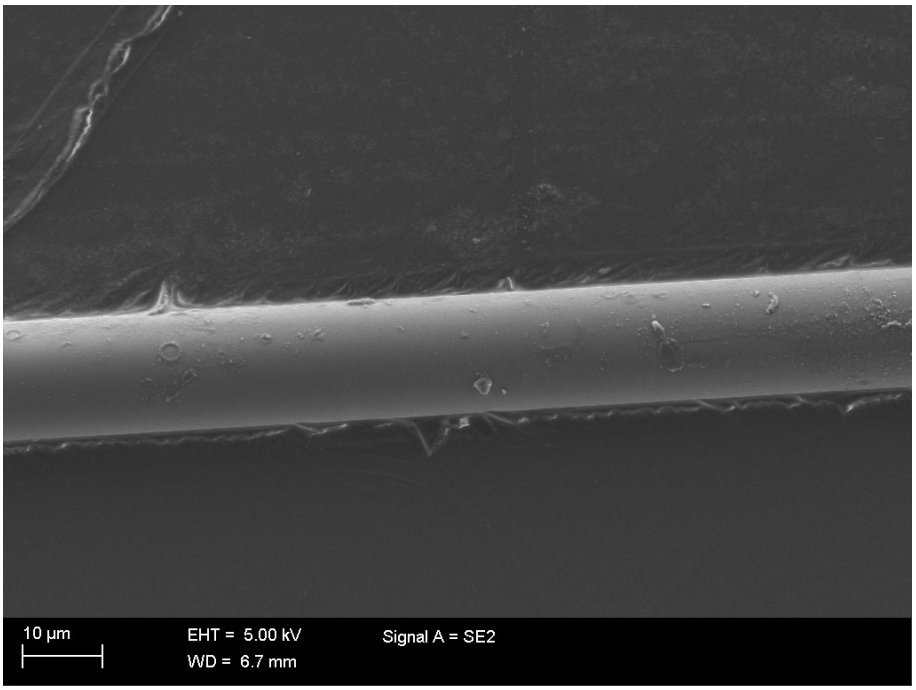

Figure 68. *SEM image of a Jushi E6CR fibre aged for 2 days in 95 °C 1 g/dm^3 sulphuric acid solution.*

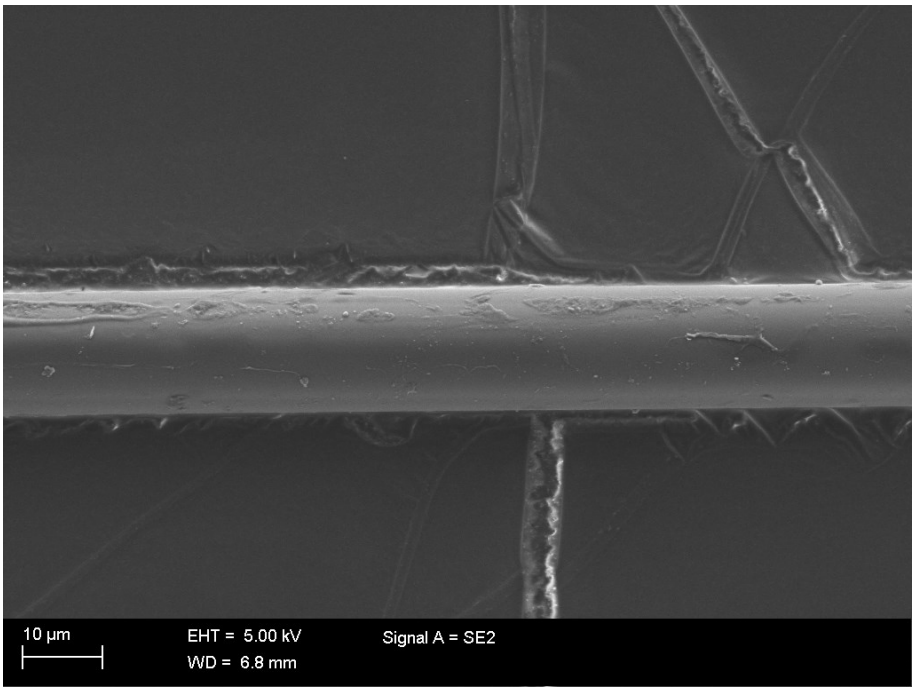

Figure 69. *SEM image of a Jushi E6CR fibre aged for 2 days in 95 °C 1 g/dm^3 sulphuric acid solution.*

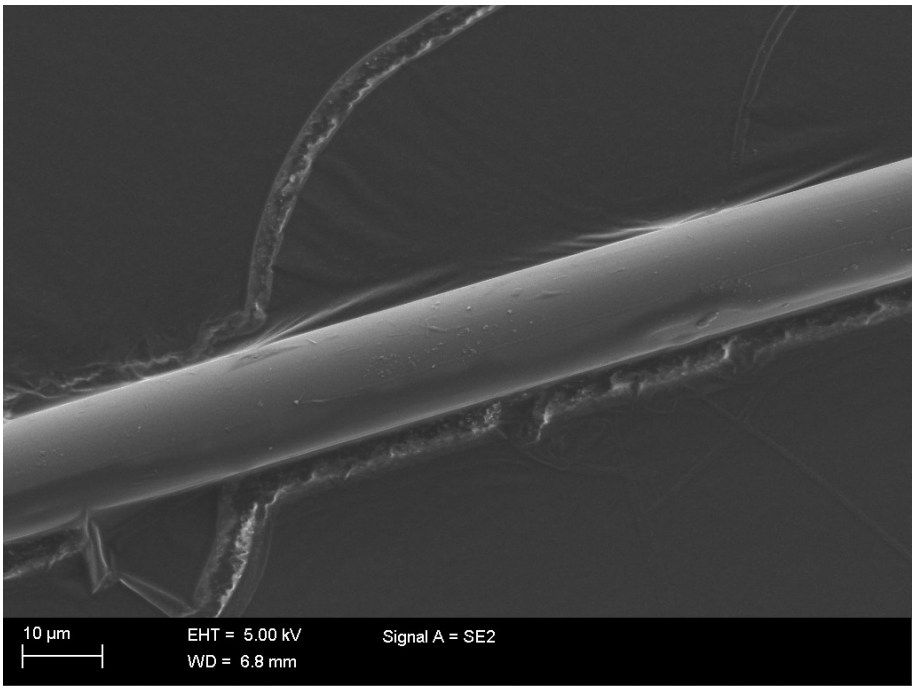

Figure 70. *SEM image of a Jushi E6CR fibre aged for 1 week in 95 °C 1 g/dm^3 sulphuric acid solution.*

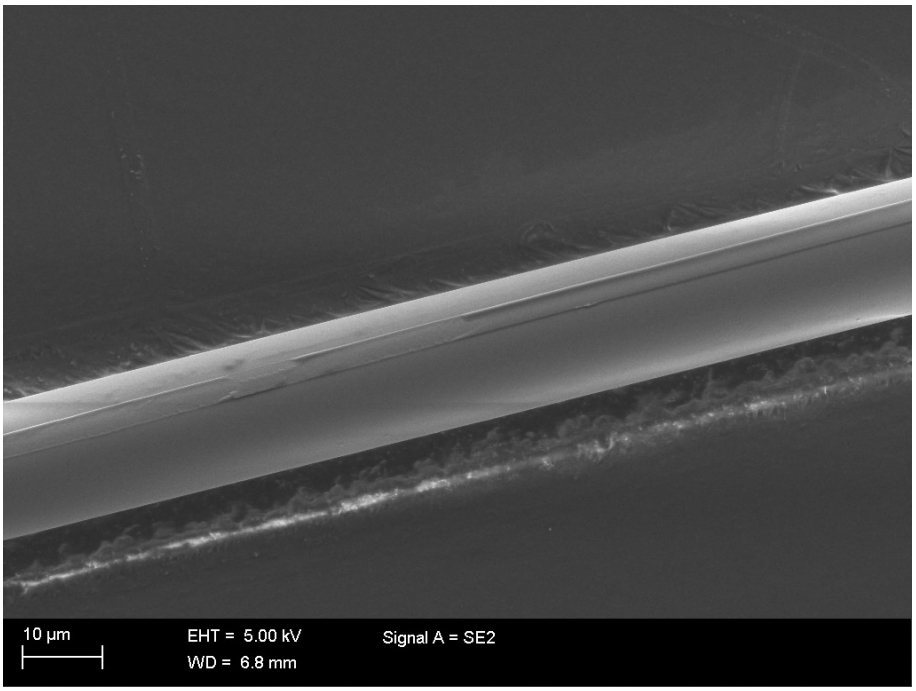

Figure 71. *SEM image of a Jushi E6CR fibre aged for 1 week in 95 °C 1 g/dm^3 sulphuric acid solution.*

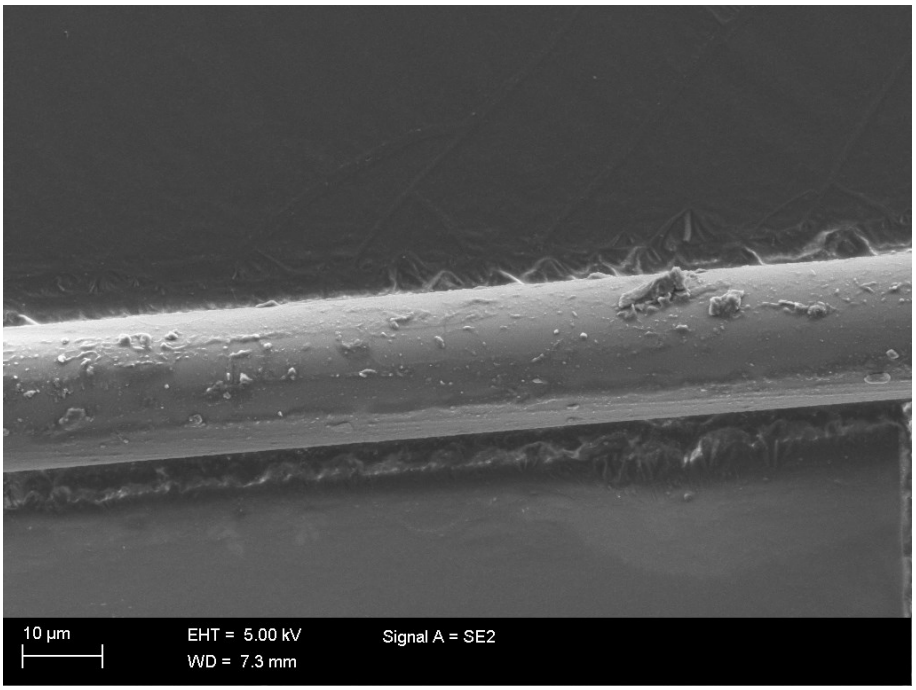

Figure 72. *SEM image of a Jushi E6CR fibre aged for 2 weeks in 95 °C 1 g/dm^3 sulphuric acid solution.*

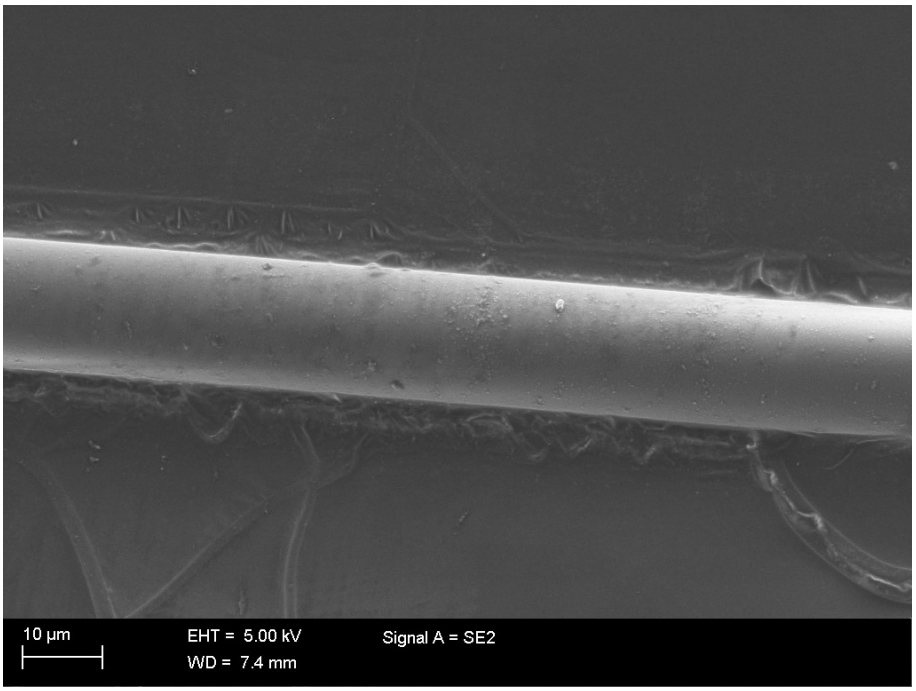

Figure 73. *SEM image of a Jushi E6CR fibre aged for 1 week in 95 °C 1 g/dm^3 sulphuric acid solution.*

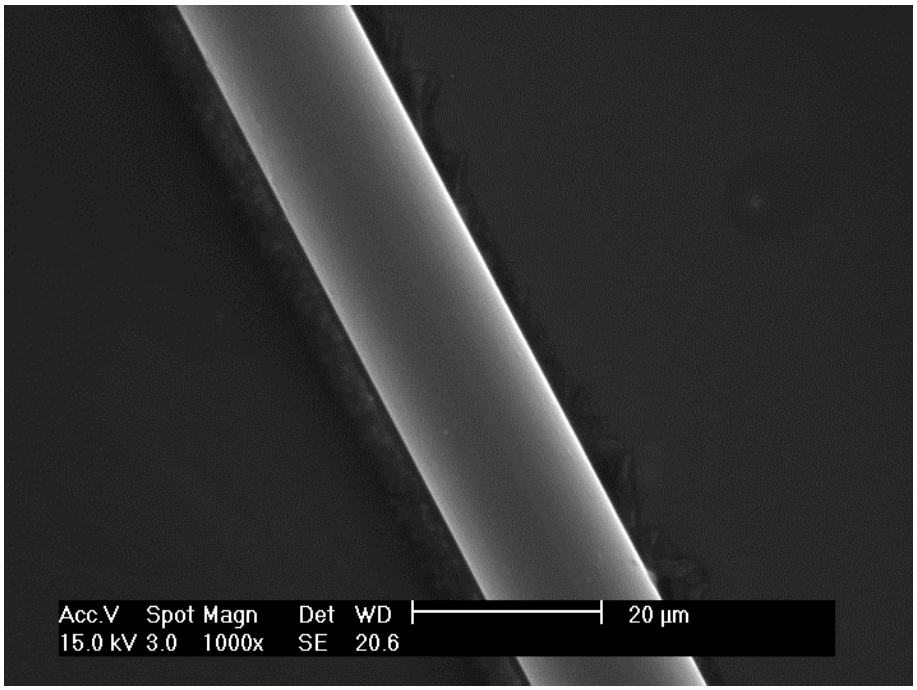

Figure 74. *SEM image of a Ahlstrom R338 fibre aged for 1 day in 95 °C deionized water.*

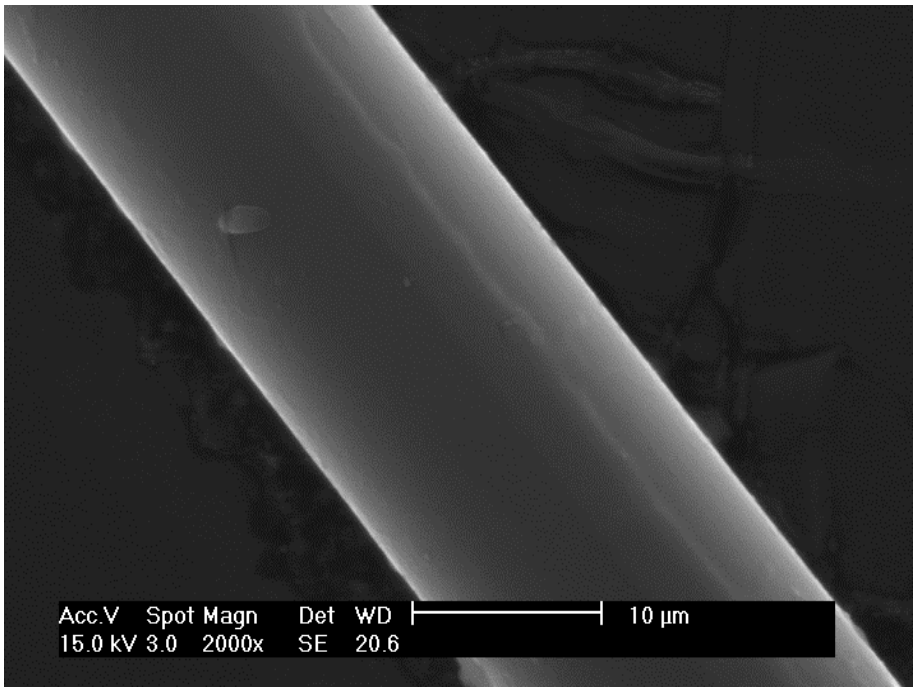

Figure 75. *SEM image of a Ahlstrom R338 fibre aged for 1 day in 95 °C deionized water.*

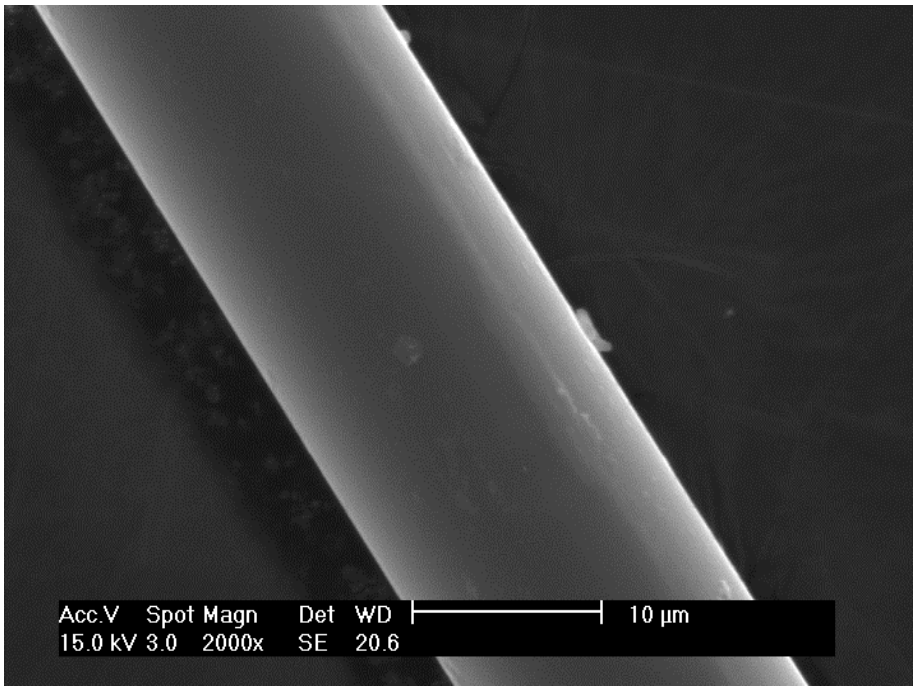

Figure 76. *SEM image of a Ahlstrom R338 fibre aged for 2 days in 95 °C deionized water.*

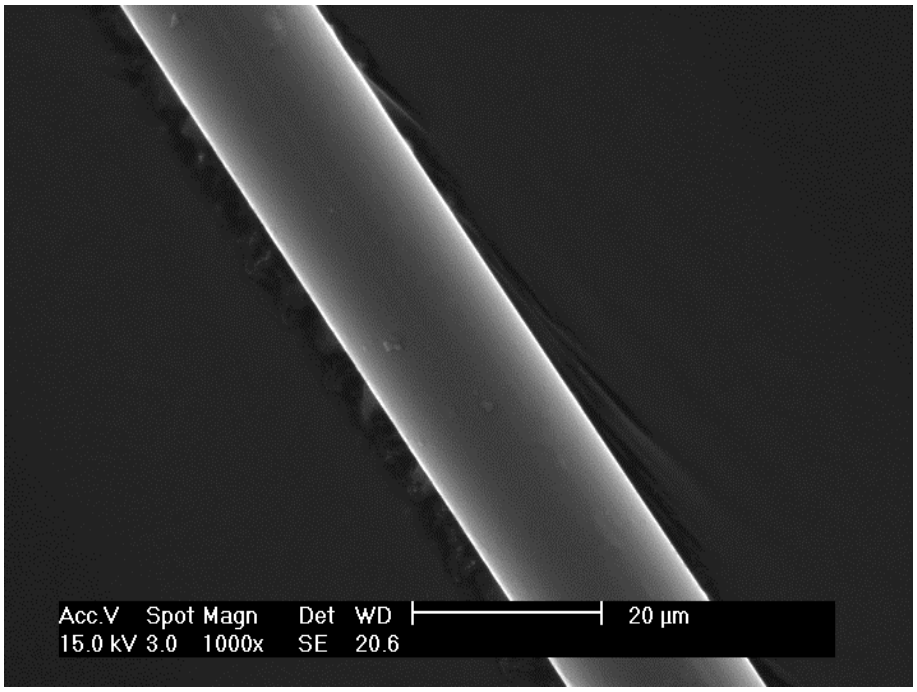

Figure 77. *SEM image of a Ahlstrom R338 fibre aged for 2 days in 95 °C deionized water.*

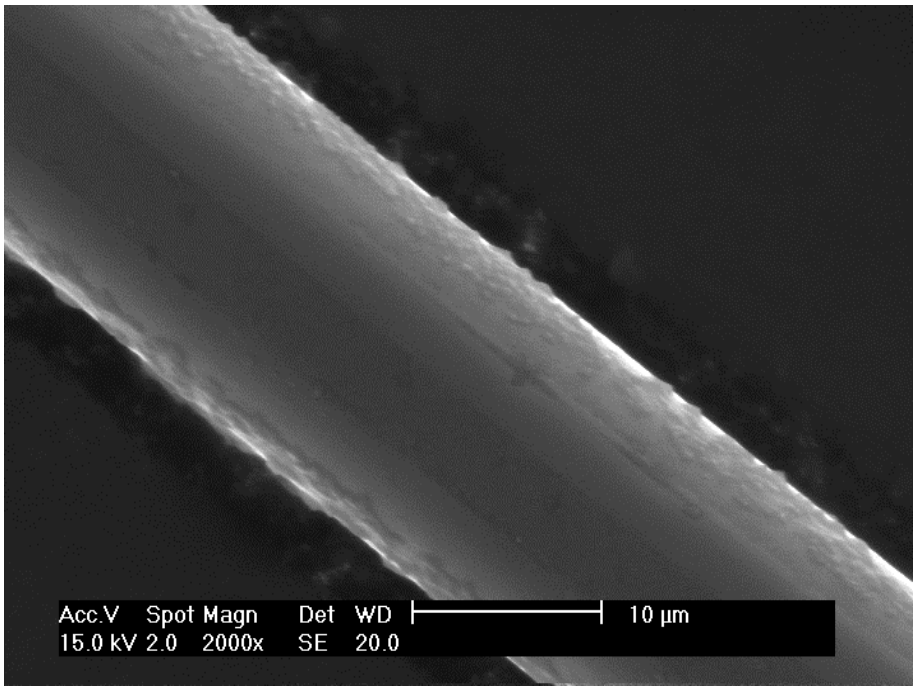

Figure 78. *SEM image of a Ahlstrom R338 fibre aged for 1 week in 95 °C deionized water.*

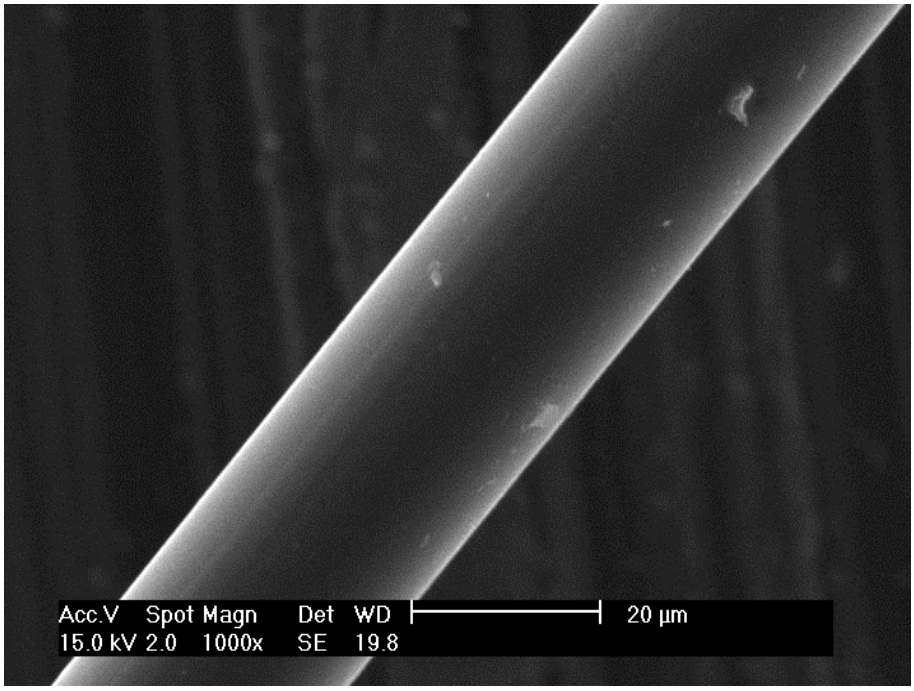

Figure 79. *SEM image of a Ahlstrom R338 fibre aged for 1 week in 95 °C deionized water.*

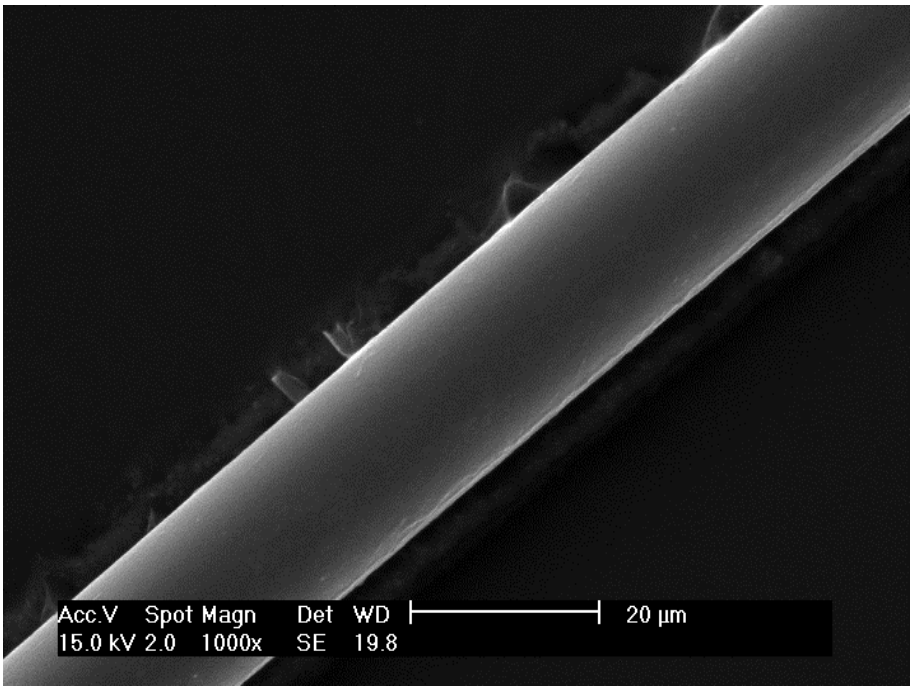

Figure 80. *SEM image of a Ahlstrom R338 fibre aged for 2 weeks in 95 °C deionized water.*

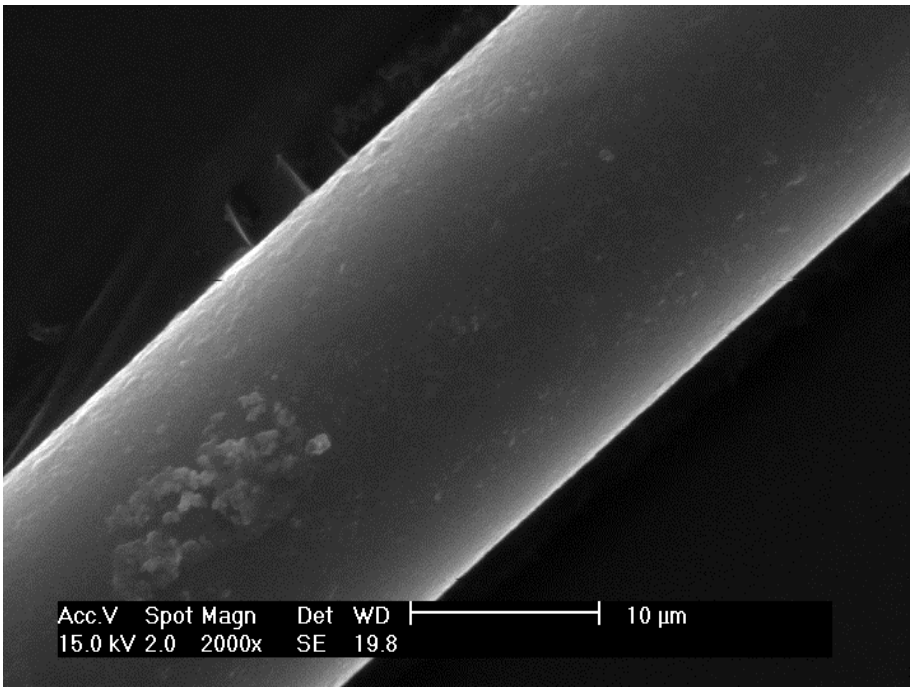

Figure 81. *SEM image of a Ahlstrom R338 fibre aged for 2 weeks in 95 °C deionized water.*

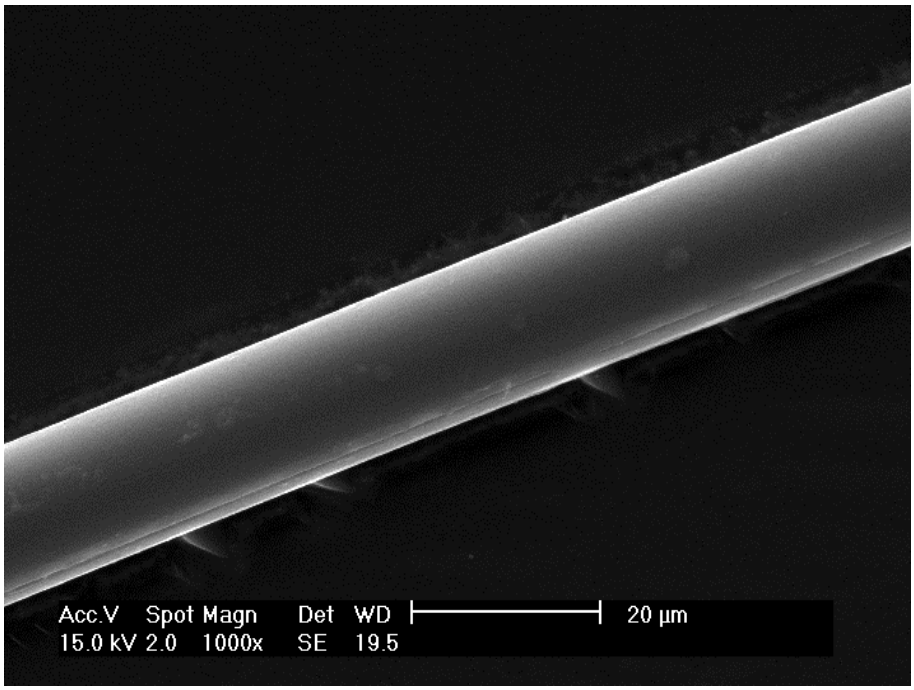

Figure 82. *SEM image of a Ahlstrom R338 fibre aged for 1 day in 95 °C 1 g/dm^3 sulphuric acid solution.*

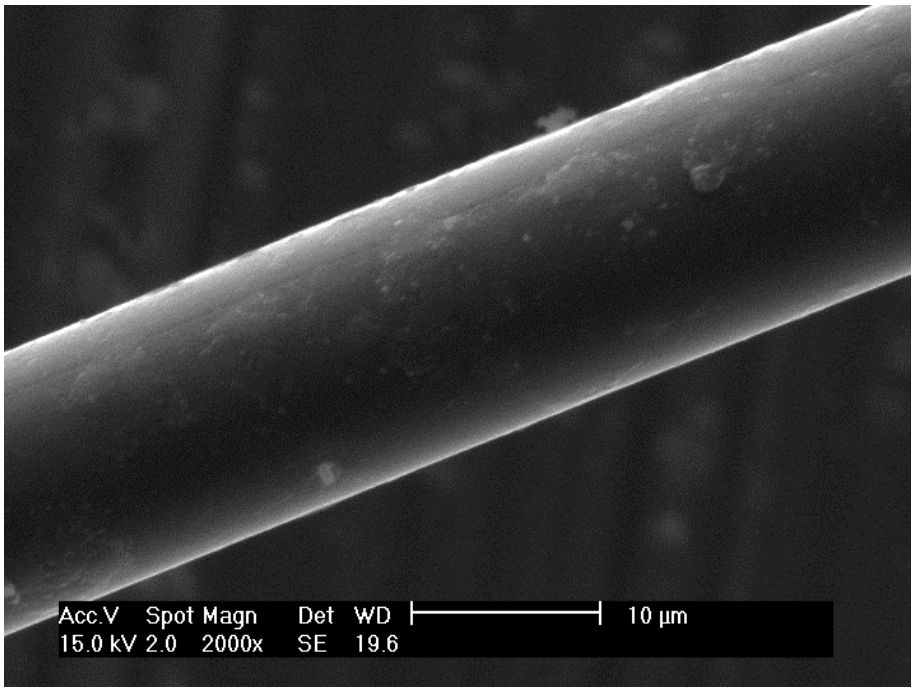

Figure 83. *SEM image of a Ahlstrom R338 fibre aged for 1 day in 95 °C 1 g/dm^3 sulphuric acid solution.*

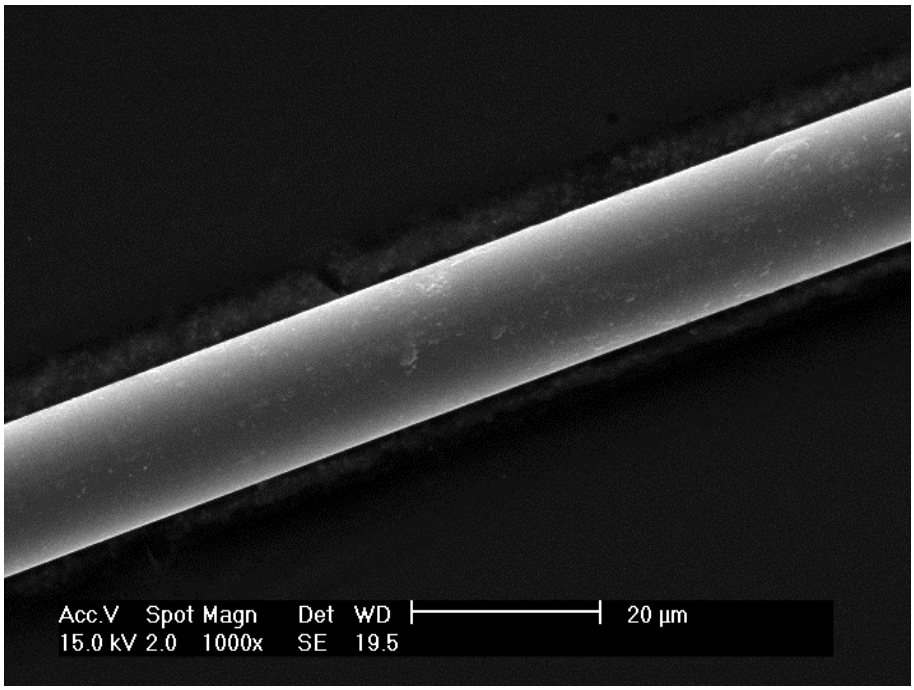

Figure 84. *SEM image of a Ahlstrom R338 fibre aged for 2 days in 95 °C 1 g/dm^3 sulphuric acid solution.*

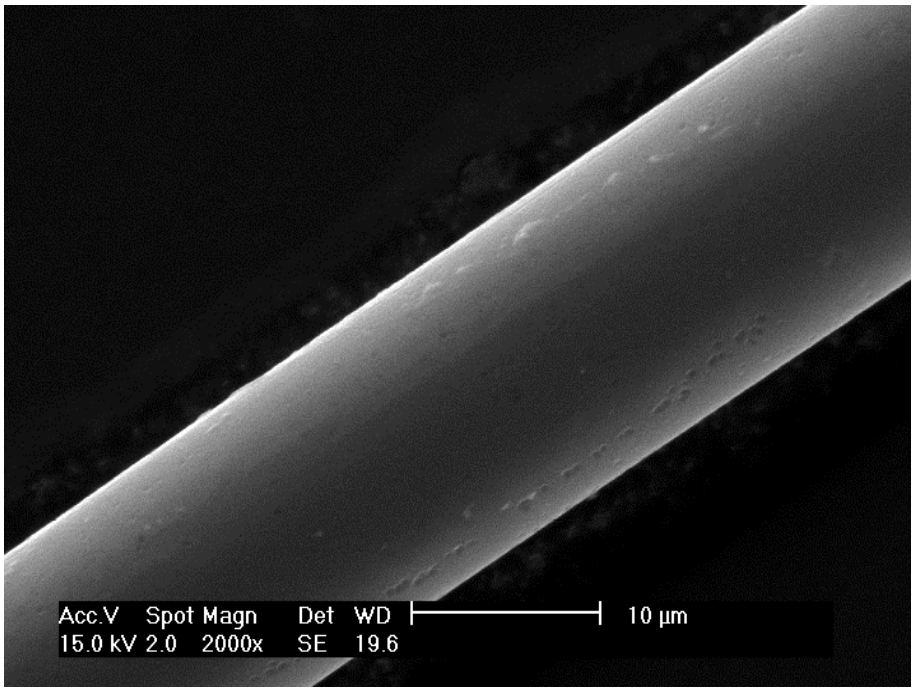

Figure 85. *SEM image of a Ahlstrom R338 fibre aged for 2 days in 95 °C 1 g/dm^3 sulphuric acid solution.*

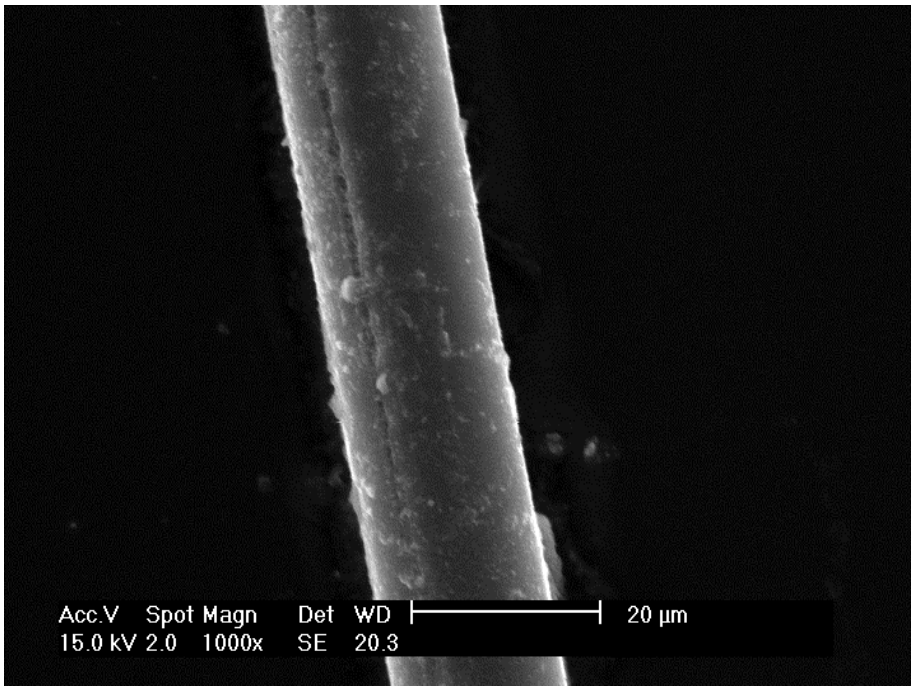

Figure 86. *SEM image of a Ahlstrom R338 fibre aged for 1 week in 95 °C 1 g/dm^3 sulphuric acid solution.*

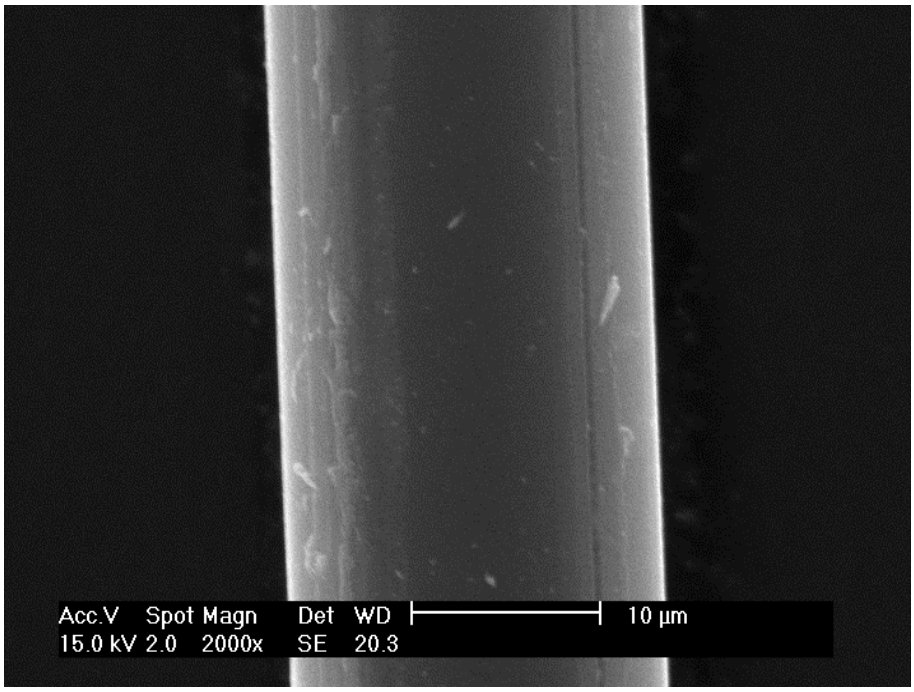

Figure 87. *SEM image of a Ahlstrom R338 fibre aged for 1 week in 95 °C 1 g/dm^3 sulphuric acid solution.*

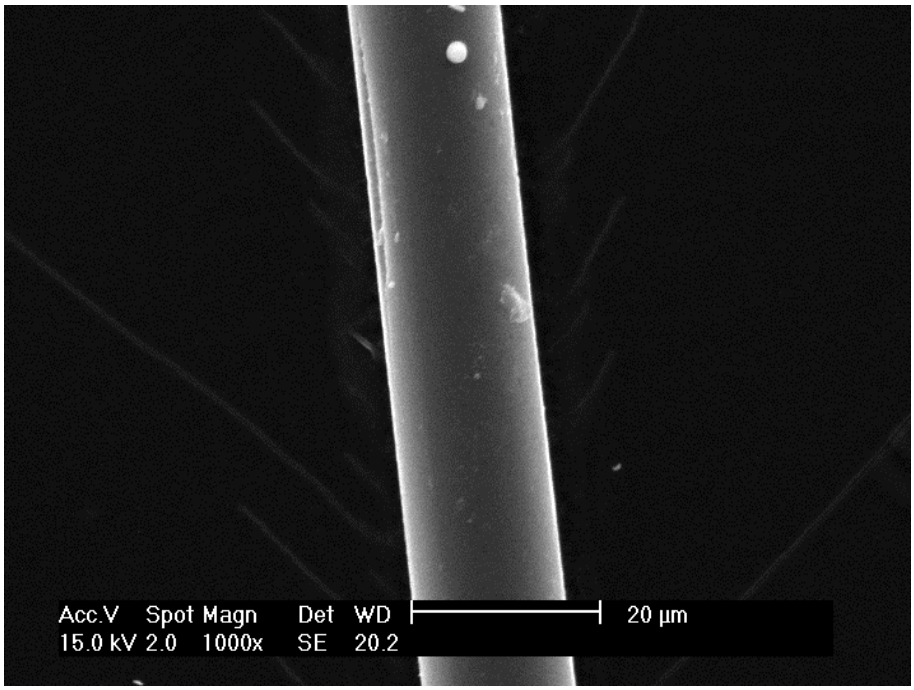

Figure 88. *SEM image of a Ahlstrom R338 fibre aged for 2 weeks in 95 °C 1 g/dm^3 sulphuric acid solution.*

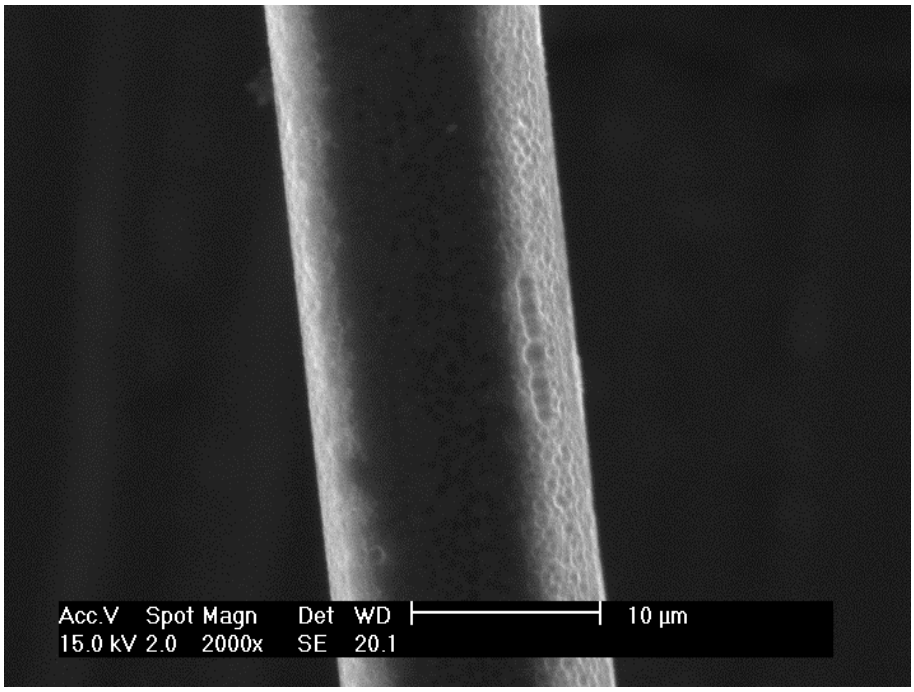

Figure 89. *SEM image of a Ahlstrom R338 fibre aged for 2 weeks in 95 °C 1 g/dm^3 sulphuric acid solution.*

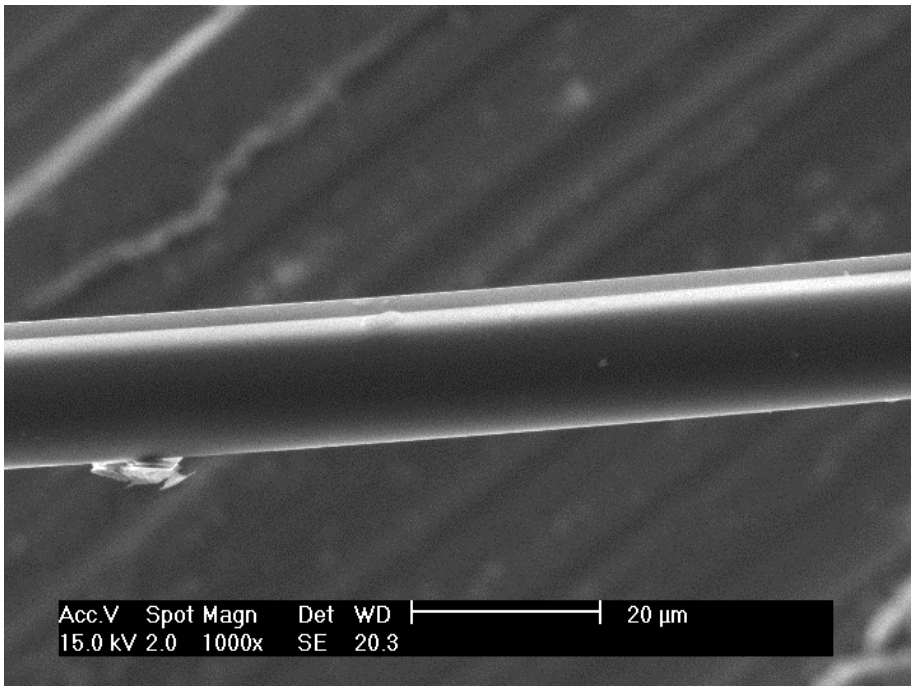

Figure 90. *SEM image of a Ahlstrom R338 fibre aged for 1 day in 95 °C 50 g/dm^3 sulphuric acid solution.*

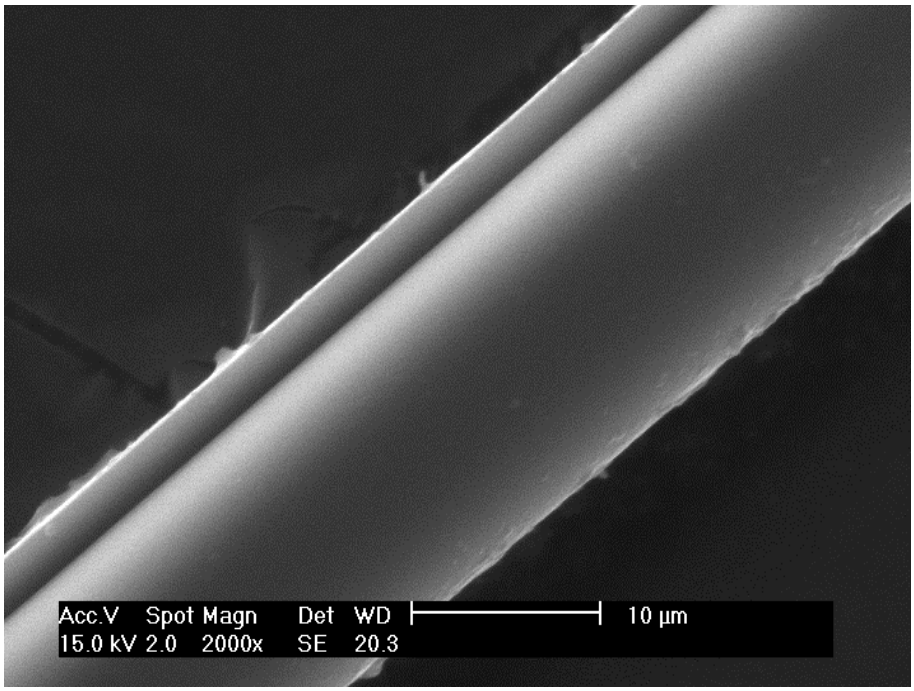

Figure 91. *SEM image of a Ahlstrom R338 fibre aged for 1 day in 95 °C 50 g/dm^3 sulphuric acid solution.*

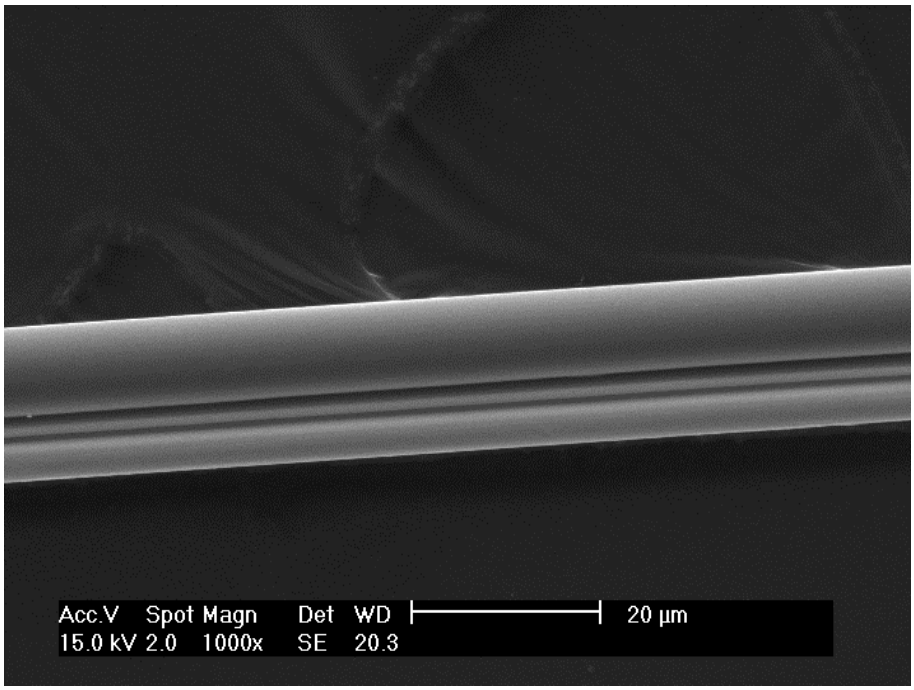

Figure 92. *SEM image of a Ahlstrom R338 fibre aged for 2 days in 95 °C 50 g/dm^3 sulphuric acid solution.*

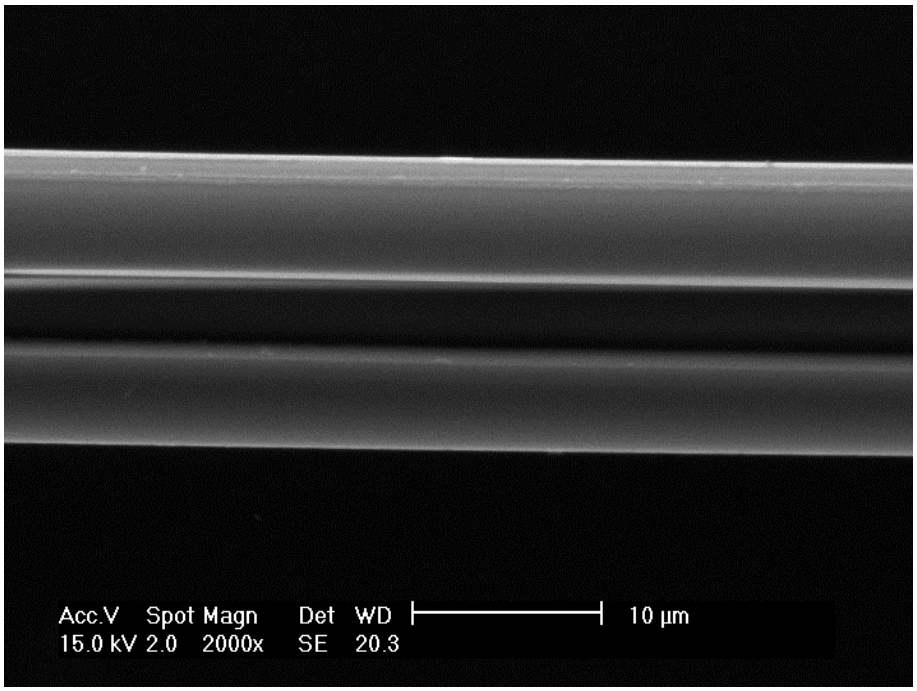

Figure 93. *SEM image of a Ahlstrom R338 fibre aged for 2 days in 95 °C 50 g/dm^3 sulphuric acid solution.*

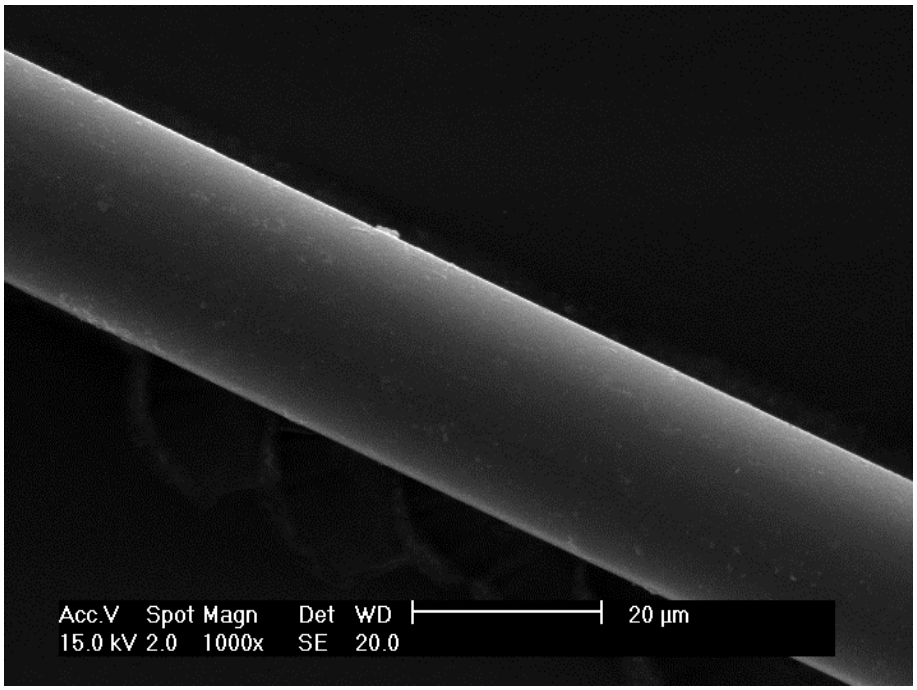

Figure 94. *SEM image of a Ahlstrom R338 fibre aged for 1 week in 95 °C 50 g/dm^3 sulphuric acid solution.*

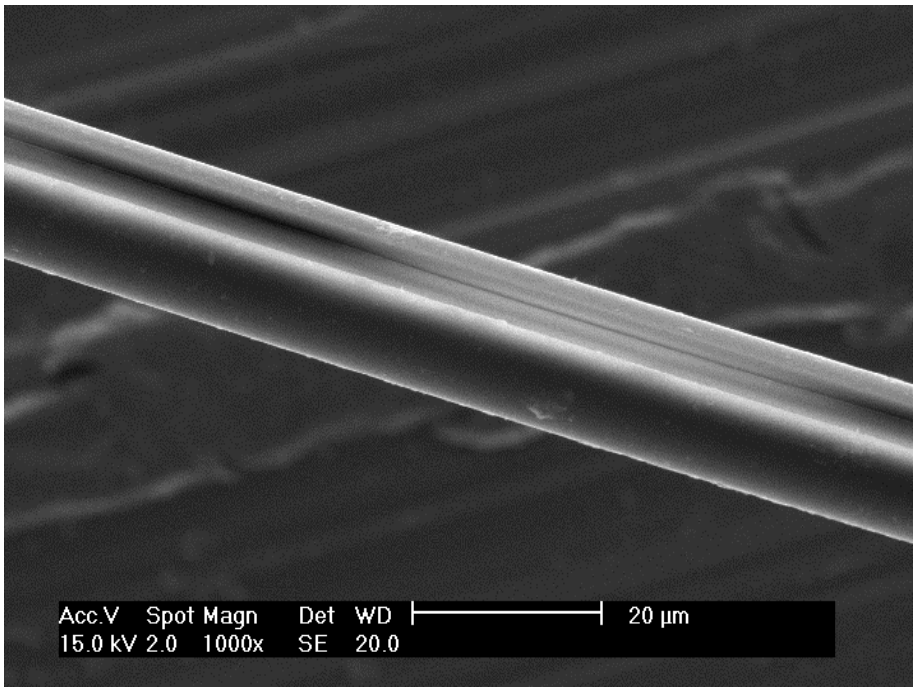

Figure 95. *SEM image of a Ahlstrom R338 fibre aged for 1 week in 95 °C 50 g/dm^3 sulphuric acid solution.*

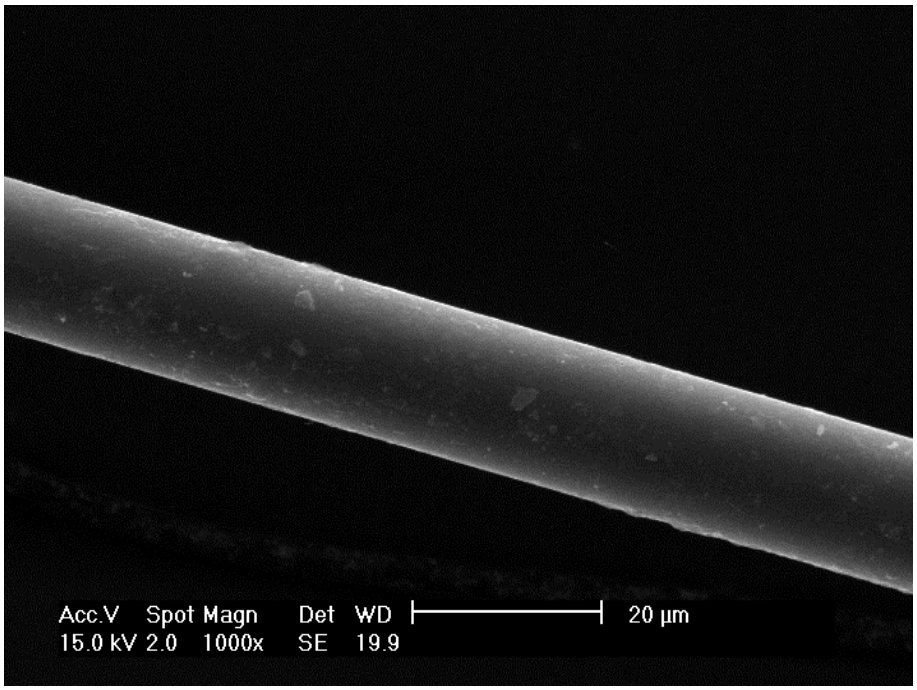

Figure 96. *SEM image of a Ahlstrom R338 fibre aged for 2 weeks in 95 °C 50 g/dm^3 sulphuric acid solution.*

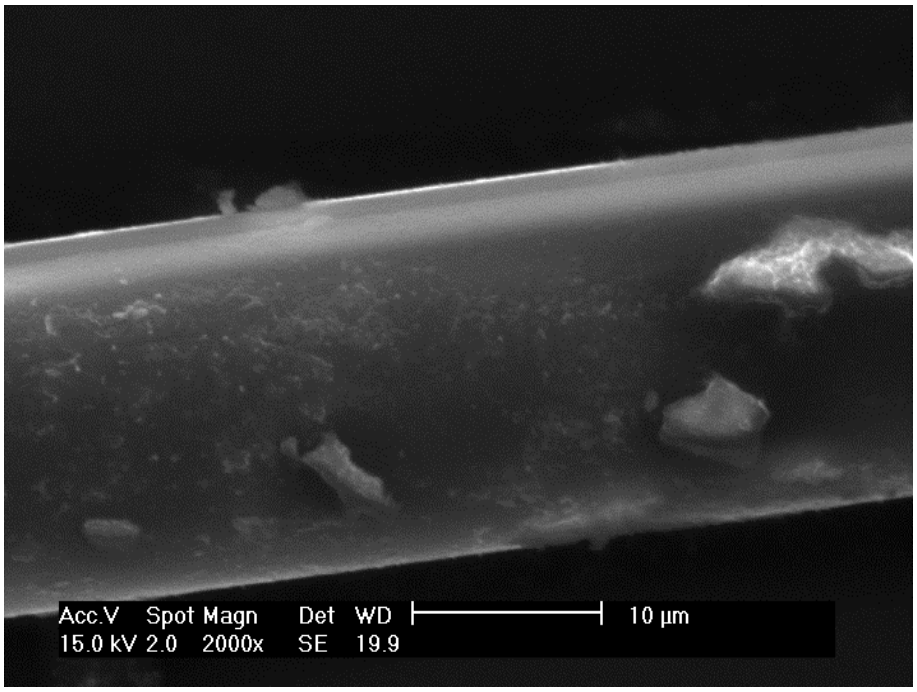

Figure 97. *SEM image of a Ahlstrom R338 fibre aged for 2 weeks in 95 °C 50 g/dm^3 sulphuric acid solution.*

APPENDIX 2: COMPLETE GLASS FIBRE FTIR SPECTRA

The complete measuring range of 340 – 4000 cm^{-1} for the glass fibre FTIR measurements are presented here. The transmittance values are shifted in these figures to make the observation of the individual spectra easier.

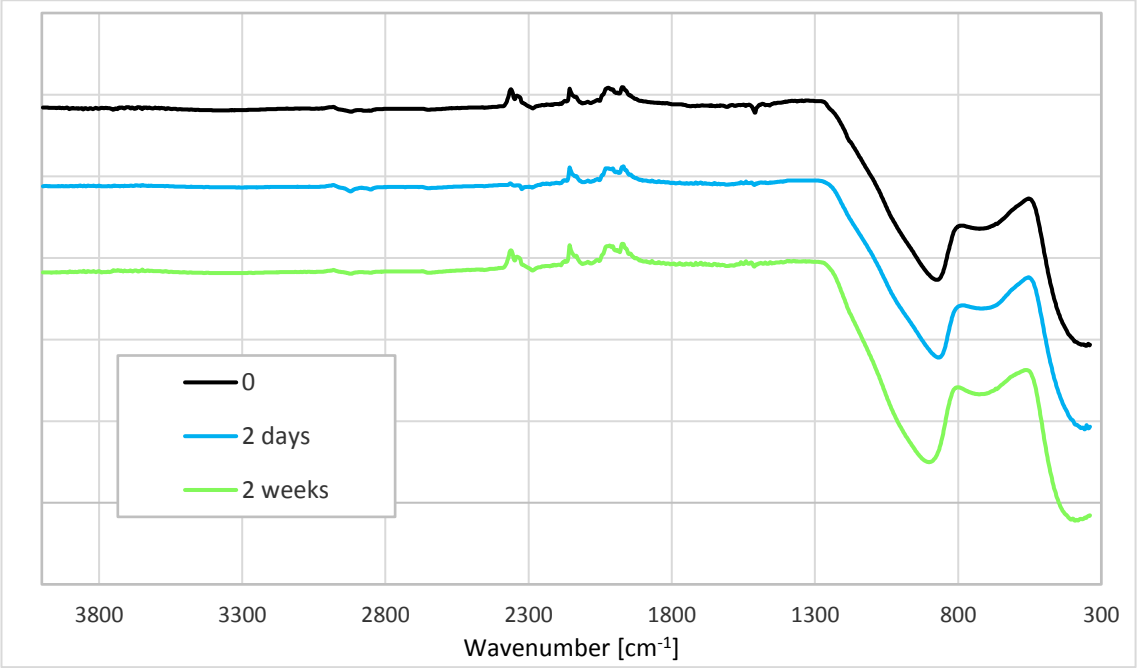

Figure 98. *FTIR spectra of Jushi E6CR fibres aged in 95 °C deionized water.*

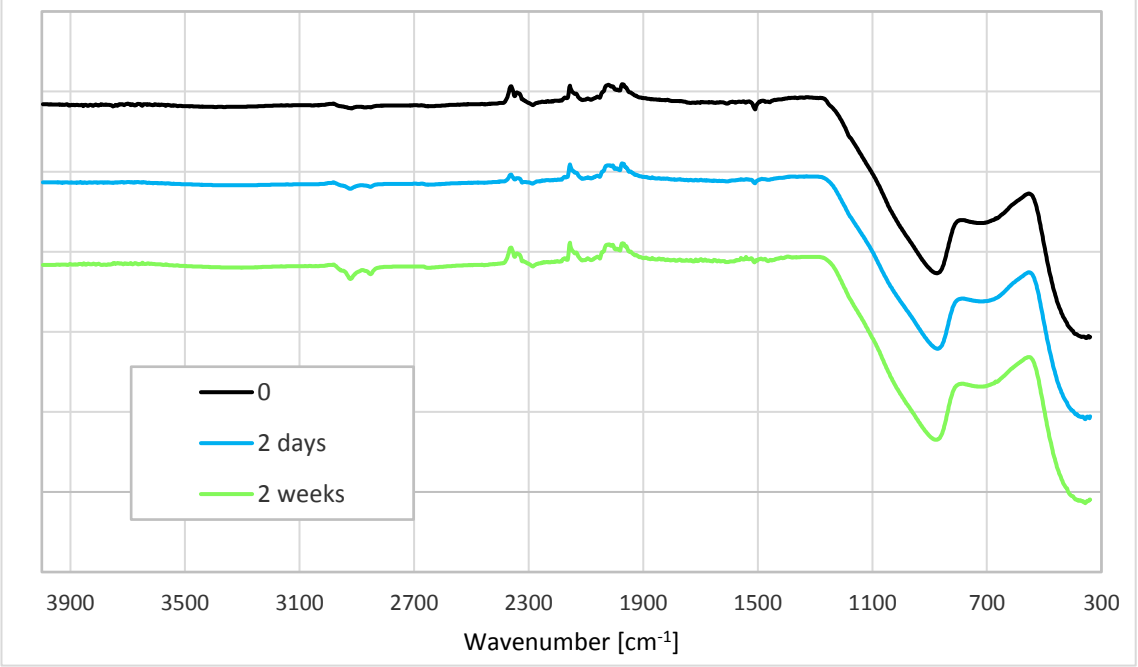

Figure 99. *FTIR spectra of Jushi E6CR fibres aged in 95 °C 1 g/dm³ sulphuric acid solution.*

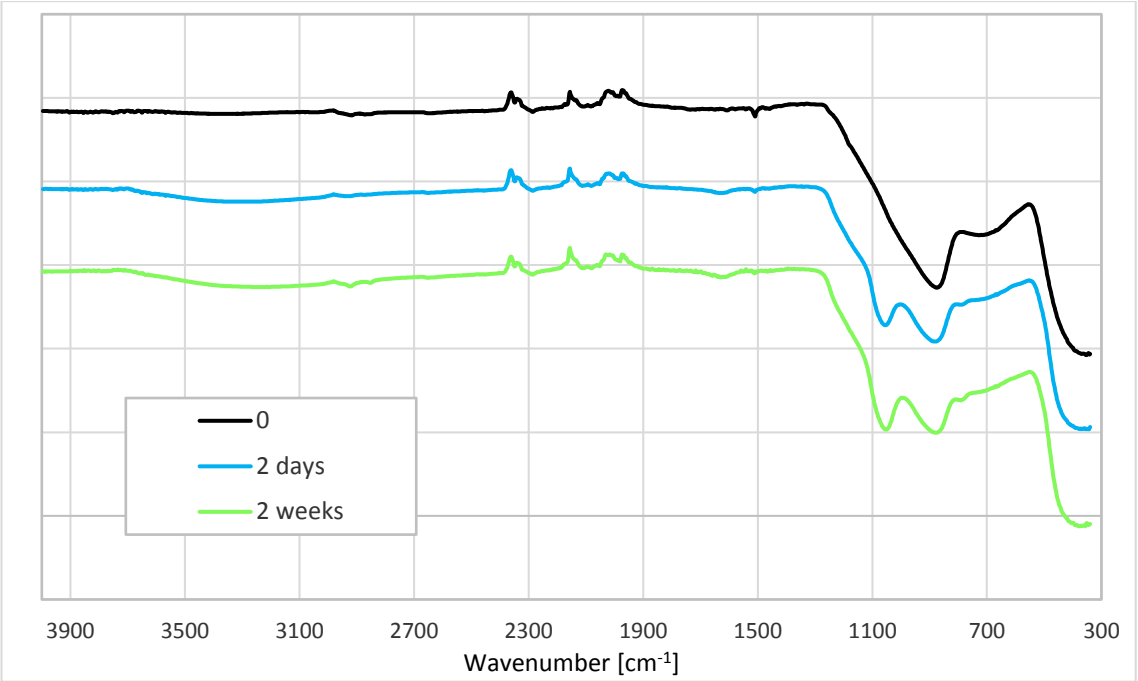

Figure 100. *FTIR spectra of Jushi E6CR fibres aged in 95 °C 50 g/dm³ sulphuric acid solution.*

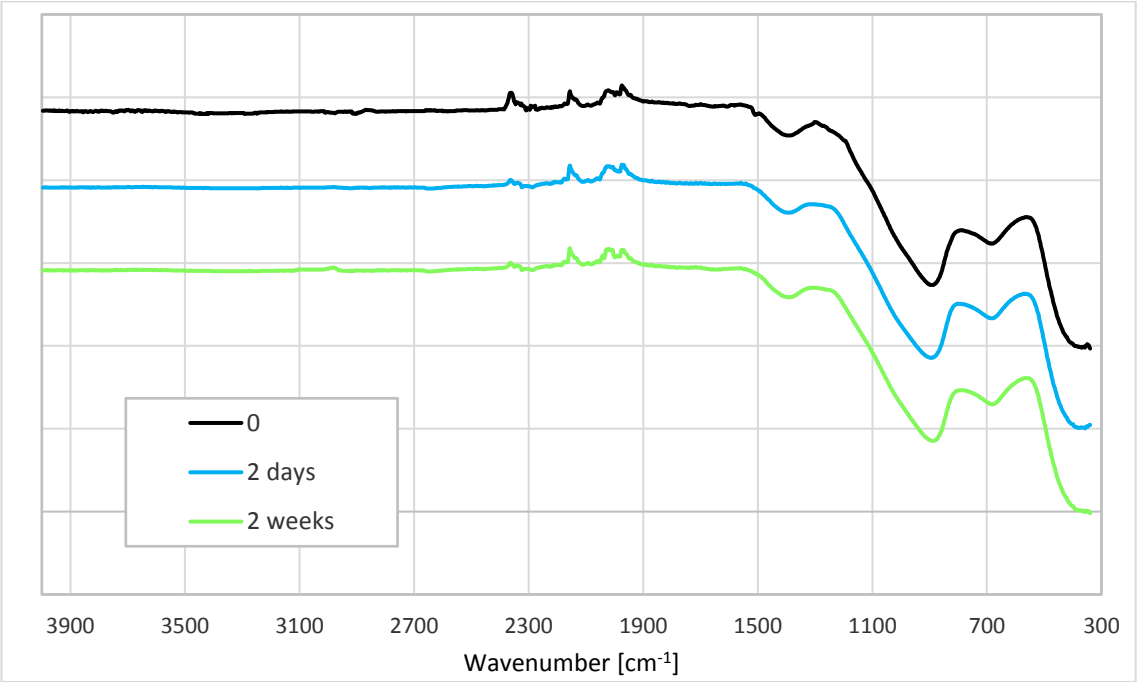

Figure 101. *FTIR spectra of Ahlstrom R338 fibres aged in 95 °C deionized water.*

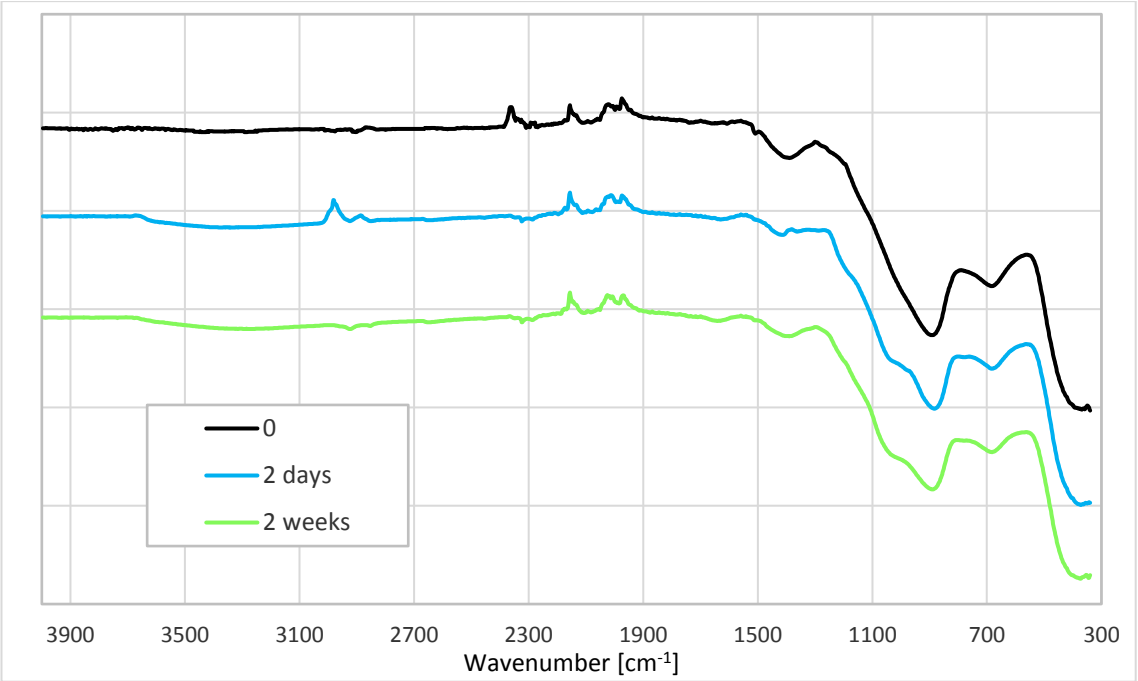

Figure 102. *FTIR spectra of Ahlstrom R338 fibres aged in 95 °C 1 g/dm³ sulphuric acid solution.*

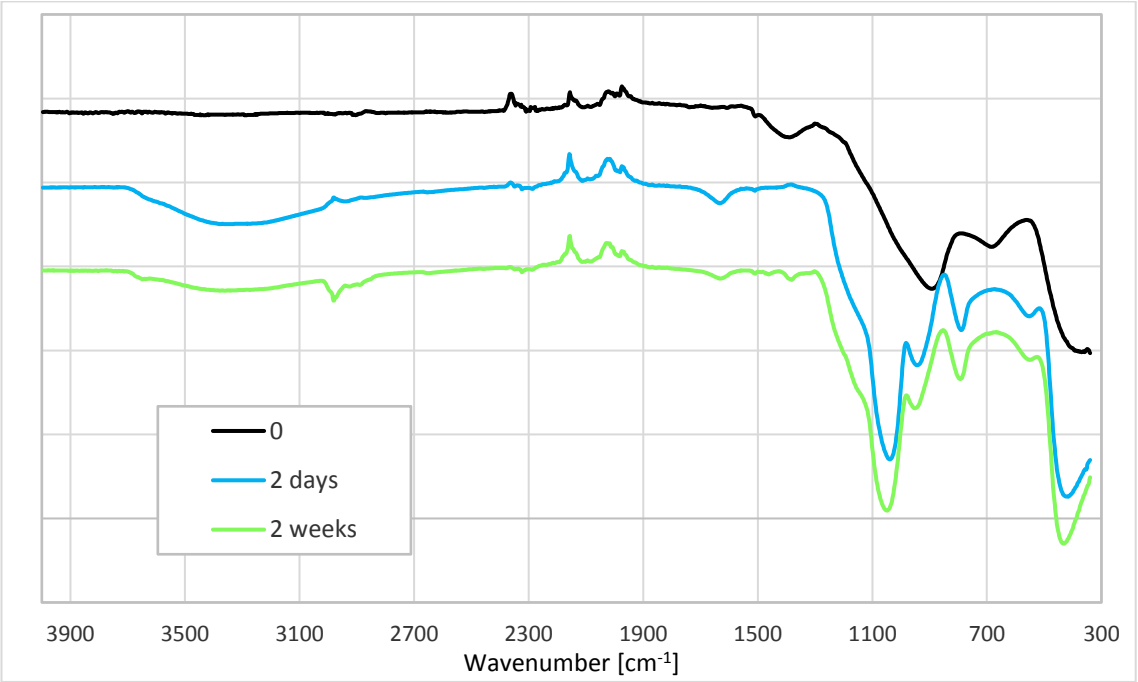

Figure 103. *FTIR spectra of Ahlstrom R338 fibres aged in 95 °C 50 g/dm³ sulphuric acid solution.*